Design and Analysis of Dynamically Grouped Multilevel Space-Time Trellis Code

A THESIS

SUBMITTED IN FULFILLMENT OF THE REQUIREMENT

FOR THE AWARD OF DEGREE OF

DOCTOR OF PHILOSOPHY

IN

ELECTRONICS AND COMMUNICATION ENGINEERING

SUBMITTED BY

DHARMVIR JAIN

REGISTRATION No.: 950906026

SUPERVISOR

Dr. SANJAY SHARMA

(PROFESSOR)

ELECTRONICS AND COMMUNICATION ENGINEERING DEPARTMENT

THAPAR UNIVERSITY, PATIALA-147004 (INDIA)

2014

CERTIFICATE

I, **Dharmvir Jain,** hereby declare that the thesis entitled, "**Design and Analysis of Dynamically Grouped Multilevel Space-Time Trellis Code**," submitted to Thapar University, Patiala, in partial fulfilment of the requirement for the award of the Degree of **Doctor of Philosophy** in **the Electronics and Communication Engineering** is a record of original, bonafide, and independent research work done by me during 2010-2014. The research work and the thesis have been conducted under the supervision and guidance of **Dr. Sanjay Sharma**, Professor and Head, Electronics and Communication Engineering Department, Thapar University. It has not formed the basis for the award of any Degree/Diploma/Associate-ship/Fellowship or other similar title to any candidate of any university.

Dharmvir Jain Date: 14/11/2014

This is to certify that above statement made by the candidate is correct to the best of my knowledge.

Dr. Sanjay Sharma

Professor (Supervisor)

Electronics and Communication Engg. Deptt.

Thapar University, Patiala

ABSTRACT

The wireless communication systems are expected to support high speed multimedia services such as high speed internet access, mobile gaming, and high definition video transmission. The rapidly growing demand of these services is driving the communication technology towards reliable and high data rate transmission. In this research work, design and analysis of different dynamically grouped multilevel space-time trellis codes have been presented in order to support the rising demand for higher data rate and higher reliability in the wireless communication systems. The simulation results depict that the proposed codes provide better performance than existing multilevel space-time trellis codes (MLSTTCs) and grouped multilevel space-time trellis codes (GMLSTTCs).

MLSTTCs and GMLSTTCs consider channel state information (CSI) at the receiver only without considering the CSI at the transmitter. In this research work, effects of the CSI at the transmitter have been considered to improve the performance of MLSTTCs and GMLSTTCs. The CSI has been used to dynamically select a component space-time trellis code (STTC), adaptively group the transmit antennas, and provide a beamforming scheme for dynamic distribution of the transmit power across the transmit antennas.

MLSTTCs and GMLSTTCs use predefined STTCs as the component codes in the multilevel coding. A code set selection algorithm has been proposed for dynamic selection of the generator sequences with the help of the CSI at the transmitter. The selected generator sequences are used to design dynamic space-time trellis codes (DSTTCs). The simulation results show that the coding gain of DSTTCs is superior to existing STTCs by 0.7 dB at frame error rate (FER) of 10^{-2}. DSTTCs are used as the component code in multilevel coding for designing multilevel dynamic space-time trellis codes (MLDSTTCs) and grouped multilevel dynamic space-time trellis codes (GMLDSTTCs). It may be inferred from the results that MLDSTTCs are superior to

MLSTTCs by 1.1 dB at FER of 10^{-1} and GMLDSTTCs are superior to GMLSTTCs by 1.6 dB at FER of 10^{-2}.

GMLSTTCs use static grouping of transmit antennas. In the presented research work, the performance of GMLSTTCs has been improved by performing the adaptive grouping of the transmit antennas based on the CSI. Adaptively grouped multilevel space-time trellis codes (AGMLSTTCs) have been designed by grouping the transmit antennas with the help of the CSI at the transmitter. An adaptive antenna grouping algorithm has been proposed to perform the transmit antenna grouping. Instantaneous channel power gain is calculated between each transmit antenna and all the receive antennas. A subset of transmit antennas having maximum instantaneous channel power gain is selected to form a group of transmit antennas. From the presented results, it is evident that AGMLSTTCs are superior to GMLSTTCs by 1.5 dB at the FER of 10^{-2}.

In GMLSTTCs, the transmit power is equally distributed across all transmit antennas. The performance of GMLSTTCs has been improved by dynamically allocating the power to the transmit antennas. Weighted adaptively grouped multilevel space-time trellis codes (WAGMLSTTCs) and weighted adaptively grouped multilevel dynamic space-time trellis codes (WAGMDLSTTCs) have been designed by weighting the transmitting signals based on the CSI at the transmitter. It has been shown that the performance of WAGMLSTTCs is better than GMLSTTCs by 2.6 dB and the performance of WAGMDLSTTCs is superior to GMLSTTCs by 3.2 dB.

ACKNOWLEDGEMENT

First and foremost, I am beholden to the Almighty and I bow before Him for his umpteen blessings and bestowing in me the grit and confidence to carry out this research work.

I extend my thanks to **Dr. Prakash Gopalan**, Hon'ble Director and **Dr. O.P Pandey**, Dean (Research and Sponsored Projects) for giving me this opportunity to undertake the Ph.D.

I would like to put on record my heartfelt and sincere gratitude to my research guide **Dr. Sanjay Sharma**, Professor and Head, Electronics and Communication Engineering Department, Thapar University, Patiala. I feel bound to be grateful to my guiding soul for his valuable support, advice, and encouragement.

I am honour bound and profoundly thankful to the doctoral committee members **Dr. Sanjay Sharma**, Professor and Head of Department, Electronics and Communication Engineering Department, Thapar University, Patiala, **Dr. Rajesh Khanna**, Professor, Electronics and Communication Engineering Department, Thapar University, Patiala, and **Dr. Amit Kumar Kohli**, Associate Professor, Electronics and Communication Engineering Department, Thapar University, Patiala, for their consistent help.

I would like to extend special thanks to my colleagues and friends **Dr. Rajeev Ratan** and **Mr. Deepak Batra** for their valuable suggestions, support, and encouragement. It is great privilege to express my profound thankfulness, deep love, and fondness to my wife **Ruchi** and my children **Lavanya** and **Bhavya**, who stood like a rock in my difficult times. Their love, patience, persistent encouragement, and good virtuous understanding enabled me to complete the research work successfully.

Finally, I will remain obligated to and filled with appreciation towards my parents for their love, affection, sacrifices, perseverance, and prayers all through my life.

Dharmvir Jain

TABLE OF CONTENTS

CHAPTER 2

MULTILEVEL CODING AND SPACE-TIME TRELLIS CODING

CHAPTER 3

IMPROVEMENT IN PERFORMANCE OF MLSTTCs AND GMLSTTCs BASED ON DYNAMIC COMPONENT CODE SELECTION

CHAPTER 4

IMPROVEMENT IN PERFORMANCE OF GMLSTTCs BASED ON ADAPTIVE GROUPING OF TRANSMIT ANTENNAS

CHAPTER 5

IMPROVEMENT IN PERFORMANCE OF AGMLSTTCs BASED ON BEAMFORMING AND DYNAMIC COMPONENT CODE SELECTION

LIST OF FIGURES

LIST OF TABLES

ACRONYMS AND ABBREVIATIONS

1G	:	First Generation
2G	:	Second Generation
3G	:	Third Generation
4G	:	Fourth Generation
AGMLSTTCs	:	Adaptively Grouped Multilevel Space-time Trellis Codes
AWGN	:	Additive White Gaussian Noise
BER	:	Bit Error Rate
BICM	:	Bit-Interleaved Coded Modulation
CDMA	:	Code Division Multiple Access
CSI	:	Channel State Information
DSTC	:	Distributed Space-Time Coding
DSTTCs	:	Dynamic Space-time Trellis Codes
DTPA	:	Dynamic Transmit Power Allocation
FEC	:	Forward Error Correcting Codes
FER	:	Frame Error Rate
GMLDSTTCs	:	Grouped Multilevel Dynamic Space-time Trellis Codes
GMLSTTCs	:	Grouped Multilevel Space-Time Trellis Codes
GSM	:	Global System for Mobile Communications
HCM	:	Hybrid Coded Modulation
LST	:	Layered Space-Time
MIMO	:	Multiple-Input Multiple-Output
MLC	:	Multilevel Coding
MLDSTTCs	:	Multilevel Dynamic Space-time Trellis Codes
MLSE	:	Maximum Likelihood Sequence Estimation
MLSTTCs	:	Multilevel Space-time Trellis Codes
MRC	:	Maximal Ratio Combining

MRM	:	Multi-Resolution Modulation
MSED	:	Minimum Squared Euclidean Distance
PDF	:	Probability-Density Function
PEP	:	Pair-Wise Error Probability
PSK	:	Phase Shift Keying
OFDM	:	Optical Frequency Division Multiplexing
OSTBC	:	Orthogonal Space-Time Block Codes
QAM	:	Quadrature Amplitude Modulation
QOSTBCs	:	Quasi Orthogonal Space-time Block Codes
QPSK	:	Quadrature Phase Shift Keying
RAS	:	Receive Antenna Selection
RSTTC	:	Recursive Space-Time Trellis Code
SISO		Single-Input Single Output
SM	:	Spatial Modulation
SNR	:	Signal-To-Noise Ratio
SOSTBCs	:	Super-Orthogonal Space-Time Block Codes
SOSTTCs	:	Super-Orthogonal Space-Time Trellis Codes
SP-MLC	:	Sphere-Packed Multilevel-Coded
STBCs	:	Space-Time Block Codes
STCS	:	Space–Time Code Selection
ST-MLCs	:	Space-Time Multilevel Codes
ST-MSD	:	Space-time Multistage Decoder
STTCs	:	Space-Time Trellis Codes
TAS	:	Transmit Antenna Selection
TCM	:	Trellis Coded Modulation
UMTS	:	Universal Mobile Telecommunications System
VBLAST	:	Vertical Bell Laboratories Layered Space-Time

WAGMLDSTTCs	:	Weighted Adaptively Grouped Multilevel Dynamic Space Time Trellis codes
WAGMLSTTCs	:	Weighted Adaptively Grouped Multilevel Space-time Trellis codes
WCDMA	:	Wideband Code Division Multiple Access
WiMAX	:	Worldwide Interoperability for Microwave Access
WMLSTTCs	:	Weighted Multilevel Space-Time Trellis Codes
WSTTCs	:	Weighted Space-time Trellis Codes

CHAPTER 1

INTRODUCTION BASED ON LITERATURE REVIEW

1.1 INTRODUCTION

The evolution of wireless communication started in 1880's with the transmission of electromagnetic waves through air. Since then a phenomenal growth in wireless communications has been unveiled. With the convenience of mobile communications and ease of deployment of systems without wires, wireless communication has enjoyed explosive growth since the 1990s', and it is now an essential part of our daily life. The desire to communicate from anywhere at any time has increased the demand for high speed and reliable communication. There has been tremendous increase in number of electronic devices such as laptops, tabs, mobile phones, high resolution digital cameras, and wireless local area networks for homes and businesses, etc. These devices are having capability to process large amounts of data at high speed. As a result, there has been substantially increase in requirement of data transmission techniques that can provide not only high data transmission rate but also provide reliable communication with minimum errors.

The wireless communication systems have evolved and developed with increase in requirement of data transmission at high data rate. The first generation (1G) wireless systems came in early 1980's to offer mainly speech related services. Due to limitations in analog techniques of 1G wireless systems, second generation (2G) systems evolved which employed digital protocols such as global system for mobile communications (GSM), code division multiple access (CDMA), and other digital signal processing techniques for transmission of data. Most of the cellular networks, that provide services such as voice communication, image, and text messaging, are based on 2G techniques.

Envisioning providing multimedia communications, third generation (3G) wireless systems such as universal mobile telecommunications system (UMTS) and wideband code-division multiple access (WCDMA) are characterized by maximum data rates of up to 2 megabits per second. These systems are currently employed in more than 195 countries with more than 850 million end users. 3G finds application in wireless voice telephony, mobile Internet access, video calls, and mobile TV.

The demand for broadband wireless access is increasing with the explosive growth of the internet services. The aim of fourth generation (4G) is to provide data rates greater than 100 megabits per second and higher reliability in wireless communication. A 4G system, in addition to the usual voice and other 3G services, provides mobile ultra-broadband internet access to laptops with USB wireless modems, smartphones, and other mobile devices at the speed of more than 100 megabits per second. Reliable transmission with high peak data rates is expected to be 1 gigabits per second or even higher for 4G systems and systems beyond 4G. Thus, there is a two-part challenge for the design engineers of wireless systems: one is to increase the data rates with less number of errors, and other is to improve power and bandwidth efficiency of the wireless systems.

The wireless communication channel is random and unpredictable by its nature. Due to this nature, channel error rates over the wireless channel are more than channel error rates over a wired channel. The signal propagating through free space is attenuated due to absorption, reflection, and scattering of signal by objects in the environment. The relative movements of objects and mobile devices are other causes of severe attenuation of the signal. These attenuations in the signal substantially decrease the strength of the signal which results in an increase in errors and therefore degrades the performance of the wireless systems significantly.

A number of promising solutions have been generated by the research community to

improve the performance of wireless systems by mitigating the effects of the multipath fading. The effects of fading can be substantially mitigated by using diversity techniques. Three prominent forms of diversity techniques exploited for fading channels are: temporal diversity, spectral diversity, and spatial diversity. It has been found that the spatial diversity can be explored in the wireless systems by employing multiple transmit and multiple receive antennas. Multiple-input multiple-output (MIMO) systems have been designed that use spatial diversity by employing the multiple antennas both at transmitter and receiver to provide significant improvement in the channel capacity and error performance without increasing the power consumption. For instance, the transmit antennas in MIMO systems are useful for increasing the antenna gain, reducing the transmit power, and suppressing the interference.

A promising method to provide spatial diversity and achieve high spectral efficiency with minimum errors is space-time coding. Space-time trellis coding, a family member of space-time coding, is based on spatial diversity and finds its application in the cellular communications and in most of the wireless networks. A main issue in space-time trellis coding is large redundancy and exponential increase in complexity at high spectral efficiency.

Multilevel coding (MLC) is a transmission scheme that is used in the wireless communication systems to achieve high spectral efficiency. In spite of the advantages of improving the spectral efficiency, multilevel signals are not reliable because the multilevel signals are easily distorted by channel noise. Therefore, the multilevel coding requires an error-correcting scheme to make the multilevel signals immune to the channel noise and therefore, to provide reliability in the data transmission.

Thus, there was a strong need for a transmission scheme which can provide benefits of the multilevel coding and the space-time trellis coding without having the

disadvantages of the multilevel coding and the space-time trellis coding i.e. a transmission scheme that can provide high data rate, low error rate, and has manageable complexity.

1.2 MOTIVATION FOR RESEARCH

Although, space-time trellis codes (STTCs) have been designed to substantial improve the diversity, data rate, and coding gain, but there is an exponential increase in the complexity of STTCs at high data rates. Generally, design criterion for STTCs needs a vigorous computer search. The search space for the computer search increases exponentially with increase in the size of the constellation. The search space also increases with increase in number of states and the number of transmit antennas. Due to this, practically design engineers are reluctant to use large size constellations in STTCs to provide high data rate transmission.

Although, multilevel coding has been designed to significantly increase the spectral efficiency, but the multilevel signals have a disadvantage that they are easily corrupted by noise in the communication channel. Therefore, the multilevel signals are combined with different error-correcting schemes to provide reliable communication at high data rates.

Grouped multilevel space-time trellis codes (GMLSTTCs) have been designed based on the combination of multilevel coding and STTCs. GMLSTTCs provide not only improvement in spectral efficiency, coding gain, and diversity gain, but also linear increase in the complexity at high data rate in comparison to exponential increase in the complexity in STTCs. This scheme considers channel state information (CSI) at the receiver only which limits the performance of GMLSTTCs. GMLSTTCs use predefined antenna grouping, static component codes, and equal power allocation to the transmit antennas. Therefore, there was requirement of a transmission scheme which can use CSI at the transmitter to improve the performance of GMLSTTCs.

In this thesis, the primary aim is to design and analyse an efficient transmission scheme using STTCs, MLC, and CSI at the transmitter for providing high spectral efficiency and better error performance with low complexity. The main purpose of the presented work is to analyse the use of CSI at the transmitter for dynamic selection of component codes for multilevel coding, dynamic allocation of power to transmit antennas, and adaptive grouping of transmit antennas. In order to design the efficient transmission scheme, a detailed literature survey was carried out to investigate the different multilevel coding schemes, space-time coding schemes, and effects of the CSI on different coding schemes.

1.3 MULTILEVEL CODING

Forward error correcting codes (FEC) [1] are widely used in digital communication systems for reliable transmission of information on various communication channels. However, the forward error correcting codes have a code rate less than 1bit/s and thereby the spectral efficiency is less than 1 bit/dimension for the systems using the forward error correcting codes. With the growth in the demand for high data rates, there was requirement for data transmission techniques that can provide high spectral efficiency in the limited available bandwidth.

Coded modulation, founded in 1974 by Messey [2], is a highly efficient transmission technique for improving the error performance, coding gain, and spectral efficiency of a digital communication scheme. The coded modulation combines the modulation and coding to achieve the coding gain without reducing the data rate or without compromising with the bandwidth efficiency. In late 1970s, Ungerboeck and Csajka [3] in their pioneering work extended Messey’s thoughts to design a powerful coded modulation technique by combining the modulation and channel coding using a trellis code. Since, Ungerbock's coded modulation was of trellis nature, this scheme was referred to as trellis

coded modulation (TCM).

At the same time Imai and Hirakawa [4] in their seminal work presented another powerful coded modulation technique named as multilevel coded modulation in which each individual bit is protected using a different binary error correcting code. Each binary error correcting code is mapped to M_{ary} signal constellation to provide flexible data rate.

Both of these schemes are based on the constellation partitioning to optimize Euclidean distances between the codewords as compared to Hamming distances dealt in the classical coding schemes. Both the schemes have showed that the combination of the modulation and the channel coding results in high data rate and high coding gain in comparison with other coding schemes.

Specifically, in Ungerboeck's TCM [3], [5]-[7], a signal constellation is partitioned into a plurality of subsets in such a way that the distance between the subsets is maximized. A TCM encoder splits the binary symbols into least significant binary symbols and most significant binary symbols which are encoded using different error correcting codes. The minimum Euclidean distance between coded symbols is maximized using an exhaustive computer search. Forney et al. [8], and Calderbank and Mazo [9] further contributed to the development and improvement of TCM technique since Ungerboeck's seminal work.

Originally, the Ungerboeck's approach of constellation partition was designed for one dimensional signal constellation only. Calderbank and Sloane [10] generalized the partitions of the one dimensional signal constellation to partitions of the multidimensional signal constellation sets. The authors presented partitioning of the multidimensional signal sets into multiple levels and mapping a coset code to each level. A lot of work on TCM e.g. in [11], [12] have been presented for further improving the coding gain of TCM and showing that the deficiencies of FEC can be overcome by TCM.

Research community performed a lot of work to combine the signal constellation of higher dimensions with error correcting codes to provide flexible data transmission rates using TCM. Imai and Hirakawa [4] introduced the concept of multilevel coding using several error-correcting codes that can provide flexible data transmission rates and improve the bandwidth efficiency over the additive white Gaussian noise (AWGN) channel.

In the multilevel coding technique, the modulation and error correcting codes are combined using a set of simple component codes to construct a complicated code. The input data stream is partitioned in a plurality of sub-streams which are encoded using respective error correction codes to generate the simple component codes. Each simple component code is mapped to the channel symbols from a predetermined signal constellation for transmission over the communication channel. The channel symbols are selected by partitioning the predetermined signal constellation successively into subsets until the subsets contain a single constellation point.

Motivated by Imai and Hirakawa, Ginzburg [13] extended the multilevel coding to multiple dimensions by employing a group of component codes on the multi-dimensional signal constellation. Ginzburg presented hierarchical partitioning of the signal constellation in the subsets so that distance between the subsets is optimum. The results presented by Ginzburg showed that use of the multi-dimensional signal constellation provide better performance than using the single dimensional signal constellation in multilevel coding.

Biglieri and Elia [14] and Sayegh [15] implemented the approach of partitioning the multi-dimensional signal constellations using trellis codes and block codes respectively as component codes for different levels. Tanner [16] elaborated the multilevel coding schemes by mixing the block codes and convolutional codes in the different levels. As a

special case, Duan et al. [17] presented a multilevel coding scheme by mapping each encoder output to an independent signal constellation to achieve the capacity of the AWGN channel. Ma and Ping [18] extended the scheme of Duan et al. [17] by using different power-allocation strategies in decoding to improve the bandwidth efficiency.

Imai and Hirakawa [4] suggested a suboptimal multistage decoding for decoding the multilevel signals. In multilevel coding as discussed in [4] and [19]-[21], the transmission channel is split into several logical sub-channels based on the size of the underlying signal constellation. Therefore, a multistage decoder presented in [21] can be used to decode the component codes at each level. In the multistage decoder, the decoded output of first stage is passed to the next stage for decoding of the subsequent component code. The main advantage of the multistage decoder over the maximum likelihood decoder is that the complexity of the multistage decoder is proportional to sum of the decoding complexity of each component code instead of the product as in the maximum likelihood decoder.

The conventional multistage decoding [21] involves sequentially passing output from the first stage decoder to the next stage decoder and so on. For component codes that do not achieve the channel capacity of the levels, the error correcting capability of the multilevel codes may not be fully exploited with the conventional multistage decoding. The main drawback in the conventional multistage decoding is the worst performance of the first level because it is decoded without any side information from all the other levels.

This drawback can be overcome by introducing iterative multistage decoding which is presented by Isaka and Imai in [22]. In the iterative multistage decoding, reliability information is passed to the decoders at all subsequent levels and to at least decoders on some previous levels instead of only passing the output of the decoder at the current stage to decoders on subsequent levels. A significant improvement in performance is achieved

by using the iterative multistage decoding in comparison with the conventional multistage decoding.

Bit-interleaved coded modulation (BICM) [23], [24] is one of the techniques which compete with multilevel coding. BICM is designed by combination of the binary error correcting codes and modulation by partitioning the signal constellations in a single level. BICM uses a single stage of decoding in comparison with multiple stages of decoding as in MLC.

The bit-wise interleaving idea was first investigated by Zehavi [23] to improve the diversity of coded modulation using bit-wise interleaving at the output of the encoder and using an appropriate soft-decision bit metric at input of the decoder. Based on Zehavi's findings, Caire et al. [24] presented a comprehensive information theoretical performance analysis of BICM and showed that the separation of the modulation and coding by the bit-wise interleaving increases code diversity in comparison with TCM.

The major drawback of BICM in comparison with MLC is the loss of data rate. This rate loss in BICM can be recovered by using Gray mappings [18] and iterative decoding [22]. The limitation of the Gray mapping is that it does not work in some fading channels and the importance of the Gray mapping is lost when the Euclidean distance of signal points are dependent on the channel characteristics. In such scenarios, multilevel coding provides much better performance than BICM. The examples of such scenarios are MIMO signaling presented in [25], [26], free space optical communications using the pulse modulation techniques [27], and decoders using frequency-shift keying [28].

A variety of design criteria have been proposed for designing the multilevel codes. These design criteria are used for selecting the component codes. Out of these criteria, two majorly used criteria are distance based criteria [4], [19]-[21] and capacity based design criteria [20], [29], [30]. A balanced distance design rule presented in [4] is based

on the minimum squared Euclidean distance (MSED) between the constellation points. The balanced distance design rule is used to choose component codes for all levels such that the MSED is maximized. The maximization of MSED based on the balanced distance rule results in equal protection for all the constellation points and helps in achieving a significant coding gain.

The capacity based design rule states that for the desired signal-to-noise ratio (SNR), the component code at level *l* should be selected based on the equivalent channel capacity of the level *l*. The capacity design rule provides a superior estimation of the optimal component code at each level of multilevel coding than the balanced distance rule. Another design criterion for designing the multilevel codes is the error probability rule [22]. The aim of this rule is that all levels should equally contribute to the total bit error rate (BER). This rule can be applied for designing the multilevel codes for AWGN channel and other fading channels.

Several constellation partitioning techniques have been presented in [20] and [31]-[33] for multilevel coding. The set partitioning presented by Ungerboeck aims to partition the constellation such that minimum Euclidean distance increases with each level of partitioning. This set partitioning has two major drawbacks: first is the decoding of first level is associated with a large number of nearest neighbors which results in high BER and second is that this set partitioning provides poor coding gain.

In block partitioning [34], the constellation points in first level are divided in two groups, on left and right of the y-axis. In the second level of partitioning, the constellation points in each group are divided into subgroups, above and below the x-axis. This partitioning continues until each subgroup has one constellation point. The block partitioning is in contrast with the set partitioning as the number of nearest neighbors in block partitioning is minimized at the cost of intra-set distance.

Hybrid partitioning [34] is a combination of the set partitioning and the block partitioning in which first level is partitioned based on the block partitioning and the subsequent levels are partitioned based on the set partitioning [35], [36]. Another partitioning technique is the coset partitioning [37], [38], presented by G.D. Forney in 1988, which is based on Ungerboeck's set partitioning to eliminate the exhaustive search required to find the best component codes.

The tradeoffs for designing good multilevel codes involve number of points in the underlying signal constellation, scheme used for partitioning the signal constellation, number of levels in which the signal constellation is partitioned, distance between the signal points, type of component codes, and code rates at each level. These tradeoffs are selected to provide desired error performance, data rate, and decoding complexity.

In comparison with Ungerboeck's TCM, the multilevel coding scheme decouples the code rate from dimensionality of signal constellation to provide flexible data transmission rates. The benefits of multilevel coding are high data transmission rates, improvement in the received SNR, significantly low error rates, and mitigation of co-channel-interference. The design flexibility provided by the multilevel coding is that any type of codes can act as component code in multilevel coding. Examples of such codes are trellis codes, convolutional codes, or block codes.

1.4 SPACE-TIME CODING

Spatial diversity is a prevalent technique used in the wireless systems. The spatial diversity is implemented by arranging multiple antennas in space in such a way that the distance among the antennas is large enough so that signals transmitted or received are uncorrelated. The separation among the antennas changes based on height of the antennas, frequency of the transmitting signal, and propagation environment. Generally, the antennas are required to be separated by a minimum number of wavelengths to avoid

correlation among the signals.

The spatial diversity is classified in two categories as receive diversity and transmit diversity. In receive diversity [39], [40], the multiple antennas are used at the receiver to receive the replicas of the transmitted signals and to mitigate the effects of the channel fading. In spite of advantages of the receive diversity, it is very difficult to install multiple antennas at the mobile devices because the mobile devices are required to be small, portable, and inexpensive. Therefore, it is preferred that the transmitter should have the multiple transmit antennas. As a result, the demand of transmit diversity schemes [41], [42] grew at fast rate to increase the spectral efficiency and error performance of the wireless fading channels.

Pioneering works by Winters [43], Foschini [44], and Telatar [45] have shown remarkable increase in the spectral efficiency for wireless systems using the transmit diversity and receive diversity. Under the rich scattering environments [46] with independent transmission paths, a MIMO system with N_R receive antennas and N_T transmit antennas provide an increase in spectral efficiency by a factor of min (N_R; N_T) in comparison with a system with one receive antenna and one transmit antenna.

The advantages of using the multiple transmit and receive antennas are because of two effects. One is the diversity gain since it reduces the chances that there is a deep fading of signals transmitted by several antennas simultaneously. The other is beamforming gain obtained by combining signals from different transmit antennas to achieve a high SNR. The multiple antennas at the receiver and transmitter introduce a new dimension of space on top of the conventional time dimension at the transmitter. This triggers tremendous research interests on multi-dimensional coding schemes for MIMO systems, which are generally referred to as space-time coding schemes.

Originally, the space-time coding was proposed by Tarokh et al. [47] in 1998 in their

popular work by designing codes over both time and space dimensions. The space-time coding is performed by combining the coding, modulation, and spatial diversity using the multiple transmit and receive antennas. The space-time coding provides improvement not only in the diversity gain but also in the coding gain without forfeiting the bandwidth.

Tarokh et al. in their original work devised well-known criteria for designing and governing the performance of the space-time codes. These design criteria are referred to as rank and determinant criteria. The rank criterion states that the maximum diversity gain can be attained by maximizing the minimum rank of a code distance matrix, while the determinant criterion states that the maximum coding gain can be achieved by maximizing the minimum determinant of the code distance matrix. Following Tarokh's work, much research efforts have been made to develop powerful space-time codes [48]-[54] using different design criteria and improved algorithms.

The family of space-time codes includes STTCs [48]-[52] and space-time block codes (STBCs) [53]-[54]. In STBCs, the encoding and decoding processes are performed for blocks of transmission symbols. The beauty of STBC is its simplicity, i.e. it can provide full diversity with a linear maximum-likelihood decoding.

Alamouti in [55] presented first space-time block coding scheme. Alamouti presented a basic two transmit antenna diversity scheme which has a remarkably low decoding complexity. The performance of CDMA systems based on Alamouti scheme was evaluated in mobile fading channels by Zhu et al. [56]. Because of the simplicity in the structure of STBCs, WCDMA and CDMA-2000 standards and fixed point digital signal processing [57] have been implemented using STBCs.

Tarokh et al. [54] extended the Alamouti scheme for more than two antennas at the transmitter by designing orthogonal space-time block codes (OSTBCs). OSTBCs are characterized by a code matrix whose columns are orthogonal to each other. OSTBCs are

popular for providing full transmit diversity and low decoding complexity. It has been shown in [54] that the systems using more than two transmit antennas and real signal constellations, OSTBCs can provide full rate. While for the systems using the complex signal constellation, OSTBC can provide full rate for two transmit antennas only.

Tarokh's work in [54] was extended by Su et al. [58] by presenting modified OSTBCs to provide full rate for the systems using the complex signal constellation and random number of the transmit antennas. Research community further improved OSTBCs in [59]-[62] and presented different methods for analyzing the performance of OSTBCs. In an example, the performance analysis of OSTBCs based on the channel capacity was presented in [61] and in another example, closed form of the pair-wise error probability (PEP) of OSTBCs for different fading channels was presented in [62].

The perfect orthogonality concept in OSTBCs was relaxed by another type of STBCs referred to as quasi orthogonal space-time block codes (QOSTBCs) [63]-[66]. QOSTBCs are designed for the systems having more than two transmit antennas to provide higher data rates than OSTBC but at the expense of increased decoding complexity. It has been shown that concatenating OSTBCs with convolutional codes, turbo codes, and trellis code [67] can further improve the performance of the OSTBCs.

Another family member of STBCs is super-orthogonal space-time block codes (SOSTBCs) [68]-[72] which can provide full diversity and coding gain. The coding gain in SOSTBCs is achieved by integrating trellis codes with space-time block codes. However, this integration results in reduction of data rate.

A number of other families of STBC have been also proposed for improved performance. For example, square matrix embeddable STBCs [73] are based on a square matrix of a complex symbol constellation. The simulation results have shown that that the coding gain of these codes increases exponentially with increase in the number of

transmit antennas. Another family member called algebraic STBC [74], [75] provides the full diversity and uses the sphere decoding [76] for providing low decoding complexity.

In this thesis, the main concentration has been focused on using STTCs [47] [77], [78] which are designed based on combination of the modulation, spatial diversity, and error control coding to mitigate the fading in the wireless channel. In this scheme, the information and redundant symbols are distributed to a set of transmit antennas in different time intervals to achieve correlation between the temporal and spatial dimensions. STTCs provide not only a substantial improvement in the diversity gain and spectral efficiency but also offer the coding gain for the signals transmitting over the wireless fading channels.

So far, there has been a lot of research to develop different design criteria for STTCs. Tarokh et al. [47] proposed the well-known design criteria, referred to as rank and determinant criteria, for minimizing the upper bound of PEP. The rank and determinant criteria is mostly used at high SNR for the systems having a small number of receive antennas. The rank criterion states that the maximum diversity gain is achieved by maximizing the minimum rank of a code distance matrix, while the determinant criterion states that the maximum coding gain is achieved by maximizing the minimum determinant of the code distance matrix.

Alternatively, the Euclidean distance criterion was presented by Chen et al. in [78], which states that the minimum squared Euclidean distance of the code distance matrix can be used to design the optimum STTCs. The Euclidean distance criterion is used when the diversity gain is more than four. It was further found by Tao and Cheng [79] that the Euclidean distance criterion should be used at moderate and low SNR for the systems having large number of receive antennas.

All the different design criteria derived for STTCs aim to optimize diversity gain and

coding gain. It has been shown that these design criteria are dependent on a number of parameters such as the number of antennas at the transmitter and receiver, cardinality of the employed modulation scheme, and whether a computer search is required to design the optimum STTCs. Based on these popular design criteria, several powerful STTCs [80], [81] have been designed using different computer search techniques.

To simplify computer search complexity, some systematic code design algorithms have been proposed. Banerjee and Agrawal [77] presented simple design rules to construct a generator matrix for designing STTCs for arbitrary number of transmit antennas. In their seminal work, they showed the reduction in the code search complexity to a large extent.

Although, Tarokh et al. [47] proposed the performance analysis of STTCs by minimizing the upper bounds of the PEP, several tighter bounds of PEP [82]–[85] and exact PEP [86], [87] were also presented in the research onwards.

Generally, the design criteria for STTCs in the quasi-static channels are different than the design criteria for STTCs in the rapid fading channels. Although STTCs designed for the rapid fading channels are few, the performance analysis of STTCs in rapid fading channels has attracted lots of research interests. Some of the design criteria for designing STTCs for the rapid fading channel have been presented in [88]-[91].

Liao and Prabhu [92] presented improved design criteria for STTCs in fast fading channels using a union bound analysis and showed that the performance of STTCs in the fast fading channels, at high SNR, is governed primarily by symbol Hamming distance, while the performance of STTCs in the fast fading channels, at the low SNR, is governed by the minimum Euclidean distance.

Another family of space-time coding is distributed space-time coding (DSTC). DSTC [93]-[97] has been presented for cellular mobile devices and ad hoc mobile networks

where practicality of using the multiple antennas is not possible. DSTC utilizes cooperative diversity as a substitute of multi-antenna transmission schemes for optimizing the spectral and power efficiency of wireless systems. In the cooperative diversity, the source nodes transmit the signals to partner nodes which further relay the signals to other partner nodes. Distributed space-time codes are designed by rank and determinant criteria [47] by making the code distance matrix delay tolerant. The PEP for distributed space-time codes have been analyzed in [98]-[101] and it was found that the performance of DSTC depend on a metric similar to the Euclidean distance.

Another class of STTCs is recursive STTC (RSTTC) [102], [103] which serve as an internal code for concatenation with other codes. The main advantage of RSTTCs is that they provide flexible high data rate. The simulation results showed that the data rate of RSTTCs can be adjusted by varying the number of recursive convolutional codes, the coding rate of each recursive convolutional codes, the modulation scheme, and the number of transmit antenna.

The major limitation of STTCs is that there is an exponential increase in the decoding complexity with increase in the size of constellation. This drawback of STTCs limits the attainable data rates using STTCs. Foschini [44] presented a layered space-time (LST) scheme in which the decoding complexity increases linearly with the increase in data rate. A number of LST architectures have been presented based on the usage of error control coding. For example, vertical Bell Laboratories layered space-time (VBLAST) technique [104] in which the input information sequence is de-multiplexed into sub-streams and each of them is modulated and transmitted from a transmit antenna. It has been shown that the data capacity of the wireless system using VBLAST scheme increases with the increase in number of antennas. Following this, more researches [105]-[107] have exploited the combination of LST coding and other signal processing techniques.

1.5 EFFECTS OF CHANNEL STATE INFORMATION ON SPACE-TIME CODING

Throughout the development of space-time codes, the researchers have focused on the idealistic assumption that the perfect CSI is available only at the receiver. However, practically, the perfect CSI cannot be made available due to errors in the channel estimation. To overcome this problem, either non-coherent detection methods, where no CSI is needed at the receiver, or channel estimation techniques are used to design space time codes.

Non-coherent differential modulation schemes were presented in [108] and [109]. However, it was shown that there is a performance loss with the non-coherent differential modulation schemes. To achieve satisfactory performance with the non-coherent differential modulation schemes, it is required that the channels should remain constant for a sufficient long time duration.

Although the channel estimation techniques are well understood for single-input single-output (SISO) systems [110], however the channel estimation schemes for MIMO systems [111], [112] are difficult to implement because of an additional spatial dimension required for estimation of channels for MIMO systems. In addition to the difficulties of MIMO channel estimation, the performance analysis and code design of STTCs over MIMO systems with channel estimation errors are even more challenging. The performance analysis of STTCs with imperfect channel estimation of the quasi-static fading channel has been presented in [113] and [114].

The most of the space-time coding schemes mentioned above are for open-loop systems. It has been shown that closed loop systems [115]-[118] which use the CSI at the transmitter provide better performance than open-loop systems. The CSI at the transmitter can be utilized in a number of ways. For example, using the CSI, the transmitter can

employ strategies such as adaptive coding, code selection, beamforming, and transmit antenna selection for providing improvement in the performance of the wireless systems.

1.5.1 Use of CSI at the Transmitter for Antenna Grouping

MIMO wireless communication systems use the multiple antennas at the transmitter and receiver to increase the reliability of the communication, data rate, and spectral efficiency. However, increasing the number of antennas at the transmitter and receiver beyond a particular limit does not improve the performance significantly. Moreover, there will be an increase in the cost and complexity of the systems on increasing the number of antennas. So, this motivates the use of selection diversity in MIMO systems.

Antenna selection [119]-[121] is a powerful signal processing technique used in wireless systems with multiple antennas at the transmitter and receiver. The main advantage of the antenna selection is that it decreases the system cost, reduces the computational complexity, and preserves the diversity of the system. In the antenna selection technique, a subset of antennas is optimally selected from a large number of antennas. An exhaustive search is performed on all possible combinations of the antennas so that the selected combination provides minimum error.

Two types of antenna selection criteria have been presented for selecting the antennas in MIMO systems. First one is capacity based criteria [122]-[124] in which the antennas that maximize an upper bound of channel capacity are selected. The second one is performance based criteria in which the antennas that maximize the SNR of the received signals [119] and minimize the error probability [125] are selected.

The selection of antennas can be performed at both the receiver and the transmitter. In receive antenna selection (RAS) [126]-[130], a subset of the receive antennas are selected at the receiver to reduce the number of radio-frequency chains required at the receiver, thereby, saving the cost of the system significantly. In transmit antenna selection (TAS), a

subset of the transmit antennas that provide best performance in the wireless fading channel is selected for transmission of the signals. RAS is an open-loop scheme whereas TAS is a closed loop scheme performed based on feedback from the transmitter.

A single transmit antenna selection scheme using maximal-ratio combining (MRC) has been presented in [131] and [132] to maximize the SNR at the receiver. Another scheme referred to as the TAS/STBC scheme [133], [134] in which two transmit antennas that maximize the SNR at receiver, are selected for transmission of STBCs. Similarly, in TAS/STTCs scheme [135], two transmit antennas which maximize the SNR at the receiver are selected for transmission of STTCs.

Narasimhan [136] presented an antenna selection scheme in which a subset of transmit antennas is selected for VBLAST systems operating in correlated wireless fading channels. Narasimhan presented that for a given spectral efficiency, the transmit antennas and the signal constellations are selected to maximize the SNR at the receiver. Narasimhan further presented that for a given SNR, the transmit antennas and signal constellations can be selected to maximize the data rate.

Yuan [137] assumed partial CSI at the transmitter for adaptive selection of a number of transmit antennas, and their corresponding space-time codes for transmission. Yuan further derived criteria for minimizing the probability of error for the space-time coded system with adaptive antenna selection over slow Rayleigh fading channels.

Tarokh et al. [138] presented grouping of the transmit antennas by partitioning available transmit antennas into smaller groups to increase the data rate over wireless channel. Each group of transmit antennas transmits a separate space-time code which is decoded by using a linear array processing technique and suppressing the signals transmitted by other groups of the transmit antennas. This grouping of transmit antennas for space-time coded systems improves the reliability and increases the data rate for the

signals transmitting over the wireless fading channels.

Another antenna grouping technique was presented by Huang et al. [139] in which the transmit antennas are adaptively grouped by selecting the optimum transmit antennas according to the CSI. The antenna grouping is determined at the receiver and an index from a predetermined codebook is sent to the transmitter for grouping the transmit antennas. The main advantage of this antenna grouping is that it requires a very small amount of feedback and therefore, the grouping is performed with minimal complexity. Adaptive modulation [140], [141] and beamforming [142]-[146] in combination with antenna grouping are other key areas of research which are utilized for increasing the data rates and decreasing the error rates of wireless communication systems.

1.5.2 Use of CSI at the Transmitter for Beamforming

Beamforming is a signal processing technique for providing directional transmission or reception of the signals. It is achieved by multiplying the signals with beamforming coefficients to adjust the magnitude and phase of the signals in such a way that the signals in particular direction experience constructive interference while other signals experience destructive interference. Hence, the beamforming emphasizes the signals in a particular direction while attenuates the signals in other directions. It has been shown that the beamforming improves the spectral efficiency, decreases the outage probability, and improves the error performance.

Many different beamforming techniques have been presented for different wireless systems that use different coding techniques. For example, the beamforming techniques for uncoded systems have been presented in [142]-[146] while beamforming techniques for the space-time coded systems have been presented in [147]-[153]. The beamforming techniques for the space-time coded systems are mainly implemented using CSI at transmitter. The combination of STBCs and the beamforming presented in [147]-[150]

has shown that diversity gain and beamforming gain can be achieved by using the beamforming.

The application of beamforming has been extended to STTCs and it has been shown that the optimum allocation of power at the transmit antennas can be done by using the CSI at the transmitter. However, implementation of the beamforming strategies for STTCs using the CSI is not straightforward and presents a number of challenges. The design of adaptively weighted space-time trellis codes [154] has been presented by combining the STTCs with a beamforming scheme using the CSI at the transmitter. It has been shown that these codes provide significant improvement in the coding gain.

The dynamic allocation of the transmit power across two transmit antennas has been presented in [155] based on the partial CSI at the transmitter. However, the beamforming coefficients in [155] are not optimal for a large number of states and more than two transmit antennas.

Santoso et al. [156] extended this work and presented a novel beamforming strategy for an arbitrary number of transmit antennas. Santoso et al. designed STTCs with dynamic transmit power allocation (STTCs/DTPA) using the partial CSI at the transmitter. In this strategy, the transmitter selects the two best transmit antennas and dynamically distributes power among the selected two transmit antennas. The simulation results have shown that a high diversity order, optimum coding gain, and weighting gains can be achieved using STTCs/DTPA with minimum decoding complexity at the receiver.

Li et al. [157]-[159] presented the performance analysis of weighted STTCs (WSTTCs) for fast fading channels. Li et al. proposed a new design criterion and presented an improved PEP upper bound for WSTTCs. The simulation results have shown that WSTTCs attain not only the full diversity order and significant coding gain but also improve the SNR at receiver in comparison to the standard STTCs.

1.5.3 Use of CSI at the Transmitter for Code Selection

The primary motivation of using the antenna selection in MIMO systems was a strong necessity for increasing the diversity, coding gain, and reducing the hardware cost. However, the main limitation of the antenna selection techniques is that the space time codes remain same and do not change with the CSI. Recent research has emphasized on the selection of space-time codes to further optimize the performance of space coded systems.

Mavares et al. [160] presented a space–time code selection (STCS) scheme which selects the space-time codes for the selected antennas based on the comparison of equivalent SISO channel envelopes with a set of predefined threshold levels. Using this code selection scheme, the transmission of space-time codes is adapted to the CSI at the receiver. This code selection scheme has shown an improvement in the performance at the cost of marginal increase in the decoding complexity.

Liu and Jafarkhani [161] presented selection of inner codes for concatenation with outer codes using the channel phase feedback at the transmitter. This code selection scheme is easy to implement with low decoding complexity and provides an improved peak to average power ratio at the receiver.

Celebi et al. presented a STBC selection method [162] in which full rate balanced STBCs are selected using partial CSI at the transmitter. This STBC selection approach increases SNR at the receiver in comparison to Alamouti's scheme with the antenna selection. An adaptive selection of STBCs [163] based on the perfect CSI has shown increase in the received SNR at the destination. Ginige et al. [164] presented dynamic code selection technique to optimize peak-to-average-power ratio of a CDMA system.

Blanz and Schotten [165] presented dynamic space-time coding in which a codeset having optimum generator sequences is selected that matches best with current CSI at the

transmitter. Teran et al. [166] presented a constant-rate space-time code selection technique in which the selection of both the space-time codes and the number of transmit antennas is performed using four bits of the feedback information. The simulation results have shown that this technique increases the spectral efficiency with a slight reduction in performance. The major advantage of this code selection technique is that it makes BER performance almost independent of the relative velocity between the transmitter and the receiver.

1.6 COMBINATION OF MULTILEVEL CODING AND SPACE-TIME CODING

Tarokh et al. in their inspirational work [47] initially presented producing powerful and high data rate space-time codes using the combination of multilevel coding with space-time codes. A multilevel coding scheme is presented using a 8-phase shift keying (PSK) signal constellation and three transmit antennas to provide a data rate of 5bit/s and diversity order of two. The encoding of the information bits is performed by partitioning the 8-PSK constellation into multiple levels and using a simplified decoding at the receiver. However, there is a loss of performance due to the simplified decoding because of magnification of error coefficient in the simplified coding. The drawbacks of this multilevel coding scheme motivated for alternative multilevel space-time coding strategies that can provide high data rates with minimum number of errors.

Since then many strategies [167]-[170] have been presented for combining the multilevel coding and different error correcting codes to improve the data rate and error performance. Lampe [167] presented space-time multilevel coding using a binary partition of two dimensional constellations and using STBCs as component codes for systems having a single transmit antenna and a single receive antenna. Yuan et al. [168], [169] presented the concatenation of MLC with OSTBCs to reduce the errors in Rayleigh fading channel. Both the distance-based and capacity-based approaches were considered

for choosing the component codes.

Woerz and Hagenauer [170], [171] proposed multilevel codes based on the combination of convolutional codes and block codes in the different levels. The multistage decoding was improved by including the reliability information from the previous stages.

Martin et al. [172], [173] proposed space-time multilevel codes (ST-MLCs) using a multi-dimensional constellation partitioning scheme [174]. A $2N_t$ dimensional real constellation was partitioned such that each component code span N_t transmit antennas. A space-time multistage decoder (ST-MSD) was developed to reduce the decoding complexity. Martin et al. further compared the performance of the ST-MLCs with turbo codes and showed that their performance is much superior to turbo codes.

Oruc et al. [175] presented a combination of multilevel coding technique with full-diversity, full-rate super-orthogonal space-time trellis codes (SOSTTCs) for two-transmit and two receive antenna systems over fast Rayleigh fading channels. The simulation results have shown that this scheme provides high coding gains and improvement in error performance in comparison with the conventional SOSTTCs.

Chih [176] presented the construction of multilevel space-time codes by combining several component STBCs with set partitioning of an expanded signal constellation. Tee et al. [177] presented a sphere-packed multilevel-coded (SP-MLC) modulation technique which combines multilevel coding with STBCs to improve the diversity gain. This technique captures time and space diversity using a multi-dimensional sphere packed modulation and maximizes the coding gain by optimally detecting the sphere packed modulated symbols.

Chui and Calderbank [178] and Diggavi et al. [179] presented multilevel diversity embedded space-time codes for parallel MIMO channels (e.g. MIMO-OFDM channels).

It was shown that these diversity embedded space-time codes provide an improvement in diversity and peak SNR for video broadcasting in WiMAX.

Ma [180] presented multilevel space-time codes based on the combination of MLC, STBCs, and spatial modulation (SM). The partitioning of an expanded transmission matrix was presented based on a distance criterion for mapping the component STBCs. It was shown that for the same spectral efficiency and the same space diversity order, the performance of this scheme is much superior to conventional STBC-SM scheme.

Many researchers have also focused on the combination of MLC and STTCs because of the limitations of STTCs. The main limitation of STTCs is an exponential increase in the decoding complexity at high data rate. The complexity of STTCs increases exponentially with increase in the size of constellation, number of transmit antennas, and states in the code trellis. To address these issues, an alternative transmission scheme was required that combines MLC and STTCs to provide high data rate with manageable decoding complexity.

The MLC and STTCs combined in [181] provide a promising alternative to the currently available STTCs, which has advantages of STTCs without having the disadvantages of high complexity. Multilevel space-time trellis codes (MLSTTCs) have been designed by using multiple STTCs as component codes in multilevel coding. MLSTTCs provide not only improvement in spectral efficiency but also improvement in diversity and coding gain.

The spectral efficiency of MLSTTCs has been further improved by GMLSTTCs [182]. GMLSTTCs provide improvement in spectral efficiency of MLSTTCs by transmitting more than one symbol per time slot. The increase in transmission of symbols per time slot is achieved by grouping the transmit antennas and using separate component STTCs for each group of the transmit antennas.

MLSTTCs and GMLSTTCs use CSI at the receiver only. Sharma in his pioneer work [183] presented weighted multilevel space-time trellis codes (WMLSTTCs) designed by combining beamforming and MLSTTCs. In WMLSTTCs, the transmit power is dynamically allocated to the transmit antennas by using the beamforming coefficients that are calculated based on the CSI at the transmitter. The simulation results have shown that the performance of WMLSTTCs is superior to MLSTTCs.

1.7 PROBLEM FORMULATION

The desire to communicate from anywhere and at any time has increased the demand for high speed and reliable data communication. This demand for the high data rate and reliability has made the research in the wireless communications an interesting and challenging field. The spectrum or bandwidth is often limitedly allocated to the service provider and there is a slow increase in the allotment of new spectrum to the service provider. The electronic devices are generally small in size and consume little power to conserve battery life. Thus, the design engineers for wireless systems face a two-fold challenge: one is to increase the data rates with less number of errors and second is to improve power and bandwidth efficiency of the wireless systems.

The main obstacle to accomplish both the challenges is random and unpredictable nature of the wireless channel. The signal propagating through free space is attenuated due to absorption, reflection, and scattering of the signal by the objects in the environment. The relative movement of objects and mobile devices are other causes of severe attenuation in the signal. These attenuations in the signal substantially decrease the strength of the received signal and therefore degrades the performance of the wireless systems significantly.

In order to support high bit rates and good error performance in the fading channels, research efforts have been carried out to develop efficient transmission schemes using

different coding and modulation techniques. Space-time trellis coding is presented as unique coding scheme that integrates channel coding and modulation using transmit diversity and receiver diversity. This scheme provides better performance by improving the data rate and the reliability of communication over fading channels.

In spite of the advantages of STTCs, the design engineers are reluctant to use STTCs in modern high data rate wireless communication systems due to their inherent disadvantages of high complexity at high data rates. Multilevel coding is a technique which has been designed to significantly increase the spectral efficiency, but the multilevel signals have a disadvantage that they are easily corrupted by noise in the communication channel. Therefore, multilevel signals are combined with different error-correcting schemes to provide reliable communication at high data rates.

Multilevel coding when combined with STTCs presented an efficient alternative to STTCs, which provide advantages of STTCs such as improved diversity and coding gain without having the drawbacks of STTCs such as search complexity and decoding complexity. For example, MLSTTCs and GMLSTTCs have been presented to choose any desired balance between code performance, complexity, and throughput.

MLSTTCs and GMLSTTCs consider the CSI at the receiver only and do not consider the CSI at the transmitter. MLSTTCs and GMLSTTCs use predefined component STTCs, static antenna grouping, and equal power distribution across the transmit antennas which limits the performance of MLSTTCs and GMLSTTCs. Therefore, there is a strong need to improve the performance of MLSTTCs and GMLSTTCs using the CSI at the transmitter. In this research work, the efforts have been made to improve the performance of MLSTTCs and GMLSTTCs by dynamic selection of component STTCs, adaptive antenna grouping, and beamforming with the help of CSI at the transmitter.

1.8 RESEARCH OBJECTIVES

In the light of aforementioned aspects, the research objectives for the investigation are as follows:

1. To design optimum dynamically grouped multilevel space-time trellis code for improved performance.
2. To analyze the proposed STTC scheme for quasi-static channel with CSI at the transmitter.
3. To simulate the proposed STTC.
4. To evaluate and compare the performance of proposed STTC with existing STTC.

1.9 THESIS OUTLINE

The thesis will be organized in six chapters. The details of the contents of each chapter of the thesis are as follows

- Chapter one presents introduction, motivation for research, problem formulation, objectives of the thesis, and organization of the thesis. An exhaustive literature survey about the different space-time coding schemes, multilevel coding schemes, and codes designed by combination of multilevel codes and space-time trellis codes has been conducted in this chapter. This chapter describes various techniques and algorithms presented in the literature for code selection, antenna grouping, and transmission weighting for improving the performance of space-time codes.
- Chapter two presents performance evaluation of the existing space-time codes in quasi-static Rayleigh fading channel. This chapter describes the quasi-static Rayleigh fading channel model, generic model for multilevel coding, design and performance analysis of STTCs using the rank and determinant criteria as well as trace criterion.

- Chapter three describes the effect of dynamic code selection on the performance of STTCs, MLSTTCs and GMLSTTCs. This chapter presents design and analysis of DSTTCs using the CSI at the transmitter. A code set selection algorithm is proposed here for the dynamic selection of generator sequences. DSTTCs are applied in the multilevel coding to design MLDSTTCs and GMLDSTTCs. The performance comparison of STTCs vs DSTTCs, MLSTTCs vs MLDSTTCs, and GMLSTTCs vs. GMLDSTTCs is shown by varying the number of receive antennas.
- Chapter four describes the effect of adaptive antenna grouping on the performance of GMLSTTCs. An adaptive antenna grouping algorithm is proposed here for the adaptive grouping of transmit antennas. In this chapter, the emphasis is on design of AGMLSTTCs and performance comparisons of AGMLSTTCs with GMLSTTCs by varying the number of receive antennas.
- Chapter five describes the effect of beamforming on the performance of GMLSTTCs. This chapter presents combination of adaptive antenna grouping and transmission weighting with GMLSTTCs to improve the performance of GMLSTTCs. Here, the focus is on design and analysis of WAGMLSTTCs and performance comparisons of GMLSTTCs, AGMLSTTCs, and WAGMLSTTCs by varying the number of receive antennas. This chapter further presents performance analysis of the codes designed by the combination of GMLSTTCs, dynamic code selection, adaptive antenna grouping, and beamforming.
- Finally, the chapter six sums up the research work. Further, a brief description about the future work/scope has been presented as a motivational seed for the germination of research work. The thesis concludes with the research publications as well as the list of references found useful during the course of investigation.

1.10 SUMMARY OF THE CHAPTER

This chapter acts as a capsule for the motivation of the thesis. An exhaustive literature survey has been presented for the multilevel coding techniques, space-time coding techniques, and the effects of the CSI on these techniques. Based on this, the objectives of thesis have been identified, in which the main motive is to improve the performance of the multilevel space-time coded communication system by using CSI at the transmitter. In the next chapter, the performance of existing space-time trellis codes has been evaluated which will be used for designing the proposed codes.

CHAPTER 2

MULTILEVEL CODING AND SPACE-TIME TRELLIS CODING

2.1 INTRODUCTION

Imai and Hirakawa [4] introduced the concept of the multilevel coding using the several error correcting codes which provide flexible data transmission rates and improvement in bandwidth efficiency of the AWGN channel. In the multilevel coding technique, the modulation and error correcting codes are combined to construct a complicated code. The input data stream is partitioned in a plurality of sub-streams which are encoded using respective encoders to generate the simple component codes. Each component code is mapped to channel symbols from a predetermined signal constellation for transmission over a communication channel. The channel symbols are selected by partitioning the predetermined signal constellation successively into subsets until the subsets contain a single constellation point. The major benefit of employing the multilevel coding technique is that it enables a design engineer to design a flexible system which can provide desired data rate, coding gain, and error performance.

STTCs [47] [78] are designed based on the combination of modulation, spatial diversity, and error control coding to mitigate the fading in the wireless channel. In this scheme, the information and redundant symbols are distributed over time and a set of transmit antennas for achieving a correlation in temporal and spatial dimensions. STTCs provide not only a substantial improvement in diversity gain but also offer coding gain for the signals transmitting over the fading channels. In other words, STTCs improve the reliability and spectral efficiency of communication over the fading channels.

In this chapter, a brief introduction has been provided for multilevel coding of information data stream and decoding of multilevel codes using a multistage decoder. A

comprehensive study and analysis of design criteria for STTCs are presented in this chapter. These design criteria are used to design optimum STTCs for different fading channels. These design criteria are in general formulated by analyzing the expressions for the pair-wise error probability of STTCs. The performance of STTCs adhering to the different design criteria are compared by simulations. This chapter provides the necessary context for the main work in this thesis.

2.2 QUASI-STATIC RAYLEIGH FADING CHANNEL

Rayleigh fading is a form of fading experienced by a signal propagating in an environment having a number of objects. The signal while propagting from the transmitter to the receiver takes multiple paths due to reflections, diffractions, and scattering of the signal by the objects. Due to these reflections, diffractions, and scattering, multiple replicas of the transmitted signal arrive at the receiver. These replicas superimpose over each other constructively or destructively to generate the resultant received signal.

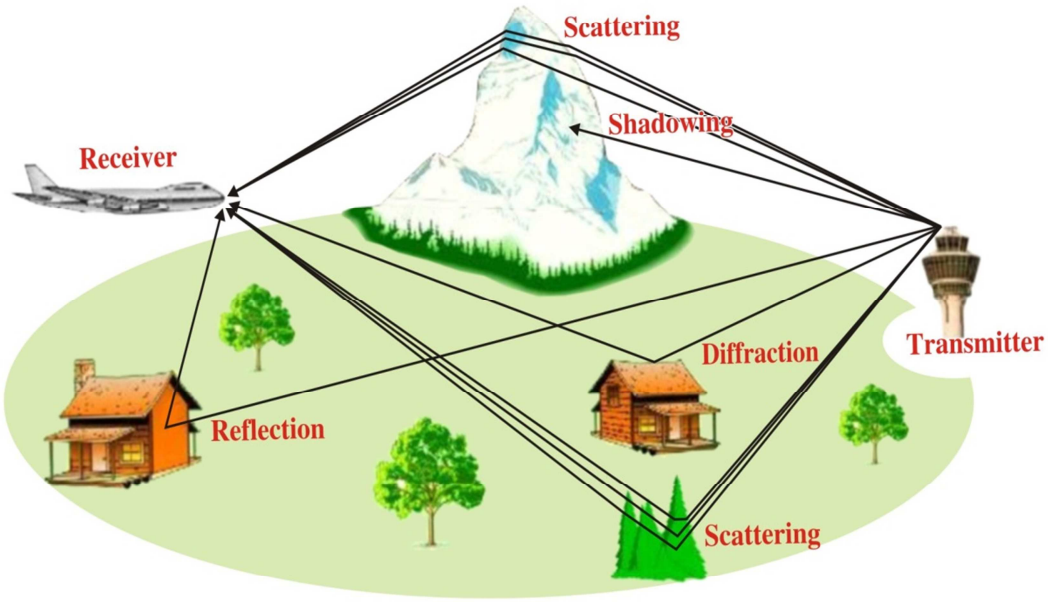

Figure 2.1: Multipath propagation

The Rayleigh fading model is used to analyse the fading channel when multipath propagation of the signal exist in the environment. In the Rayleigh fading model, the line of sight communication is not considered between the transmitter and receiver. The Rayleigh fading model is used to analyse and predict the performance of signals in cellular communication where there are multiple paths due to reflections, diffractions, scattering of the signals from buildings, vehicles, trees etc.

Figure 2.1 shows that a radio signal travelling from the transmitter to the receiver takes multiple paths. The phase of the signal varies depending on the length of path travelled by the replicas. The resultant signal is defined by combining all the replicas of signal that reach at the receiver. These replicas of the signal are combined constructively or destructive i.e. when the received replicas are in same phase, then they are added and the strength of resultant signal is high. However, if the received replicas are in out-of-phase, then the received replicas are subtracted and the strength of the resultant signal is low. Thus, the strength of resultant received signal varies when the replicas add or subtract based on their phases.

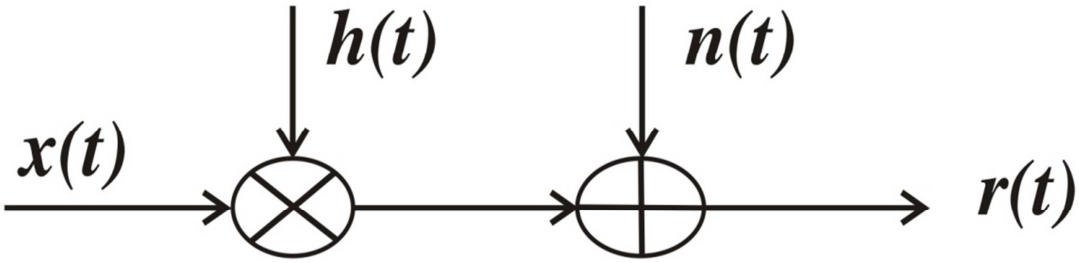

Figure 2.2: Rayleigh fading channel model

Statistically, in Rayleigh fading model, as shown in figure 2.2, the received signal is presented as the sum of faded signal and AWGN. The received signal can be expressed as

$$r(t) = h(t)x(t) + n(t) \quad (2.1)$$

where $x(t)$ represents the transmitted signal, $r(t)$ represents the signal received by the receiver, $n(t)$ represents the AWGN, and $h(t)$ represents the multipath Rayleigh fading coefficient. $h(t)$ is modelled as a complex Gaussian random variable which introduces random variation in the phase and random fluctuations in the amplitude of the transmitted signal.

In the Rayleigh fading channel, the received signal corresponding to an impulse transmitted from the transmitter is given by a train of impulses of varying magnitudes received at different time intervals and is shown in figure 2.3.

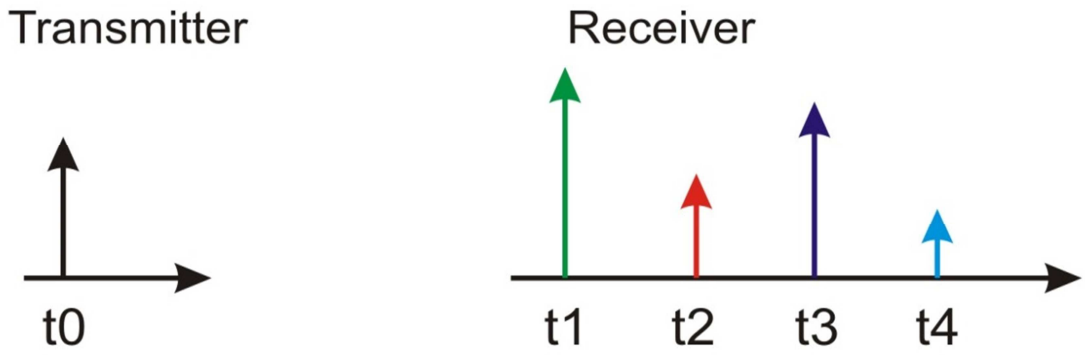

Figure 2.3: Impulse response of a multipath channel

In the Rayleigh fading channel model with multipath propagation, each path is modelled as symmetric complex Gaussian random variable. When the number of the independent paths between the transmitter and receiver are very large, the central limit theorem states that in-phase and out-of phase components of the received signal are modelled as Gaussian random variables with zero mean and variance σ_s^2. Therefore, a Rayleigh probability distribution, as shown in figure 2.4, is applied to the amplitude of the received signal. The phase of the received signal varies uniformly between $-\pi$ and π. The probability density function (PDF) of Rayleigh distribution is given by

$$p(a) = \frac{a}{\sigma_s^2} e^{-\frac{a^2}{2\sigma_s^2}} \quad a \geq 0$$

$$= 0 \qquad a < 0 \tag{2.2}$$

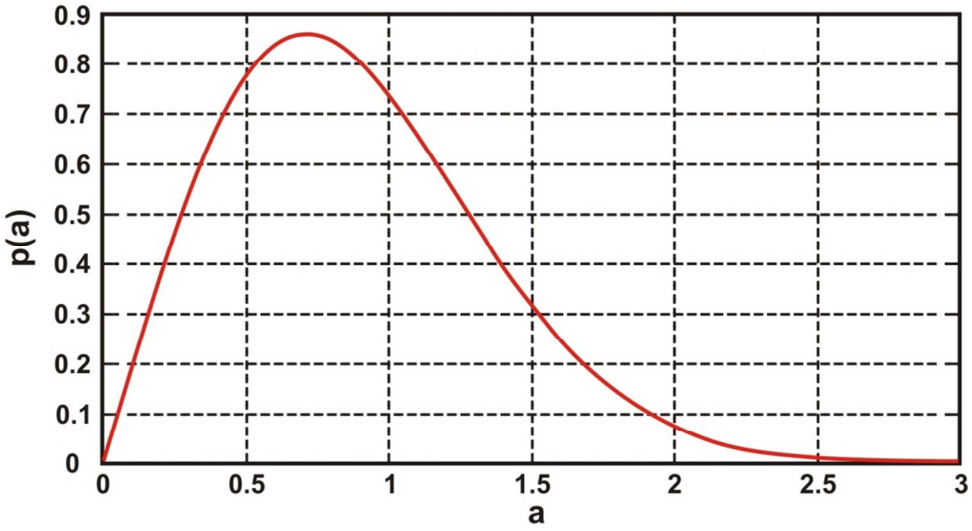

Figure 2.4: The PDF of Rayleigh distribution

In the presented work, the quasi-static Rayleigh fading channel has been considered in which the fading coefficients remain constant during the transmission of each frame. The channel fading coefficients in the quasi-static Rayleigh fading channel change when the frame changes from one frame to another. In other words, according to the assumption of the quasi-static fading channel, the channel varies so slowly over one frame of information that it can be treated as constant for a frame and varies from one frame to other.

2.3 MULTILEVEL CODING

Multilevel coding is a technique used for providing flexible data transmission rates and improvement in bandwidth efficiency over the wireless fading channel. The input data stream is partitioned into a plurality of sub-streams which are then encoded using respective error correction techniques to generate simple component codes. Each component code is mapped to the symbols from an enlarged signal constellation by partitioning the signal constellation successively into subsets until the subsets contain only a single constellation point. The mapped symbols are then modulated and combined to construct complicated codes. The complicated codes referred to as the multilevel codes are transmitted over the communication channel.

2.3.1 Multilevel Encoder

A block diagram of a system for multilevel coding of an information data stream is shown in figure 2.5. The system includes a multilevel encoder which comprises a set of *M* encoders E_1, E_2, …,E_M, for generating the *M* different binary error-correcting codes $S_1^{(t)}$,$S_2^{(t)}$,… $S_M^{(t)}$ each of which is referred to as a component code. The information data stream is split into *M* sub-streams of information which are applied to respective encoders to generate the corresponding error correcting codes. For example, when the i^{th} sub-stream is applied to the i^{th} encoder E_i, it generates the component code $S_i^{(t)}$.

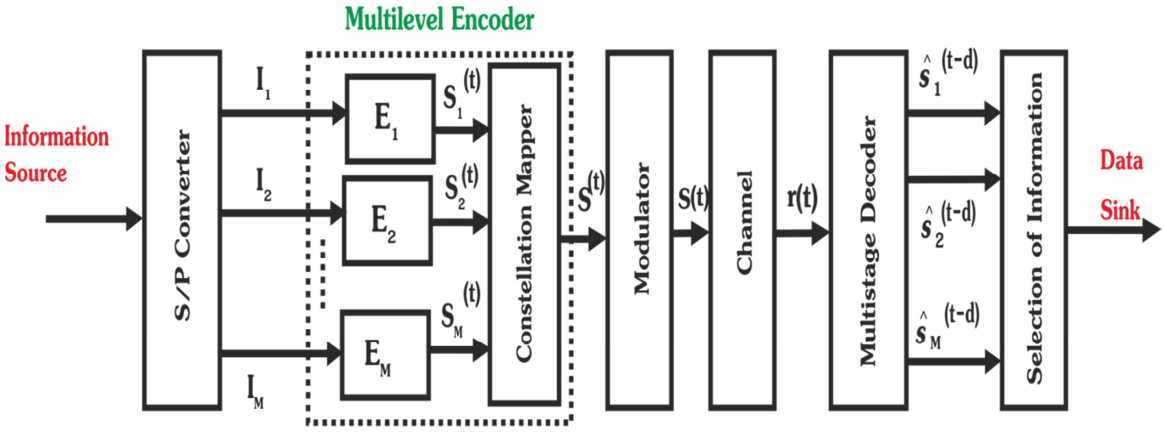

Figure 2.5: General block diagram of a system for multilevel coding

The generated codewords are mapped to symbols from an enlarged signal constellation. The mapped symbols are modulated by a desired modulation scheme e.g. quadrature phase shift keying (QPSK) or quadrature amplitude modulation (QAM). The modulated signals are then transmitted through the transmit antennas at the transmitter.

The codewords are mapped by partitioning the enlarged signal constellation successively into subsets or clusters. The partition continues till each subset has a single signal point only. The main aim of the partitioning is to maximize the minimum Euclidean distance between the symbols of a subset. In general, the minimum Euclidean distance in the subsets increases from first subset down to the last subset.

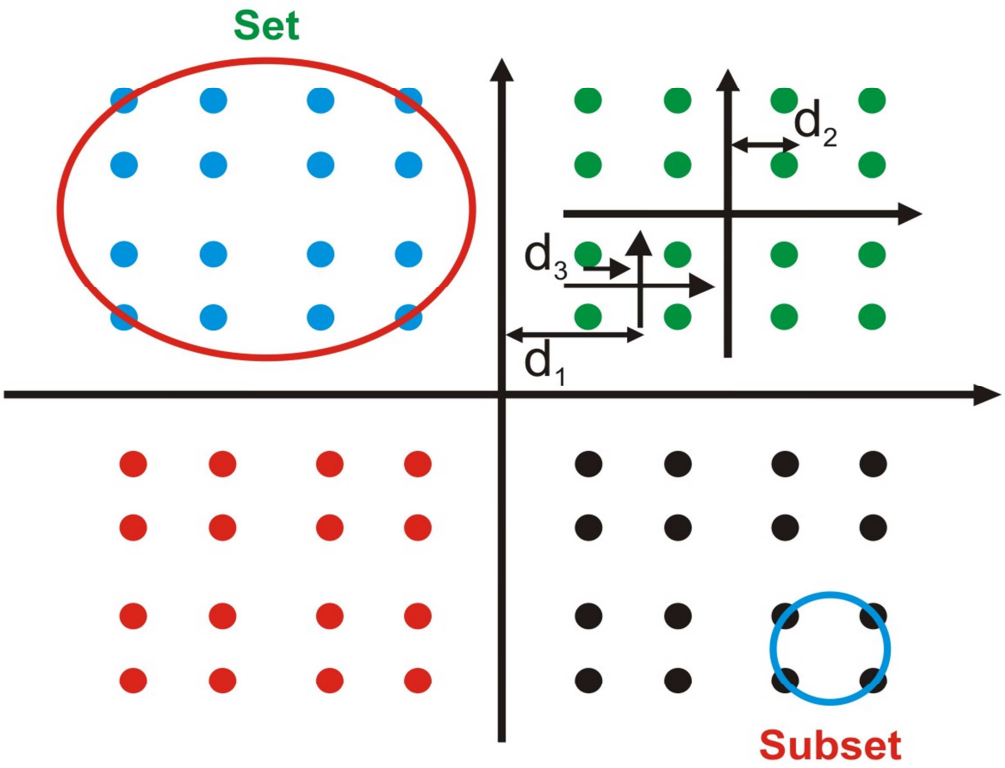

Figure 2.6: Partitioning of 64-QAM constellation

An example of partitioning of a 64-QAM constellation is shown in figure 2.6. As shown in the figure that at the first level, all constellation points are split into four sets, each set having sixteen points. At the second level, each set of sixteen points is split into four subsets such that each subset has four points. In this way, the subsets are further split till each subset contains only a single constellation point. The idea behind the partitioning is that the most significant information bits are mapped to the sets and the less significant information bits are mapped to the subsets.

2.3.2 Multistage Decoder

The decoding of the multilevel codes is performed by using a multistage decoder [21] at the receiver. Figure 2.7 shows the structure of multistage decoder in which the decoded output of first stage is passed to next stage for decoding of subsequent component code. As shown in figure 2.7, the first stage decoder decodes the codeword $s_1{}^{(t)}$ which is then applied as input to next decoding stage. In this way, the decoded outputs corresponding to

code words $s_1{}^{(t)}, s_2{}^{(t)}, \ldots s_{M-1}{}^{(t)}$ are applied as input to final stage of the decoder to decode $s_M{}^{(t)}$.

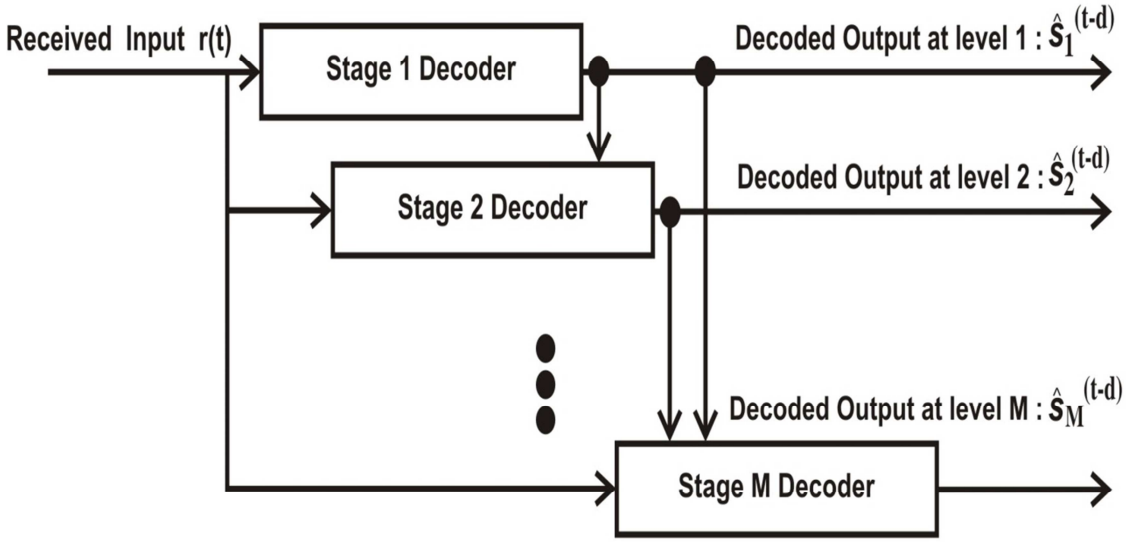

Figure 2.7: Generic Structure for Multistage decoder

The main advantage of the multistage decoder over the maximum likelihood decoder is that the complexity of the multistage decoder is proportional to the sum of the decoding complexity of each component code instead of the product in the maximum likelihood decoder. Another advantage of the multistage decoding is that it enables the design engineer to design a wireless system with flexible data rate, error performance, and desired coding gain.

2.4 SPACE-TIME TRELLIS CODING

Space-time trellis coding is a unique technique for designing codes based on combination of modulation, spatial diversity, and error control coding to mitigate fading in the wireless channel. In this scheme, the information and redundant symbols are distributed over time and a set of transmit antennas to achieve a correlation between the temporal and spatial dimensions. STTCs provide not only a substantial improvement in diversity gain and spectral efficiency but also offer coding gain for signals transmitting over the wireless fading channels.

The performance of STTCs is governed by different design criteria which allow designing STTCs for optimum performance over different fading channels. These criteria in general are formulated by analyzing the expression for pair-wise error probability of STTCs. These design criteria include rank and determinant criteria [47] for small diversity order and trace criterion [78] for large diversity order.

2.4.1 System Model: STTCs

A block diagram of a system model for space-time trellis coding is shown in figure 2.8. The system comprises a transmitter having a space-time trellis encoder for encoding the input data stream and a receiver having a maximum likelihood decoder for decoding the received encoded information. The transmitter is having *N* transmit antennas and the receiver is having *M* receive antennas. The communication channel is considered as quasi-static fading channel and the CSI is assumed to be available at the receiver however assumed to be not available at the transmitter.

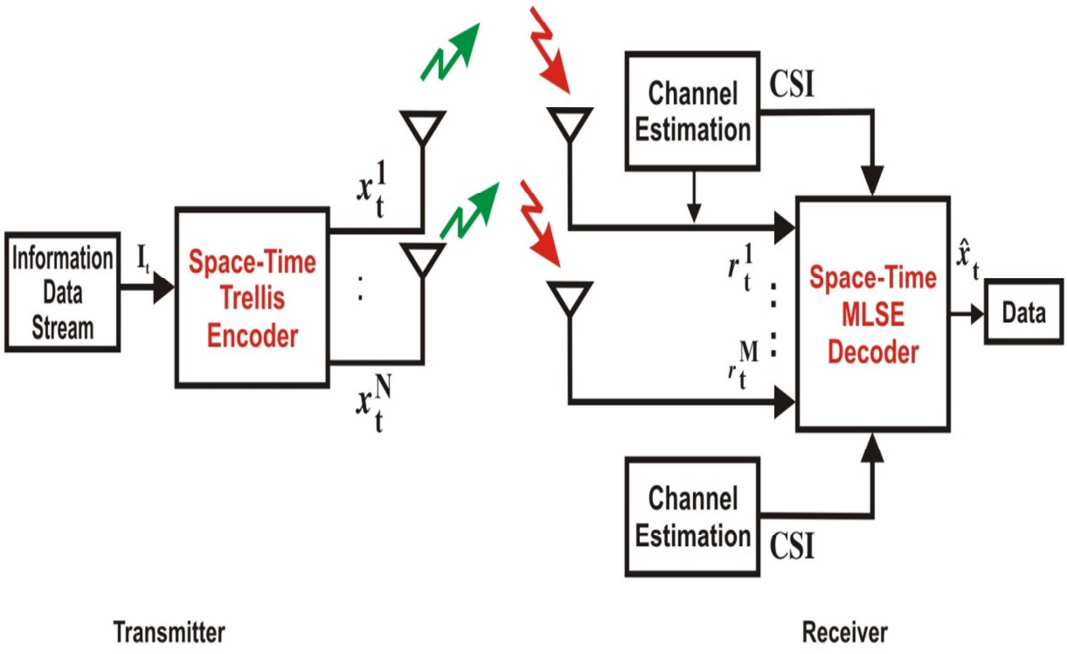

Figure 2.8: System model for STTC modulation

2.4.2 STTC Encoder

Figure 2.9 shows a STTC encoder for the system having *N* transmit antennas. The information data stream *I* is split in blocks of information sequences which are given by

$$I = (I_0, I_1, I_2 \ldots, I_t, \ldots) \quad (2.3)$$

where I_t is a block of *m* input sequences at time *t*. I_t is given by

$$I_t = (I_t^1, I_t^2, I_t^3, \ldots\ldots, I_t^m) \quad (2.4)$$

The STTC encoder includes *m* feed-forward shift registers and a plurality of multipliers for multiplying the input sequences with corresponding encoder coefficients. The encoder coefficients are also referred to as generator sequences. Each input sequence is applied to one of the feed-forward shift registers. For example, the k^{th} input sequence, $I^k = \left(I_0^k, I_1^k, I_2^k \ldots, I_t^k, \ldots\right)$ is input to the k^{th} shift register, where k = 1, 2, . . .*m*, and is multiplied with the generator sequences corresponding to the k^{th} shift register. The outputs from all the multipliers in the shift registers are combined with each other giving the encoder output $x_t = (x^1, x^2, x^3, \ldots\ldots x^N)$.

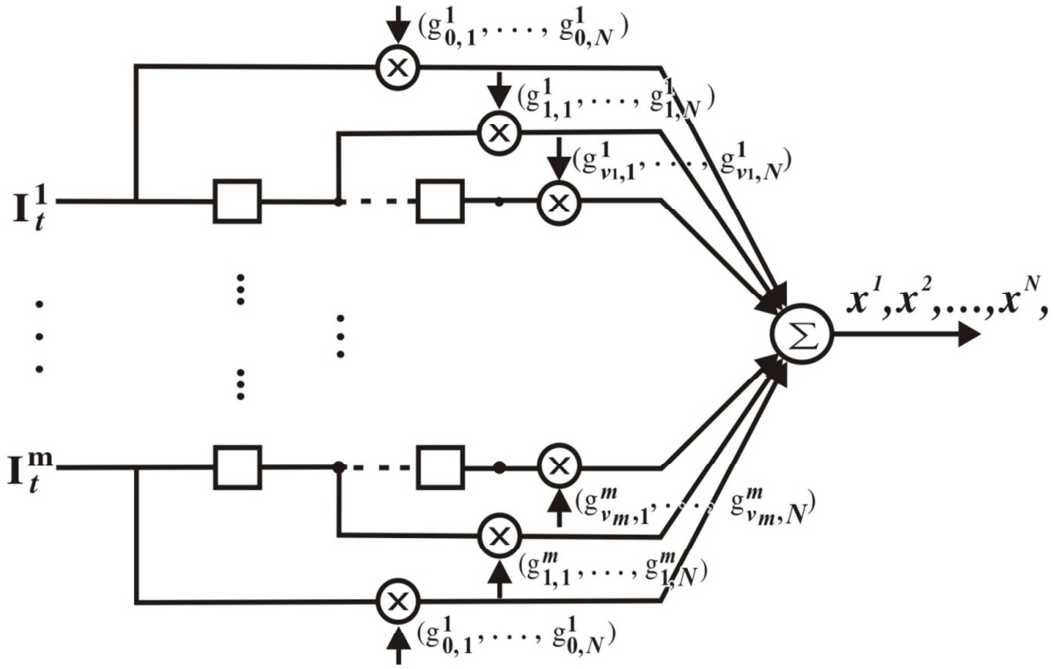

Figure 2.9: STTC Encoder

The generator sequences used for multiplying the input sequences are given by

$$g^1 = [(g^1_{0,1} \dots g^1_{0,N,}), (g^1_{1,1} \dots g^1_{1,N,}) \dots (g^1_{v1,1} \dots g^1_{v1,N,})] \quad (2.5)$$

$$g^2 = [(g^2_{0,1} \dots g^2_{0,N,}), (g^2_{1,1} \dots g^2_{1,N,}) \dots (g^2_{v2,1} \dots g^2_{v2,N,})] \quad (2.6)$$

$$g^m = [(g^m_{0,1} \dots g^m_{0,N,}), (g^m_{1,1} \dots g^m_{1,N,}) \dots (g^m_{vm,1} \dots g^m_{vm,N,})] \quad (2.7)$$

where $g^{k,}_{j,i}$ is a constellation point of the M_{ary} QAM signal constellation, $i = 1, 2, \dots, N$, $j = 1, 2, \dots, v_k$, $k = 1, 2, \dots, m$, and v_k is the memory order of the k^{th} shift register. At time t, the STTC encoder output x^i_t for transmit antenna i can be computed as

$$x^i_t = \sum_{k=1}^{m} \sum_{j=0}^{vk} g^k_{j,i} I^k_{t-j} \ mod\ M_{ary} \quad (2.8)$$

The encoded outputs $x^1_t, x^2_t, x^3_t, \dots . x^N_t$ form a space-time trellis coded symbol which is a N column vector and is given by

$$x_t = (x^1_t, x^2_t, x^3_t, \dots x^N_t)^T \quad (2.9)$$

where T represents the transpose of a matrix. N parallel outputs are transmitted simultaneously by N different antennas, whereby symbol x^i_t , $1 \le i \le N$ is transmitted by the transmit antenna i.

2.4.3 STTC Decoder

The transmitted signal undergoes multipath fading while travelling from transmitter to receiver. The signal received by the receive antenna i is calculated by combining faded replicas of the signal received from the transmitter. At receive antenna i, the received signal is given by

$$r^i_t = \sum_{j=1}^{N} {h_{ij}}^t \, x^j_t + \, n^i_t \quad (2.10)$$

where n^i_t is the noise associated with the receive antenna i at time t, ${h_{ij}}^t$ is the path gain/ fading coefficient between the j^{th} transmit and the i^{th} receive antenna $1 \le j \le N$, $1 \le i \le M$. The fading coefficients ${h_{ij}}^t$ are zero mean and unity variance Gaussian random variables.

In matrix form, the signals received by the receiver having *M* receive antennas are given by

$$\begin{bmatrix} r_t^1 \\ r_t^2 \\ \vdots \\ r_t^M \end{bmatrix} = \begin{bmatrix} {h_{11}}^t & \cdots & {h_{1N}}^t \\ {h_{21}}^t & \dots & {h_{2N}}^t \\ \vdots & \ddots & \vdots \\ {h_{M1}}^t & \cdots & {h_{MN}}^t \end{bmatrix} \begin{bmatrix} x_t^1 \\ x_t^2 \\ \vdots \\ x_t^N \end{bmatrix} + \begin{bmatrix} n_t^1 \\ n_t^2 \\ \vdots \\ n_t^M \end{bmatrix} \quad (2.11)$$

At the receiver, the space-time trellis coded symbols are decoded by a maximum likelihood sequence estimation (MLSE) decoder employing Viterbi algorithm. The Viterbi algorithm at the decoder is used for estimating the transmitted sequence of information. Each time the decoder receives an encoded symbol, it computes a branch metric using the Euclidean distance between each of the received symbol and all of the possible channel symbols that could have been transmitted. The branch metrics is given by

$$\sum_t \sum_{j=1}^{M} \left| r_t^i - \sum_{i=1}^{N} {h_{ij}}^t \, x_t^j \right|^2 \quad (2.12)$$

The path having minimum branch metric is selected by the decoder as the decoded sequence.

2.4.4 Performance Analysis of STTCs

To analyze the performance of STTCs, each transmit antenna at the transmitter is assumed to transmit a data frame of *l* codewords. For example, the data frame of *l* codewords transmitted by *1st* transmit antenna is given by

$$x^1 = x_1^1, x_2^1, x_3^1 \dots . x_l^1 \quad (2.13)$$

Since the transmitter is having *N* transmit antennas, collectively the codewords transmitted by *N* transmit antennas can be represented as

$$x = (x_1^1, x_1^2, x_1^3 \dots . x_1^N, x_2^1, x_2^2, x_2^3 \dots . x_2^N, \dots \, x_l^1, x_l^2, x_l^3, \dots . x_l^N) \quad (2.14)$$

A maximum likelihood decoder has been considered at the receiver. The decoder is

assumed to erroneously decode the transmitted codewords *x* as *e* which is given by

$$e = (e_1^1, e_1^2, e_1^3 \ldots . . e_1^N, e_2^1, e_2^2, e_2^3 \ldots . . e_2^N, e_l^1, e_l^2, e_l^3, \ldots . . e_l^N) \quad (2.15)$$

A codeword difference matrix, for calculating the difference between the each of the codeword transmitted from the transmitter and the corresponding codeword received with errors at the receiver, can be represented by

$$B(x,e) = \begin{bmatrix} e_1^1 - x_1^1 & \cdots & e_l^1 - x_l^1 \\ e_1^2 - x_1^2 & \ldots & e_l^2 - x_l^2 \\ \vdots & \ddots & \vdots \\ e_1^N - x_1^N & \cdots & e_l^N - x_l^N \end{bmatrix} \quad (2.16)$$

A codeword distance matrix calculated using the codeword difference matrix is given by

$$A(x,e) = B(x,e)B^H(x,e) \quad (2.17)$$

where $B^H(x,e)$ is the Hermitian of $B(x,e)$. The codeword distance matrix is assumed to have a rank *r*. The eigenvalues of $A(x,e)$ are calculated. N-r eigenvalues of $A(x,e)$ are zero whereas the non-zero eigenvalues of $A(x,e)$ are denoted by $\lambda_1, \lambda_2, \lambda_3 \ldots \lambda_r$.

Assuming that the perfect CSI is available at the receiver, the probability of transmitting x and determining an erroneous codeword *e* at the decoder is given by

$$P(x,e|i = 1,2..N, j = 1,2, \ldots M) \leq \exp(-d^2\,(x,e)E_s/4N_0) \quad (2.18)$$

where $N_0/2$ denotes the noise variance per dimension and

$$d^2\,(x,e) = \sum_{j=1}^{M}\sum_{t=1}^{l}\left|\sum_{i=1}^{N} {h_{ij}}^t (x_t^i - e_t^i)\right|^2 \quad (2.19)$$

denotes the squared Euclidean distance.

It follows from the above equation that the PEP of transmitting *x* and receiving *e* is given by

$$P(x \to e) \leq (\textstyle\prod_{i=1}^{r} \lambda_i)^{-n_R} \left(\frac{E_s}{4N_0}\right)^{-rn_R} \quad (2.20)$$

Based on the PEP, the design criteria are derived for designing STTCs to attain the desired improvement in the performance of the wireless system.

2.4.5 Design Criteria for STTCs Over Quasi-Static Rayleigh Fading Channel

2.4.5.1 *Rank and Determinant Criteria*

The rank and determinant criteria were introduced by Tarokh et al. [47] to design STTCs for providing the optimum performance. These criteria are proposed based on the rank and determinant of the codeword distance matrix $A(x,e)$. The rank criterion guarantees to attain the maximum diversity gain if the matrix $A(x,e)$ has full rank whereas the determinant criterion guarantees to attain the maximum coding gain by maximizing the minimum determinant of the matrix $A(x,e)$ over all codewords.

It is clear from equation 2.20 that the PEP decreases exponentially with increase in the SNR. Thus, the PEP at high SNRs mainly depends on the value of product of the minimum rank *r* and the number of receive antennas *M* over all possible codeword pairs. This product is denoted as r*M* and is referred to as the diversity gain. In order to design the STTCs for providing minimum error rate, the minimum rank r of the matrix $A(x,e)$ should be maximized. For the system having *N* transmit antennas, the maximum possible value of the rank *r* is *N*. Therefore, the maximum value of the product r*M* for the system having *N* transmit antennas is *NM*. Thus, the maximum diversity gain obtained using the rank criteria is given by *NM*.

In addition, the PEP is minimized by maximizing the product of nonzero eigen values, i.e. the product of λ_i, i=1….r of the matrix *A(x, e)* should be maximized. The product of nonzero eigen values is given by the absolute value of the sum of determinants of all the principal $r \times r$ cofactors of the matrix *A(x, e)*. This criterion is referred to as the determinant criterion as it optimizes the coding gain by maximizing the minimum determinant of the matrix $A(x,e)$ over all codewords. Therefore, for small values of rM (<4), the STTC design criteria for quasi-static Rayleigh fading channel can be summarized as:

i) Rank criterion: Maximize the minimum rank *r* of the codeword distance matrix *A(x, e)* over all pairs of distinct codewords to achieve maximum possible diversity gain.

ii) Determinant criterion: Maximize the minimum determinant of *A(x, e)* to achieve the maximum coding gain.

2.4.5.2 ***Euclidean distance criteria/Trace Criteria***

The trace criterion was introduced by Chen et al. [78] for designing STTCs over quasi-static fading channel for wireless systems with large number of diversity branches (i.e. where r$M \geq 4$). Normally, the number of diversity branches is large for wireless systems having a receiver with two or more than two receive antennas. As the number of diversity branches increases, there is a reduction in effect of fading and the quasi-static fading channel approaches to an AWGN channel. In the AWGN channel, the optimum performance is achieved by maximizing the minimum Euclidean distance between the codewords.

Similarly, when the number of independent diversity branches is large, $rM \geq 4$, the quasi-static fading channel approaches the AWGN channel and then the minimum Euclidean distance is used to optimize the performance of STTCs. Therefore, designing the optimum STTCs based on the Euclidean distance is referred to as the Euclidean distance criterion. The Euclidean distance criterion is applied to the systems where the number of receive antennas are two or more than two in contrast to the rank and determinant criteria which is applied to systems having a single receive antenna and a small number of transmit antennas.

For large diversity gain, the upper bound for PEP is given by

$$P(x \to e) \leq \frac{1}{4} exp\left(-n_R \frac{E_s}{4N_0} \sum_{i=1}^{n_T} \sum_{j=1}^{l} \left| e_j^i - x_j^i \right|^2 \right) \tag{2.21}$$

where $\sum_{i=1}^{n_T}\sum_{j=1}^{l}\left|e_j^i - x_j^i\right|^2 = tr\,A(x,e) = \sum_{i=1}^{r}\lambda_i$, $\left|e_j^i - x_j^i\right|^2$ represents squared minimum Euclidean distance, and $trA(x,e)$ represents the trace of the matrix *A(x, e)*.

It is clear from the above equations that the PEP decreases exponentially with increase in squared minimum Euclidean distance between the codewords *x* and *e*. The PEP at low SNRs mainly depends on the maximum value of squared minimum Euclidean distance. Thus, to minimize the error probability, the squared minimum Euclidean distance should be maximized or the minimum sum of all non-zero eigenvalues of matrix *A(x, e)* among all pairs of distinct codewords should be maximized. In other words, to minimize the error probability, the minimum trace of the matrix *A(x, e)* among all pairs of distinct codewords should be maximized. Therefore, Euclidean distance criterion is also referred to as the trace criterion. The Euclidean distance criterion for designing STTCs for systems having large diversity gain in quasi-static fading channels can be summarized as:

i) Maximize the mimimum rank *r* of the codeword distance matrix *A(x, e)* over all pairs of distinct codewords such that $rM \geq 4$.

ii) Maximize the minimum trace of the codeword distance matrix *A(x, e)* among all pairs of distinct codewords.

2.4.6 Construction of 4-State QAM STTCs

The encoder for constructing 4-state QAM STTC, as shown in figure 2.10, comprises two branches of the shift registers. The memory order of the upper and lower branch of the shift registers are v_1 and v_2, respectively. The input data streams I_t^1 and I_t^2 are fed into the branches of the encoder. The input data stream in each branch is multiplied by corresponding generator sequence. The generator sequence for upper branch is given by a_p^1, a_p^2 and for lower branch is given by b_q^1, b_q^2, where $a_p^k, b_q^k \in \{0,1,2,3\}$, k=1, 2, p=0, 1,…v_1 and q=0, 1, …v_2, $v_1+v_2=v$ and the number of states is 2^{υ}.

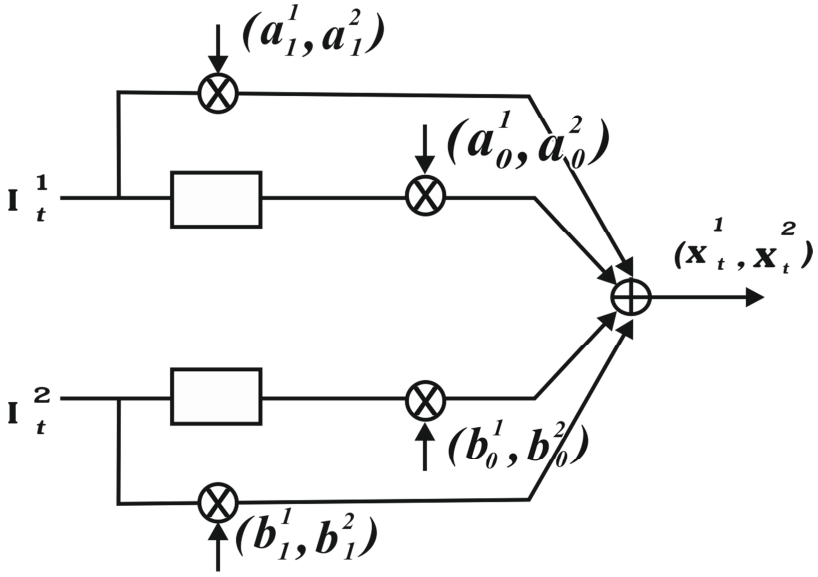

Figure 2.10: Encoder for 4-state QAM STTC

The value of v_k is calculated as

$$v_k = \left\lceil \frac{v+k-1}{2} \right\rceil \text{ where k=1, 2} \quad (2.22)$$

The output of the encoder at time t is given by

$$x_t^k = \left(\sum_{p=0}^{v1} I_{t-p}^1 \; a_p^k + \sum_{p=0}^{v2} I_{t-q}^2 \; b_{t-q}^k \right) mod\ 4 \quad (2.23)$$

$x_t^1 \; and \; x_t^2$ are transmitted simultaneously through the first and second transmit antennas.

The figure 2.11 shows a trellis diagram of 4-state QAM STTCs. In the trellis diagram, QAM symbol 0, 1, 2, and 3 correspond to bits 00, 01, 10, and 11 respectively. The trellis diagram shows that the states are represented by dots on the left and right side of the trellis. The left side of the trellis shows a matrix listing possible output combinations and the right side of the trellis shows output of the current state. The connecting lines represent a possible transition with the input bits shown beside the line. The trellis is assumed to begin at state 1 and transitions from one state to other based on the input sequence. The trellis diagram shows multiple paths for reaching from state 1 to final state. The decoder always selects the path which has minimum branch metrics.

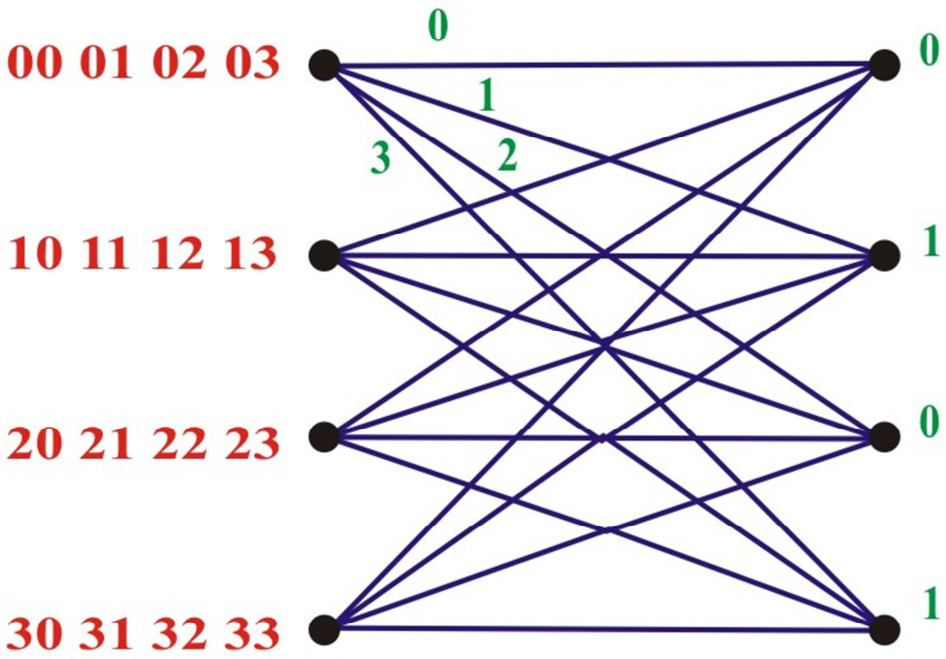

Figure 2.11: Trellis diagram for 4-state QAM STTC

2.4.7 Performance evaluation of 4-State QAM STTCs

The performance of the 4-state QAM STTCs is analyzed for two transmit antennas and 1/2/4 receive antennas. The simulation results have been presented to depict the performance of STTCs using the rank and determinant criteria and trace criterion. Each frame transmitted from the transmit antennas consists of 130 symbols. The channel is considered as a quasi-static Rayleigh fading channel and the perfect CSI is assumed to be available at the receiver. The simulation results are presented in terms of FER vs SNR.

The performance of STTCs using the rank and determinant criteria is shown in figure 2.12 and the performance of STTCs using trace criterion is shown in figure 2.13. It can be seen from the simulation results that there is a significant improvement in the performance of STTCs with an increase in number of the receive antennas. Further it can be noted that for two and four receive antennas, STTCs designed using the trace criteria outperforms STTCs designed using the rank and determinant criteria.

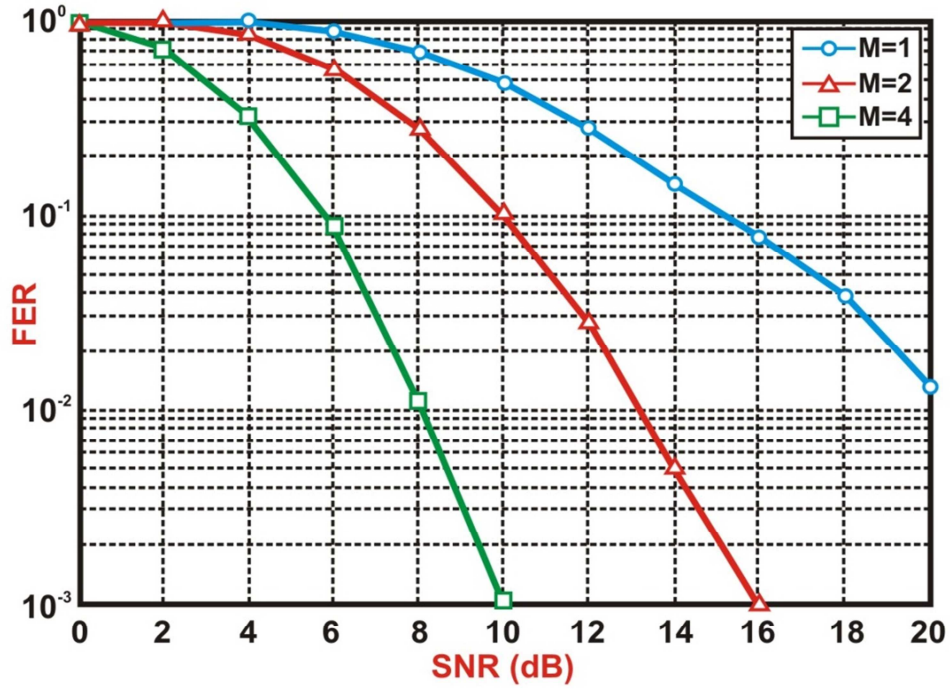

Figure 2.12: Performance comparison of 4-state QAM STTCs designed using the rank and determinant criteria

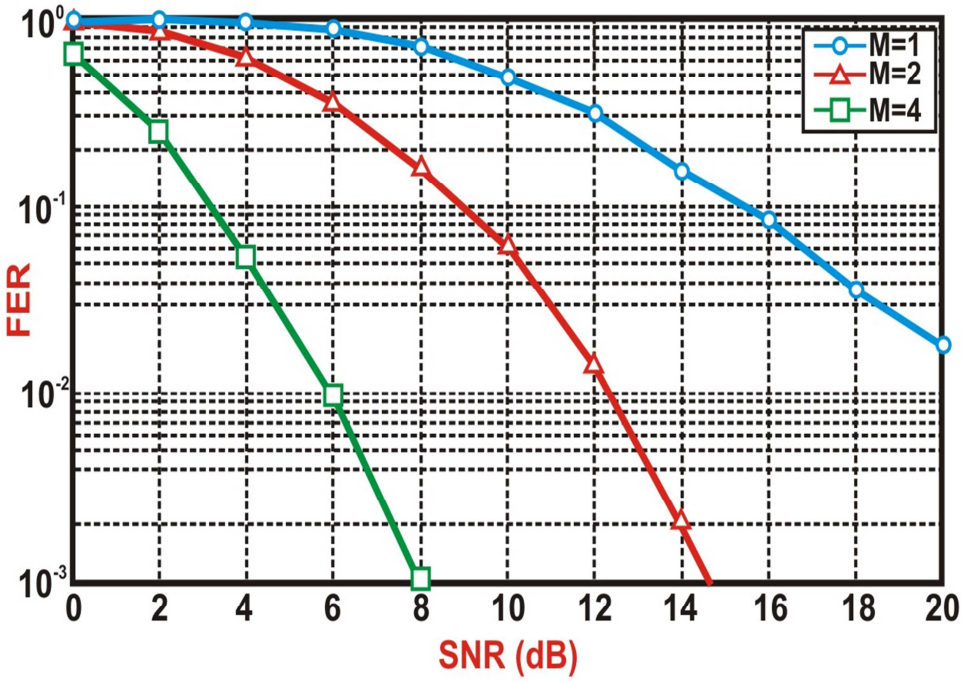

Figure 2.13: Performance comparison of 4-state QAM STTCs designed using the trace criteria

2.5 SUMMARY OF THE CHAPTER

In this chapter, the model and the characteristics of a quasi-static Rayleigh fading channel has been conferred. The quasi-static Rayleigh fading channel is considered for analyzing the performance of all the codes presented in this thesis. The multilevel encoding of an information data stream has been presented using simple component codes for providing high data transmission rate. A multistage decoder using the Veterbi algorithm has been used to decode the multilevel codes.

A comprehensive design and performance analysis of STTCs has been presented by combining modulation, spatial diversity, and error control coding to mitigate fading in the wireless channel. The STTCs construction criteria have been described by analyzing the expressions for pair-wise error probability of the codes. These design criteria include rank and determinant criteria for small diversity order ($rM < 4$) and trace criteria for large diversity order ($rM \geq 4$). The performance of the STTCs schemes adhering to these two design criteria have been compared by simulations.

In this chapter, the perfect CSI has been assumed to be available at the receiver only without considering the availability of the CSI knowledge at the transmitter. In the next chapter, the efficient design of codes based on the combination of multilevel coding and STTCs is presented using the CSI at the transmitter for improving the error performance and the data transmission rate of wireless systems.

CHAPTER 3

IMPROVEMENT IN PERFORMANCE OF MLSTTCs AND GMLSTTCs BASED ON DYNAMIC COMPONENT CODE SELECTION

3.1 INTRODUCTION

The main benefit of employing a multilevel coding technique is that it enables an engineer to design a flexible system which can provide desired data transmission rate, coding gain, and error performance. STTCs have been introduced to improve the reliability and spectral efficiency of communication over the fading channels. In-spite of the advantages of STTCs, the design engineers are seen to be reluctant to use STTCs in modern high data rate wireless communication systems due their inherent disadvantages of high complexity at the high data rates. Multilevel coding when combined with STTCs presents an efficient alternative to STTCs, which provide advantages of STTCs such as improved diversity and coding gain without having the drawbacks of STTCs such as high search complexity and decoding complexity at high data rate transmission.

In this chapter, the design and performance analysis of MLSTTCs and GMLSTTCs have been presented by combining the MLC and STTCs. The system model used for designing MLSTTCs and GMLSTTCs are open loop where it is assumed that the perfect CSI is available at the receiver only and the transmitter has no knowledge of the CSI. MLSTTCs and GMLSTTCs consider that STTCs, used as the component codes, are predefined and do not change with the change in the channel conditions.

To improve the performance of MLSTTCs and GMLSTTCs, the perfect CSI is assumed to be available both at the transmitter and the receiver. The transmitter is

assumed to receive the perfect CSI as a feedback from the receiver. In this chapter, the CSI at the transmitter has been used to choose a code set for generating dynamic STTCs. These dynamic STTCs change with the change in the CSI at the transmitter. These dynamic STTCs are used as component codes in the multilevel coding to generate novel codes which are referred to as MLDSTTCs and GMLDSTTCs respectively. The simulation results show that MLDSTTCs and GMLDSTTCs outperform over MLSTTCs and GMLSTTCs respectively.

3.2 DESIGN AND ANALYSIS OF MLSTTCs

MLSTTCs are designed by using STTCs as component codes in multilevel coding. MLSTTCs improve the coding gain, diversity gain, and increase the data rate significantly with linear increase in complexity in comparison to exponential increase in complexity in STTCs. Therefore, these codes serve as efficient and promising alternative to STTCs for providing high data rate communication.

3.2.1 System Model: MLSTTCs

MLSTTC system presented in figure 3.1 comprises a transmitter having N transmit antennas and a receiver having M receive antennas. The channel is assumed to exhibit quasi-static Rayleigh fading and the perfect CSI is assumed to be available at the receiver. The transmitter is having STTC encoders for encoding the input data streams and receiver is having a multistage decoder for decoding the received signal.

3.2.2 Encoding of MLSTTCs

At the transmitter, each STTC encoder receives a data stream, and performs space-time trellis coding on the data stream. At each of the levels 1 to L, each STTC encoder use similar generator sequences to generate STTCs which are used as component codes for multilevel coding. The outputs from STTC encoders at level 1 to L are given by

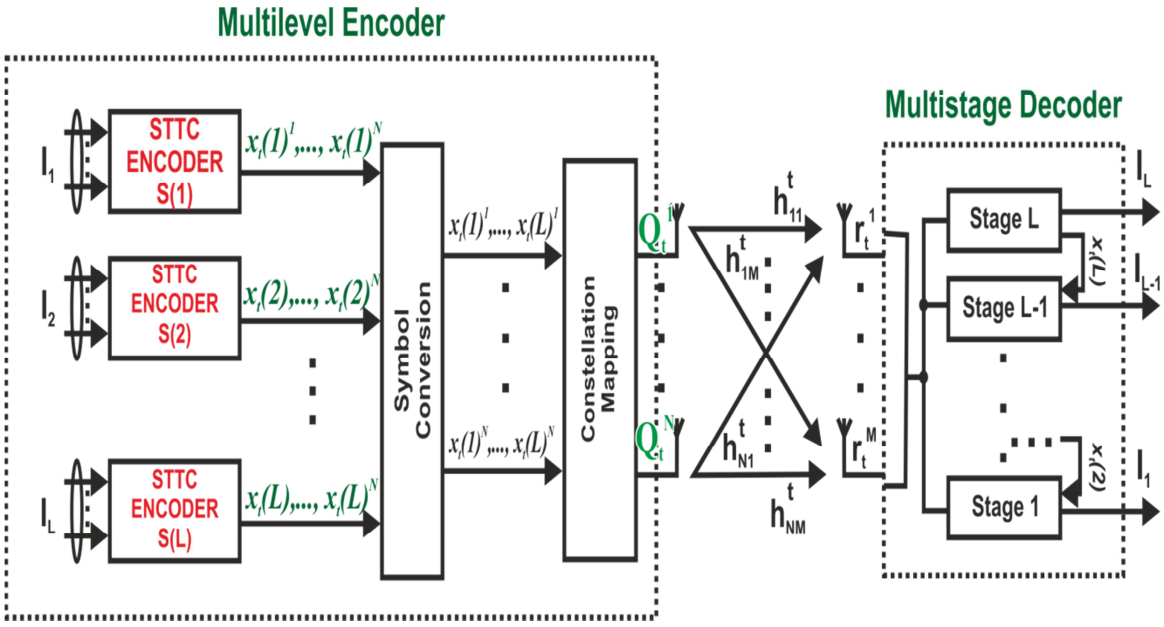

Figure 3.1: System model for MLSTTCs

$$S(1) = x_t(1)^1, x_t(1)^2 \dots x_t(1)^N \quad (3.1)$$

$$S(L) = x_t(L)^1, x_t(L)^2 \dots x_t(L)^N \quad (3.2)$$

Each STTC used in multilevel coding is designed for a 4-QAM constellation using the trace criteria. The complex form of STTC output symbols, $x_t(1)$ to $x_t(L)$ is given by

$$x_t(l) = a + jb \quad a, b \in \{1, -1\} \quad (3.3)$$

Collectively, the outputs from L levels, $S(1),\dots S(L)$, are input into a symbol translator to generate N translated symbols. These translated symbols are denoted by

$$T(1) = x_t(1)^1, x_t(2)^1 \dots x_t(L)^1 \quad (3.4)$$

$$T(N) = x_t(1)^N, x_t(2)^N \dots x_t(L)^N \quad (3.5)$$

In the translated symbols, the STTCs symbols generated by each encoder are mapped to M_{ary}-QAM signal constellation using a constellation mapper. The translated symbols are mapped to the M_{ary}-QAM signal constellation by using a multi-resolution modulation (MRM) partitioning technique which was introduced by Cover [35] and later improved by Fazel and Ruf [36]. The M_{ary}-QAM constellation is partitioned into L levels such that

$M_{ary} = 4^L$. Since there are L levels of partition, L component codes are used for encoding the information data stream.

An example of MRM partitioning of a 64-QAM constellation is shown in figure 3.2. As shown in the figure that at the first level, all the constellation points are split into four sets each having sixteen points. Each set is considered as a 16-QAM constellation. In the second level, each set of sixteen points is split into four subsets of four points. Each subset is considered as 4-QAM constellation. In this way, the subsets are further split till each subset contains only a single constellation point. The minimum Euclidean distance between two sets is more in comparison to distance between two subsets. The main use of the MRM partitioning is that the most significant information bits are mapped to the sets and the less significant information bits are mapped to the subsets. The major advantage of using MRM is that it allows using 4-QAM STTCs for constellation mapping.

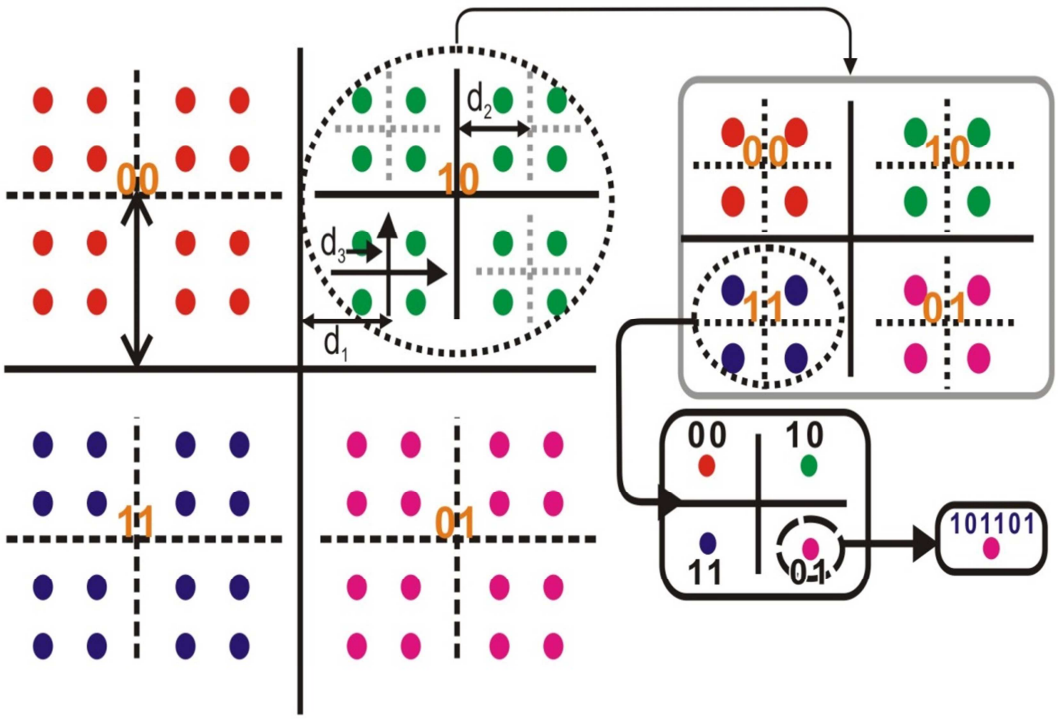

Figure 3.2: Constellation Partitioning Strategy used in MLSTTCs

Elaborating the constellation mapping further, the output of encoder *S(1)* in the translated symbol is mapped to centroid of the sets and the output of encoder *S(2)* is mapped to centroid of subset and so on with output of *S(L)* is mapped to the actual constellation points. In other words, the most significant coded bits in the translated symbols i.e. $x_t(1)^i$ corresponding to *S(1)* are mapped to the sets and the lower significant bits $x_t(2)^i$ corresponding to *S(2)* are mapped to subsets and finally the least significant bits $x_t(L)^i$ corresponding to *S(L)* are mapped to actual constellation points.

The mapped symbols are transmitted from the transmit antennas. The symbol transmitted from j^{th} transmit antenna at time *t* is represented by

$$Q_t^j = d_1 x_t(1)^j + d_2 x_t(2)^j \ldots + d_L x_t(L)^j \quad (3.6)$$

where j = 1... *N*, and $d_1 \ldots d_L$ are the subset distances associated with $x_t(1)$, ... $x_t(L)$ as shown in figure 3.2.

3.2.3 Decoding of MLSTTCs

The transmitted signals while travelling from transmitter to receiver are corrupted by Rayleigh fading. The faded and noisy signal received at receive antenna *i* is given by

$$r_t^i = \sum_{j=1}^{N} {h_{ij}}^t \, Q_t^j + n_t^i \quad (3.7)$$

Substituting the equation 3.6 in equation 3.7

$$r_t^i = \sum_{l=1}^{L} \sum_{j=1}^{N} {h_{ij}}^t \, d_l \, x_t(l)^j + n_t^i \quad (3.8)$$

The received signal is decoded by a multistage decoder as shown in figure 3.3. The multistage decoder uses the Viterbi algorithm to derive branch metrics for each stage. The decoding starts with estimating the least significant bits corresponding to component code *S(L)* by maximizing the likelihood function using the Viterbi algorithm. The estimated values of the component code *S(L)* $\left(\hat{x}_t(L)\right)$ are applied as input to the next decoding stage *L-1* to estimate the values of component code *S(L-1)*. In this way, the estimated values of component codes *S(L)* to *S(2)* are used by the decoder

at stage 1 to estimate the values of most significant bits corresponding to component code *S(1)*.

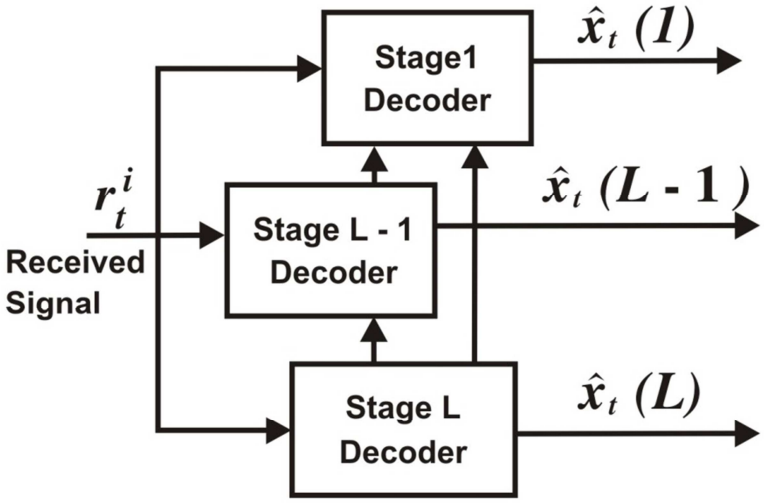

Figure 3.3: Multistage decoder for MLSTTCs

3.2.4 Branch Metrics Calculation for MLSTTCs

The branch metrics are calculated to analyse the performance of MLSTTCs. The component codes are assumed to be independent of each other. The branch metrics for the component code at level *L* i.e. $x_t(L)$ is calculated first which is then used for calculating the branch metrics for component codes at other levels.

At the decoding stage *L*, the values of $x_t(1)$ to $x_t(L-1)$ are unknown and are not considered for estimating the symbols transmitted at level *L*. The likelihood function to estimate $x_t(L)$, in the form of branch metrics, is given by

$$\mathrm{L}\big(x_t(L)\big) = log\left(\sum_{\substack{x_t(l),\\ l=1,\dots L-1}} exp\left[\frac{\left|r_t^i - \sum_{l=1}^{L}\sum_{j=1}^{N} h_{ij}{}^t d_l x_t(l)^j\right|^2}{2{\sigma_n}^2}\right]\right) \tag{3.9}$$

At the decoding stage *k*, where *1 < k < L*, the values of $x_t(k)$ are hypothesized by maximizing the likelihood function using the estimated values of stages *L* to *k+1*. It is assumed that the estimated values corresponding to stages *k-1* to 1 are unknown at the stage *k*. Based on these assumptions, the branch metric derived for stage *k*, is given by

$$log\left(\sum_{\substack{x_t(l),\\ l=1,\ldots k-1}} exp\left[\frac{\left|\begin{matrix} r_t^i-\sum_{l=1}^{k}\sum_{j=1}^{N} h_{ij}{}^t d_l x_t(l)^j \\ -\sum_{p=k+1}^{L}\sum_{j=1}^{N} h_{ij}{}^t d_p \hat{x}_t(p)^j \end{matrix}\right|^2}{2{\sigma_n}^2}\right]\right) \quad (3.10)$$

where $\hat{x}_t(p)^j$ is estimated output of the encoder p.

At the final stage, estimates of the stages 2 to L are used to the estimate the value of $x_t(1)$. The stage 1 branch metrics is given by

$$log\left(\sum_{\substack{x_t(l),\\ l=2,\ldots,L}} exp\left[\frac{\left|r_t^i-\sum_{l=1}^{L}\sum_{j=1}^{N} h_{ij}{}^t d_l x_t(l)^j\right|^2}{2{\sigma_n}^2}\right]\right) \quad (3.11)$$

3.2.5 Performance Analysis of MLSTTCs

The performance analysis of MLSTTCs has been shown by using the 16-QAM signal constellation partitioned in two levels such that d_1/d_2=2. The performance of MLSTTCs has been analysed for the wireless system with two transmit antennas by varying the number of receive antennas.

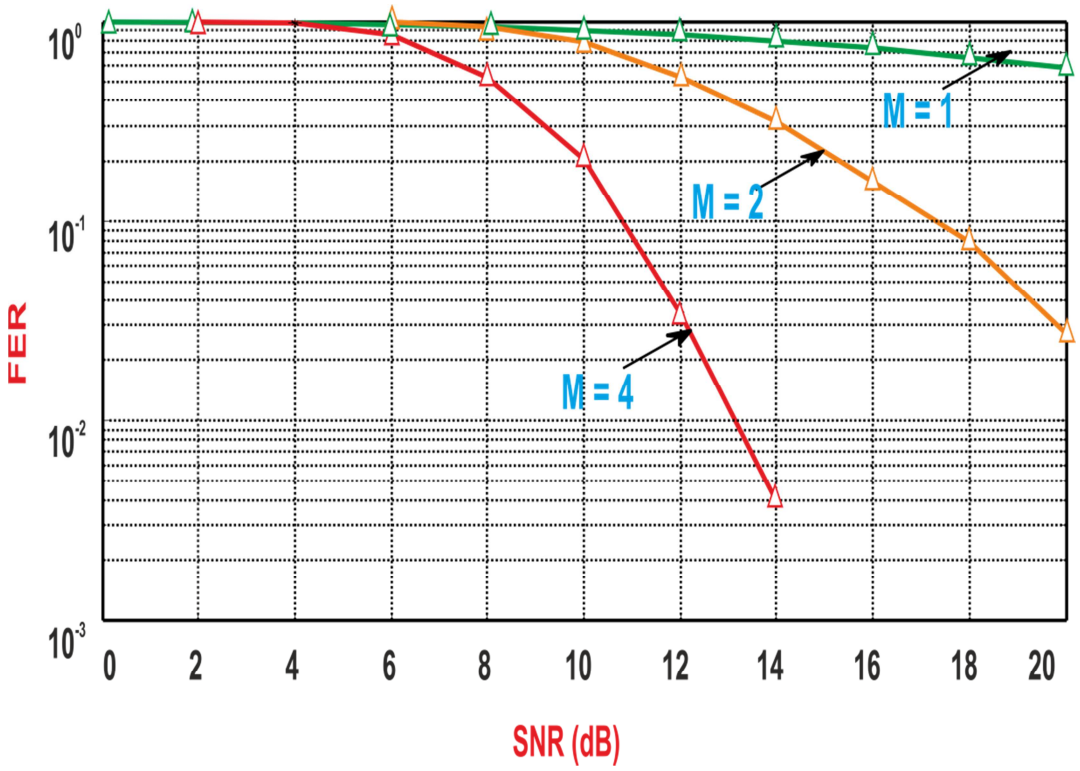

Figure 3.4: FER performance of MLSTTCs by varying number of receive antennas

Each frame transmitted from the transmit antennas consists of 130 symbols and a quasi-static Rayleigh fading channel is considered for the transmission of symbols. The perfect CSI is assumed to be available at the receiver. For simplicity, the same generator sequences are used for designing the same component STTCs for level 1 and 2. The simulation results in figure 3.4 illustrates the performance of MLSTTCs with two transmit antennas and different number of receive antennas. It is clear from the figure 3.4 that the performance of system improves with the increase in the number of receiver antennas.

3.3 DESIGN AND ANALYSIS OF MLDSTTCs

MLSTTCs use predefined STTCs as component codes in multilevel coding. The generator sequences used for designing the predefined STTCs are fixed and do not depend on the channel conditions. The performance of MLSTTCs can be improved by using dynamic STTCs as component codes by replacing the predefined STTCs. Dynamic STTCs are generated by dynamic selection of optimum generator sequences using the feedback information from the receiver. The generator sequences used to design dynamic STTCs change according to the change in the CSI at the receiver. Therefore, dynamic STTCs change dynamically with the change in the CSI.

Novel MLDSTTCs have been designed using dynamic STTCs as the component codes. The simulation results have shown that the performance MLDSTTCs is better than MLSTTCs.

3.3.1 System Model: MLDSTTCs

A MIMO system having N transmit antennas and M receive antenna is presented in figure 3.5. The channel is assumed to exhibit quasi-static Rayleigh fading. The system comprises a transmitter having STTC encoders for encoding the input data stream and a receiver having a multistage decoder for decoding the received signal. The receiver sends feedback information to the transmitter based on the comparison of current channel

profile at the receiver with a plurality of possible predefined channel profiles at the receiver. The feedback information is sent to the transmitter as an index of a predefined channel profile closest to the current channel profile at the receiver. It is assumed that the feedback is reliably delivered to the transmitter without any errors, and the feedback delay is neglected.

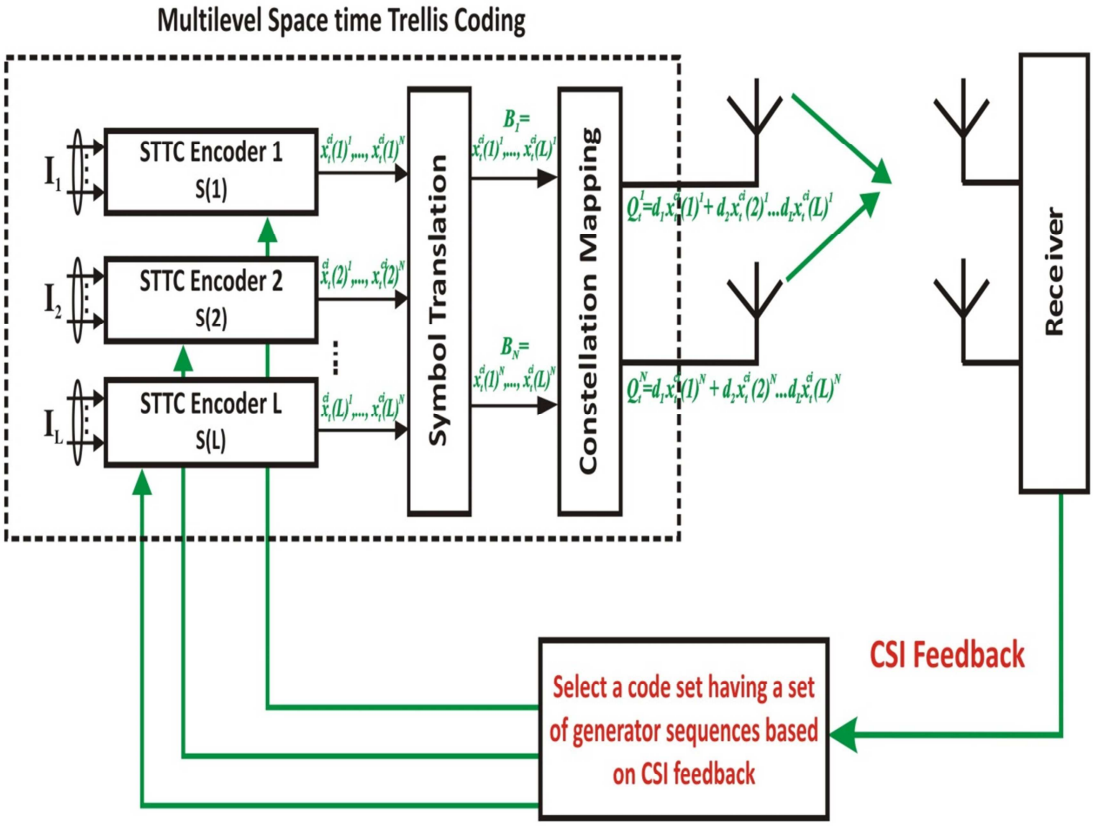

Figure 3.5 Block diagram of MLDSTTC system

3.3.2 Encoding for MLDSTTCs

The input data stream is de-multiplexed into several independent sub-streams which are applied to the STTC encoders. A code set from the multiple code sets is selected that matches best with the current channel profile using a code set selection algorithm. Each code set has a different set of generator sequences for each STTC encoder. Each code set provides best performance corresponding to a particular channel profile. As the channel profile changes from one profile to another, the code set of generator sequences used for

encoding the data stream also changes from one codeset to another. The outputs of the STTC encoders are mapped to symbols from an enlarged constellation. The mapped symbols are distributed to different antennas and then transmitted simultaneously.

3.3.2.1 Code Set Selection Algorithm

The steps of code set selection algorithm are:

• Calculate the sum of channel power gain between all transmit antennas *N* and all the receive antennas *M* for current profile at the receiver.

$$G=\sum_{j=1}^{N}\sum_{i=1}^{M}\left|h_{ij}{}^{t}\right|^{2}\ 1\le i\le M,\ 1\le j\le N \tag{3.12}$$

• Compare the power gain at the current channel profile with power gains corresponding to the predefined channel profiles.

• Determine a predefined channel profile which has the power gain closest to the power gain of the current channel profile.

• Send an index of the predefined channel profile closest to the power gain of the current channel profile to the transmitter.

• Retrieve, at transmitter, a code set of generator sequences corresponding to the index of the determined predefined channel profile.

The code set selection algorithm can be performed at the transmitter and receiver. When the perfect CSI is assumed to be available at the transmitter, the code set algorithm is performed at the transmitter, and path gains at the transmitter are used to calculate the power gain.

3.3.2.2 Dynamic Space-Time Trellis Encoder

Figure 3.6 shows a STTC encoder *l* with feedback from the receiver. A code set having a set of generator sequences is selected for the STTC encoder that provides best performance at the current channel profile at the receiver. The selected code set CS^{ci} at channel profile *ci* is given as

$$CS^{ci} = [(G_1^{1,ci}, G_1^{2,ci}, \dots G_1^{m,ci}), (G_2^{1,ci}, G_2^{2,ci}, \dots G_2^{m,ci}),$$

$$\dots (G_l^{1,ci}, G_l^{2,ci}, \dots G_l^{m,ci}), \dots \ G_L^{1,ci}, G_L^{2,ci}, \dots G_L^{m,ci}] \quad (3.13)$$

where $(G_l^{1,ci}, G_l^{2,ci}, \dots G_l^{m,ci})$ is set of generator sequences for the STTC encoder *l*.

The STTC encoder *l* receives *m* binary input sequences corresponding to data stream I_l that are multiplied by the generator sequences for the corresponding encoder *l* in the selected code set. The generator sequences for the STTC encoder *l* at the channel profile *ci* are given by

$$G_l^{1,ci} = [(g_{0,1}^{1,ci} \dots g_{0,N}^{1,ci}), (g_{1,1}^{1,ci} \dots g_{1,N}^{1,ci}) \dots (g_{v1,1}^{1,ci} \dots g_{v1,N}^{1,ci}] \quad (3.14)$$

$$G_l^{2,ci} = [(g_{0,1}^{2,ci} \dots g_{0,N}^{2,ci}), (g_{1,1}^{2,ci} \dots g_{1,N}^{2,ci}) \dots (g_{v2,1}^{2,ci} \dots g_{v2,N}^{2,ci})] \quad (3.15)$$

$$G_l^{m,ci} = [(g_{0,1}^{m,ci} \dots g_{0,N}^{m,ci}), (g_{1,1}^{m,ci} \dots g_{1,N}^{m,ci}) \dots (g_{vm,1}^{m,ci} \dots g_{vm,N}^{m,ci})] \quad (3.16)$$

where $g_{j,i}^{k,ci}$, $k = 1, 2, \dots, m$, $j = 1, 2, \dots, vk$, $i = 1, 2, \dots, N$, is an element of the 4-QAM constellation set and v_k is the memory order of the k^{th} shift register.

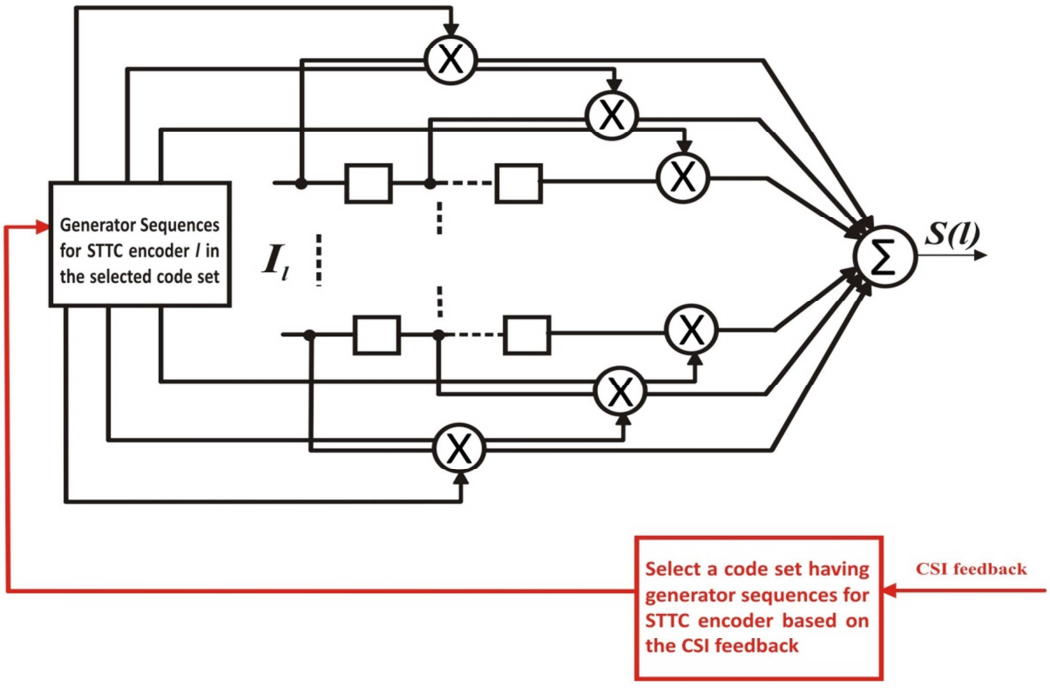

Figure 3.6: Dynamic space-time trellis encoder

The multiplier outputs from all shift registers are added to generate dynamic STTCs. The output from the STTC encoder *l* is given by

$$S(l) = x_t^{ci}(l)^1, x_t^{ci}(l)^2 \dots x_t^{ci}(l)^N \quad (3.17)$$

The equation 3.17 represents dynamic STTC at channel profile *ci*. The dynamic STTCs provide higher degrees of diversity for data transmission to the receiver and allow faster adaptation to the channel conditions using the feedback from the receiver.

As shown in figure 3.5, MLDSTTC system uses *L* STTCs encoders performing space-time trellis coding on their respective input streams. The encoder output for STTC encoder 1 is given by

$$S(1) = x_t^{ci}(1)^1, x_t^{ci}(1)^2 \dots x_t^{ci}(1)^N \quad (3.18)$$

Similarly, the encoder output for STTC encoder *L* is given by

$$S(L) = x_t^{ci}(L)^1, x_t^{ci}(L)^2 \dots x_t^{ci}(L)^N \quad (3.19)$$

Each generated dynamic STTC is used as a component code in multilevel coding by partitioning an underlying M_{ary}-QAM signal constellation using the MRM approach as discussed in section 3.2.2.

The outputs from all *L* encoders, *S(1)...S(L)*, are applied to a symbol translator. The translated outputs are denoted by

$$B(1) = x_t^{ci}(1)^1, x_t^{ci}(2)^1 \dots x_t^{ci}(L)^1 \quad (3.20)$$

$$B(N) = x_t^{ci}(1)^N, x_t^{ci}(2)^N \dots x_t^{ci}(L)^N \quad (3.21)$$

The translated outputs are applied to a constellation mapper. $x_t^{ci}(L)$ in each translated output is mapped to the actual constellation points while $x_t^{ci}(1) \dots x_t^{ci}(L-1)$ respectively are mapped to the virtual subset centre points. The mapped symbols are then transmitted through *N* antennas. The symbol Q_t^j transmitted at time *t* and channel condition *ci* by the j^{th} transmit antenna is denoted by

$$Q_t^j = d_1 x_t^{ci}(1)^j + d_2 x_t^{ci}(2)^j \dots d_L x_t^{ci}(L)^j \quad (3.22)$$

where j = 1... N, and d_1... d_L are the subset distances corresponding to $x_t^{ci}(1)$, ... $x_t^{ci}(L)$.

3.3.3 Decoding of MLDSTTCs

The received signal is a noisy superposition of independently Rayleigh faded versions of the transmitted signals. The signal received at the receive antenna i is given by

$$r_t^i = \sum_{j=1}^{N} {h_{ij}}^t \, Q_t^j + \, n_t^i \tag{3.23}$$

where n_t^i is the noise associated with the receive antenna i at time t. Substituting the equation 3.22 in equation 3.23, r_t^i is given as

$$r_t^i = \sum_{l=1}^{L} \sum_{j=1}^{N} {h_{ij}}^t \, d_l \, x_t^{ci}(l)^j + \, n_t^i \tag{3.24}$$

The received signal is decoded by the multistage decoder as shown in figure 3.3 which uses the Viterbi algorithm to derive the branch metrics for each stage over the duration of a data frame. The decoder on stage L decodes the component code encoded by the STTC encoder L and estimate the value of $x_t^{ci}(L)$. The estimated value of $x_t^{ci}(L)$ (i.e $\hat{x}_t^{ci}(L)$) is applied as input to decoding stage *L-1* to decode the values of $x_t^{ci}(L-1)$. Similarly, at the final stage, estimated values from stages L to 2 are used to estimate the value of x_t^{ci}*(1).*

3.3.4 Branch Metrics Calculation for MLDSTTCs

At the decoding stage L, the values of x_t^{ci}*(1)* to $x_t^{ci}(L-1)$ are unknown and are treated as nuisance variables. The likelihood function to estimate $x_t^{ci}(L)$ in the form of branch metrics is given by

$$\mathrm{L}\left(x_t^{ci}(L)\right) = log\left(\sum_{\substack{x_t^{ci}(l), \\ l=1,\ldots L-1}} exp\left[\frac{\left|r_t^i - \sum_{l=1}^{L}\sum_{j=1}^{N} {h_{ij}}^t d_l x_t^{ci}(l)^j\right|^2}{2{\sigma_n}^2}\right]\right) \tag{3.25}$$

At the decoding stage k, where $1 < k < L$, the values of $x_t^{ci}(k)$ are hypothesized by maximizing the likelihood function using the estimated values of stages L to $k+1$. It is assumed that the estimated values corresponding to the stages *k-1* to 1 are unknown. Based on these assumptions, the branch metric derived for stage k is given by

$$log\left(\sum_{\substack{x_t^{ci}(l),\\ l=1,\ldots k-1}} exp\left[\frac{\left|\begin{array}{l} r_t^i-\sum_{l=1}^{k}\sum_{j=1}^{N} h_{ij}{}^t d_l x_t^{ci}(l)^j \\ -\sum_{p=k+1}^{L}\sum_{j=1}^{N} h_{ij}{}^t d_p \hat{x}_t^{ci}(p)^j \end{array}\right|^2}{2\sigma_n{}^2}\right]\right) \quad (3.26)$$

where $\hat{x}_t^{ci}(p)^j$ is estimated output of the encoder *p*.

At the final stage, estimates of stages 2 to *L* are used to the estimate the value $x_t^{ci}(1)$. The stage 1 branch metrics is given by

$$log\left(\sum_{\substack{x_t^{ci}(l),\\ l=2,\ldots,L}} exp\left[\frac{\left|r_t^i-\sum_{l=1}^{L}\sum_{j=1}^{N} h_{ij}{}^t d_l x_t^{ci}(l)^j\right|^2}{2\sigma_n{}^2}\right]\right) \quad (3.27)$$

3.3.5 Simulation Results for MLDSTTCs

The performance analysis of MLDSTTCs has been shown by using 16-QAM signal constellation partitioned in two levels such that d_1/d_2=2. The performance of MLDSTTCs has been analysed for the wireless systems having two transmit antennas and up to four receive antennas. Each frame transmitted from the transmit antennas consists of 130 symbols and a quasi-static fading channel is considered for transmission of symbols.

The perfect CSI is assumed to be available at the receiver. The feedback information indicating index of the code set is sent to transmitter. A zero delay feedback channel is considered because a delay in the feedback means that the feedback is outdated due to variations of the channel conditions. Thus, when the transmitter receives the feedback information, it may correspond to an old channel profile. Therefore, due to the feedback delay, the feedback information will be imperfect and will result in loss of performance.

The performance of MLDSTTCs has been analysed by considering four different possible predefined channel profiles at the receiver. The generator sequences for each STTC encoder in the selected code set CS^{ci} at predefined channel profiles *ci* are given in table 3.1. For simplicity, the same generator sequences have been used for each encoder on level 1 and level 2 at each channel profile.

Table 3.1: Code set for different predefined channel profiles

Predetermined Channel Profile	Selected Code Set	Set of Generator sequence in the selected Code Set	
		Encoder S(1)	Encoder S(2)
C1	CS^{c1}	$G_l^{1,ci}$ = [(02), (20)] $G_l^{2,ci}$ = [(01), (10)]	$G_l^{1,ci}$ = [(02), (20)] $G_l^{2,ci}$ = [(01), (10)]
C2	CS^{c2}	$G_l^{1,ci}$ = [(02), (21)] $G_l^{2,ci}$ = [(11), (20)]	$G_l^{1,ci}$ = [(02), (21)] $G_l^{2,ci}$ = [(11), (20)]
C3	CS^{c3}	$G_l^{1,ci}$ = [(12), (20)] $G_l^{2,ci}$ = [(01), (20)]	$G_l^{1,ci}$ = [(12), (20)] $G_l^{2,ci}$ = [(01), (20)]
C4	CS^{c4}	$G_l^{1,ci}$ = [(02), (22)] $G_l^{2,ci}$ = [(01), (22)]	$G_l^{1,ci}$ = [(02), (22)] $G_l^{2,ci}$ = [(01), (22)]

In figure 3.7, the performance of dynamic STTCs has been evaluated and compared with the performance of STTCs by varying the number of receive antennas. The performance comparisons show that the performance of the dynamic STTCs has been improved by about 0.7 dB at FER of 10^{-2} due to dynamic selection of the optimum generator sequences.

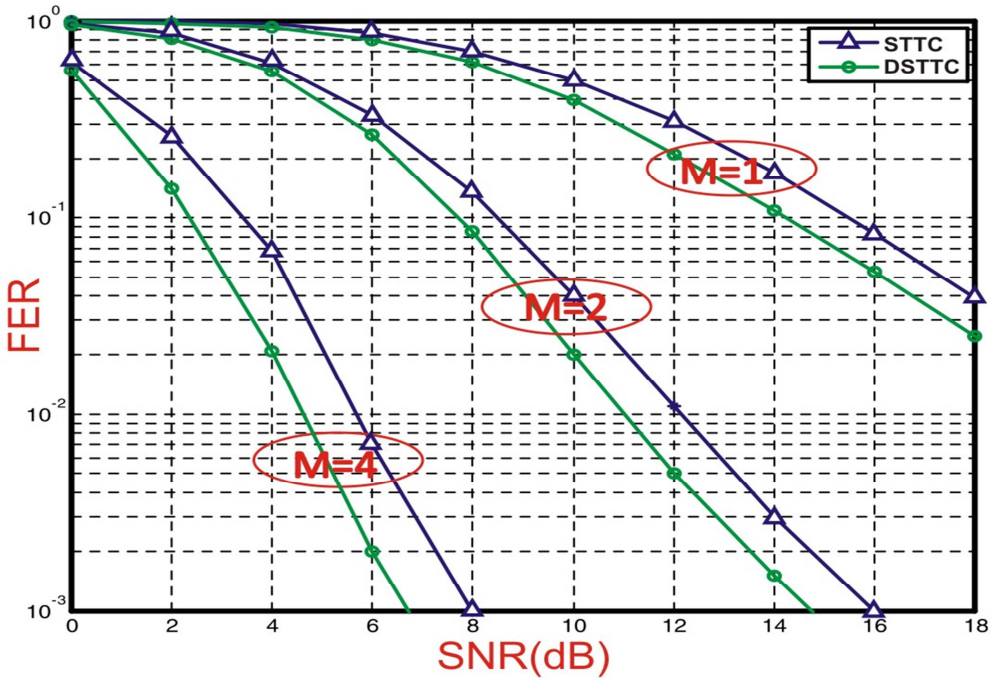

Figure 3.7: Performance comparison of STTCs and DSTTCs with 2 transmit and 1, 2 and 4 receive antennas

The performance evaluation of MLDSTTCs using two bits feedback and varying the number of receive antennas is shown in figure 3.8. Figure 3.8 also shows the performance comparison of MLDSTTCs and MLSTTCs. It can be seen that FER performance of the MLDSTTCs is superior by about 1.1 dB to MLSTTCs at FER of 10^{-1}.

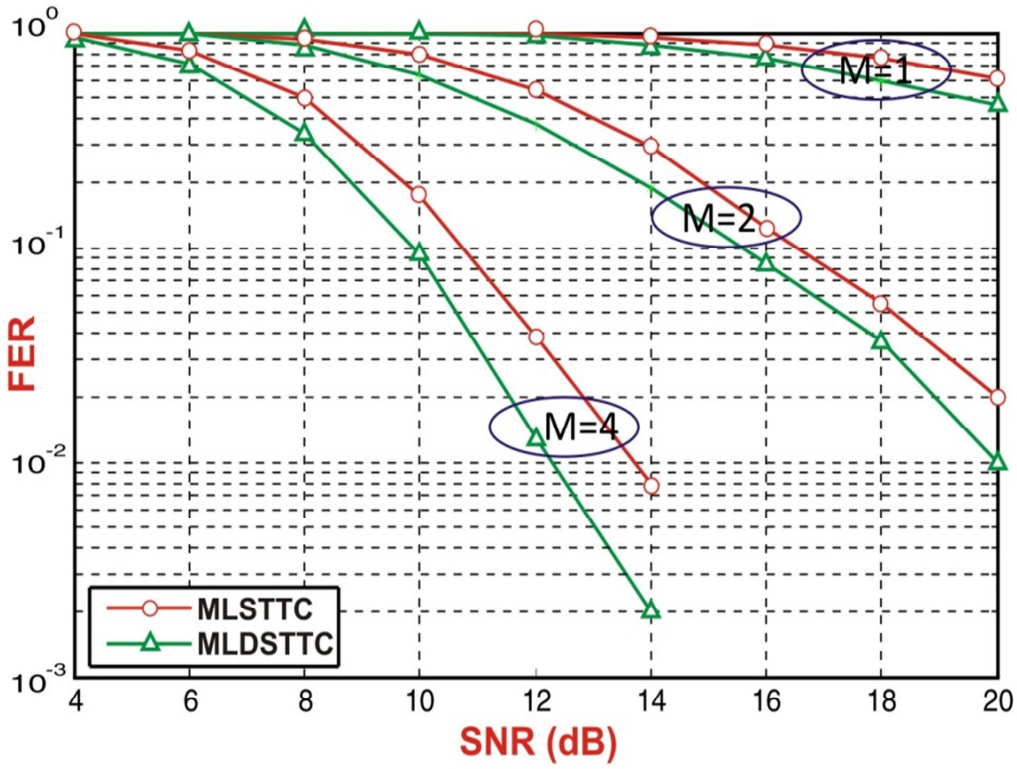

Figure 3.8: Performance comparison of MLSTTCs and MLDSTTCs using 2 transmit and 1, 2 and 4 receive antennas

Figure 3.9 shows error performance of MLDSTTCs for 2 transmit antennas and 2 receive antenna by varying the number of feedback bits. The receiver is assumed store 2^n predefined channel profiles for providing n bits of feedback. For example, when eight predefined channel profiles are considered at the receiver, then three bits of feedback information is sent from the receiver to the transmitter. The simulation results show that by increasing the number of feedback bits i.e. by increasing the number of predetermined number of channel profiles at receiver, the error performance of MLDSTTCs is improved.

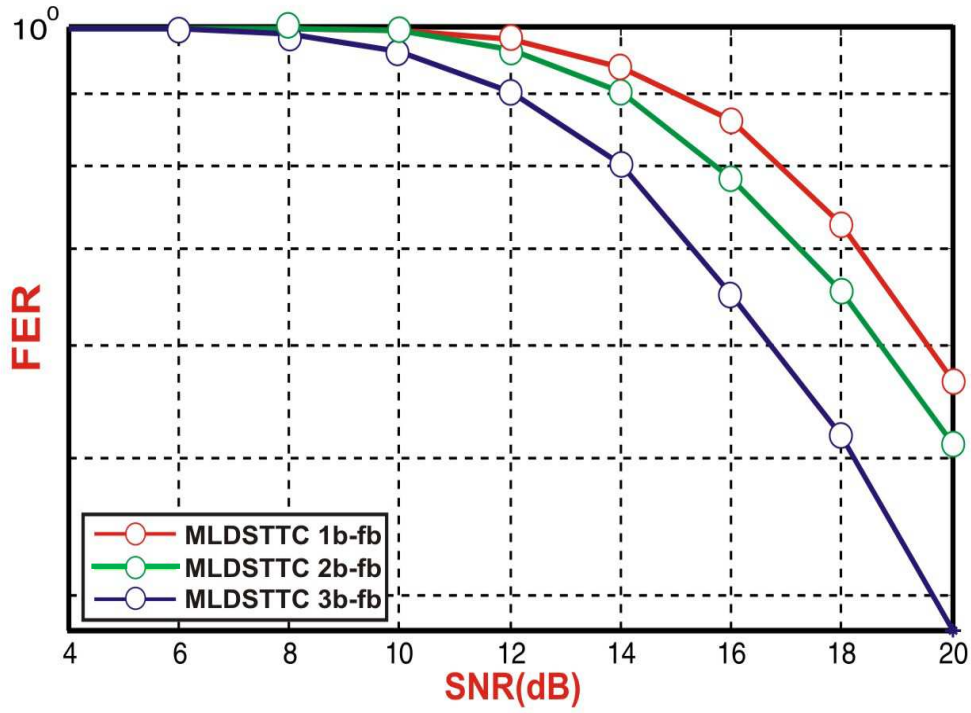

Figure 3.9: Performance comparison of MLDSTTCs for 2 transmit and 2 receive antenna using 1, 2, 3 feedback bits

3.4 DESIGN AND ANALYSIS OF GMLSTTCs

MLSTTCs use a single component code at each level and do not use grouping of transmit antennas. To improve the spectral efficiency of MLSTTCs, GMLSTTCs are designed by using the predefined grouping of the transmit antennas in MLSTTCs. GMLSTTCs use of a single component code at some levels and multiple component codes on remaining levels. The grouping of transmit antennas and using multiple component codes at particular levels enable to transmit two or more number of symbols in one time slot.

The levels that use single component code transmit the coded information to all the transmit antennas simultaneously whereas the levels which use the multiple component codes transmit the coded information to their respective groups of transmit antennas. For example, for a level *i* using two component codes, the coded information corresponding to first component code is transmitted to first group of antennas and the coded

information corresponding to second component code is transmitted to the second group of transmit antennas. In this way, depending on the number of component codes, multiple symbols are transmitted per time slot to improve the spectral efficiency. GMLSTTCs provide a spectral efficiency of 6 bits/s/Hz in comparison to 4 bits/s/Hz provided by MLSTTCs using 16 QAM constellation partitioned in two levels.

3.4.1 System Model and Encoding for GMLSTTCs

A block diagram for GMLSTTC system is given in figure 3.10. At the transmitter, each STTC encoder receives a data stream, and performs space-time trellis coding on the data stream. The encoders 1 to L-1 generate STTCs which span all N transmit antennas. The STTC encoder l output is given by

$$S(l) = x_t(l)^1, x_t(l)^2, ..., x_t(l)^N \text{ where } l=1, 2,\ldots L\text{-}1 \quad (3.28)$$

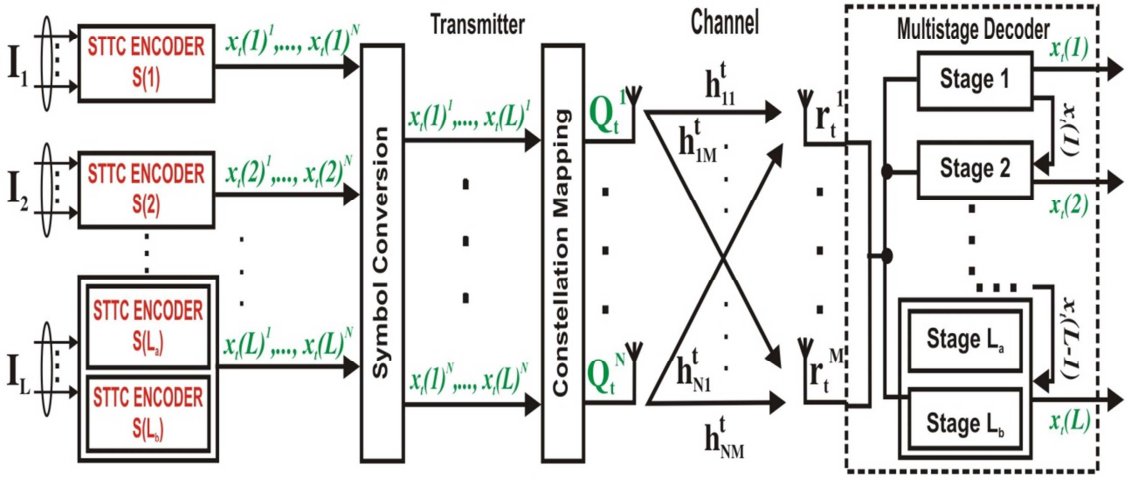

Figure 3.10: Block diagram of GMLSTTC system

Two parallel STTC encoders L_a and L_b are used at level L for generating two STTCs, each spanning through a group of $N/2$ transmit antennas. For example, STTC encoder L_a is used for generating STTCs which span through a first group of transmit antennas 1 to $N/2$ whereas STTC encoder L_b is used for generating STTCs which span through another group of transmit antennas $N/2+1$ and N.

The groups of antennas are predefined while designing GMLSTTCs and cannot be changed dynamically using the current CSI at transmitter or receiver. The main purpose of grouping the transmit antennas at level L is to transmit multiple symbols in one time slot to improve the spectral efficiency. The STTC encoder L_a output is given by

$$S(L_a) = x_t(L_a)^1, x_t(L_a)^2, ..., x_t(L_a)^{N/2} \quad (3.29)$$

In the same way, STTC encoder L_b output is represented as

$$S(L_b) = x_t(L_b)^{N/2+1}, x_t(L_b)^{N/2+2}, ..., x_t(L_b)^N \quad (3.30)$$

The output at level L, which is combination of output of STTC encoders L_a and L_b, is given by

$$S(L)= x_t(L_a)^1, x_t(L_a)^2, ..., x_t(L_a)^{N/2}, x_t(L_b)^{N/2+1}, x_t(L_b)^{N/2+2}, ..., x_t(L_b)^N \quad (3..31)$$

3.4.2 $\mathcal{M}$-way constellation partitioning

The partitioning strategy used in designing GMLSTTCs is $\mathcal{M}$-way partitioning. In $\mathcal{M}$-way partitioning, the given signal constellation is partitioned in subsets such that the Euclidean distance increases with each level of partition. An example of $\mathcal{M}$-way partitioning of 16-QAM in two partitions is illustrated in figure 3.11.

The 16-QAM constellation is partitioned in subsets, each comprising four constellation points as shown by circle in blue color. Each subset of four points is further partitioned into four subsets, each subset comprising a single constellation point as shown by a dotted circle in figure 3.11. The Euclidean distance of level 2 (d_2) is greater than the Euclidean distance of level 1 (d_1). One or more number of components codes can be used at level depending upon the number of encoders used at the corresponding level. The component code $S(1)$ at level 1 selects one of the subsets and the component codes $S(L_a)$ and $S(L_b)$ at level 2 select the constellation points from the selected subset.

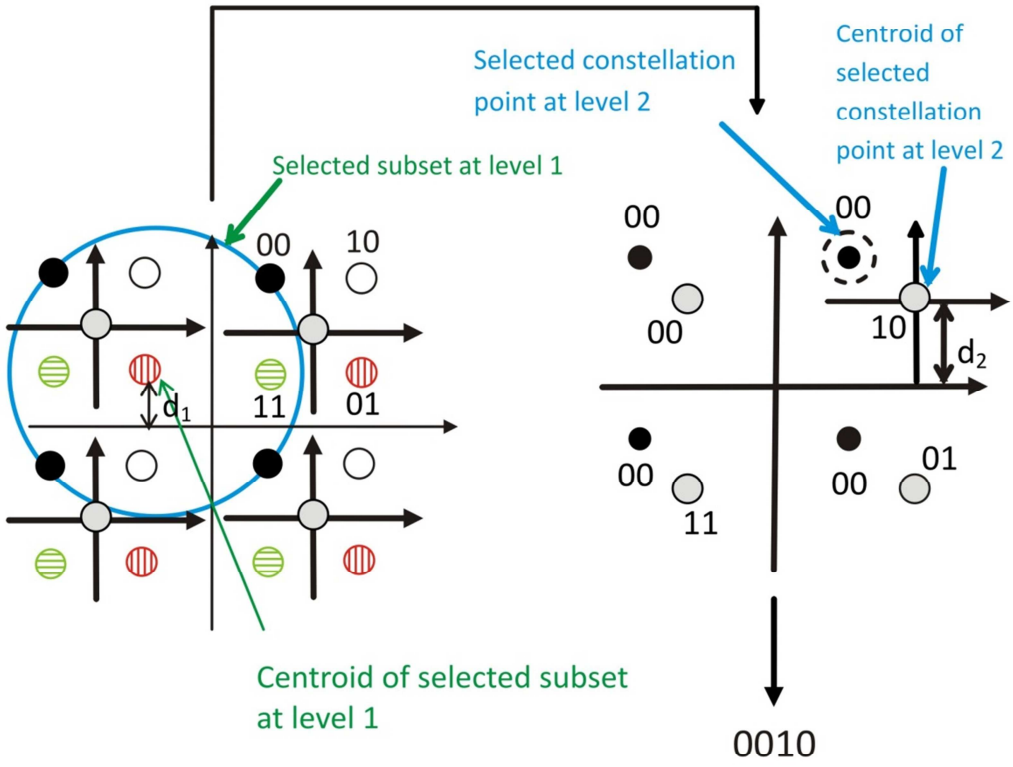

Figure 3.11: $\mathcal{M}$-way partitioning for 16-QAM constellation

Collectively, the outputs from the L encoders, i.e. *S(1),...S(L),* are fed in a symbol translator to generate N translated symbols which are mapped to M_{ary}-QAM signal constellations using a constellation mapper. The mapped signals are then transmitted through N antennas. The symbol Q_t^j transmitted from j^{th} transmit antenna at time t is given by

$$Q_t^j = d_1 x_t(1)^j + d_2 x_t(2)^j \dots d_L x_t(L_b)^j \quad (3.32)$$

where $j = 1, ...,N$, and $d_1, ..., d_L$ represent the subset distances for levels 1 to L.

3.4.3 GMLSTTC Decoder

The transmitted signals while travelling from the transmitter to the receiver are corrupted by Rayleigh fading. The faded and noisy signal received at the receive antenna i is given by:

$$r_t^i = \sum_{j=1}^{N} h_{ij}{}^t \, Q_t^j + n_t^i \quad (3.33)$$

The received signal is decoded by a multistage decoder employing two parallel decoders at final stage which is shown in figure 3.12. A Viterbi algorithm is used by the multistage decoder to derive the branch metrics for each stage. At 1st stage, the component code *S(1)* is estimated as $\hat{x}_t\,(1)$ and the estimated value $\hat{x}_t\,(1)$ is passed to the second decoding stage to estimate the value of $\hat{x}_t\,(2)$. Similarly, the decoder at final stage, which comprises of two parallel decoders, uses the estimated values of previous stages to estimate the values of $S(L_a)$ and $S(L_b)$.

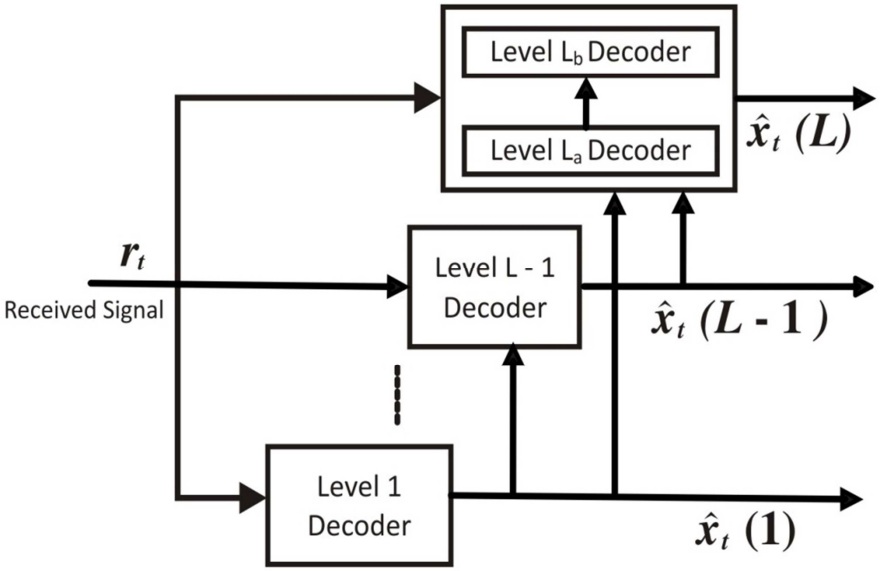

Figure 3.12: Multi-stage decoder for GMLSTTCs

3.4.4 Branch Metric Calculation for GMLSTTCs

A MIMO system with four transmit antennas and a 16-QAM signal constellation partitioned in two levels have been considered to evaluate the performance of GMLSTTCs. The STTC encoder at level 1 generate component STTC, *S(1)* which spans all four transmit antennas. At level 2, two STTC encoders generate identical component STTCs, each spanning a predefined group of two transmit antennas. The transmit

antennas in first group are assumed as 1 and 2 and antennas in second group are assumed as 3 and 4.

In the 1st stage of decoding, the multistage decoder employing the Viterbi algorithm is used to hypothesize the value of $x_t(1)$. The value of $x_t(2)$ is not known at the 1st stage and therefore is not considered while estimating the value of $x_t(1)$. Each STTC encoder operate independently, therefore, $x_t(1)$, and $x_t(2)$ are considered as mutually independent. It is also assumed that the channel is independent of the component STTCs and the probability of transmission of different component codes is same. Based on these assumptions, the branch metric for component code $S(1)$ is computed by

$$\max_{\substack{\tilde{x}_t^a(2)\in\{x_t^a(2)\}\\ \tilde{x}_t^b(2)\in\{x_t^b(2)\}}} \sum_{i=1}^{M} \Big| r_t^i - \sum_{j=1,2} {h_{ij}}^t d_2\, \tilde{x}_t^a(2)^{\mathrm{j}} - \sum_{j=3,4} {h_{ij}}^t d_2\, \tilde{x}_t^b(2)^{\mathrm{j}} - \sum_{j=1}^{N} {h_{ij}}^t d_1\, x_t(1)^{\mathrm{j}} \Big|^2 \quad (3.34)$$

In the second stage, one decoder is used to decode $S(L_a)$ and another decoder is used to decode $S(L_b)$. The branch metric for $S(L_a)$ is given by

$$\max_{\tilde{x}_t^b(2)\in\{x_t^b(2)\}} \sum_{i=1}^{M} \Big| r_t^i - \sum_{j=1,2} {h_{ij}}^t d_2\, x_t^a(2)^{\mathrm{j}} - \sum_{j=3,4} {h_{ij}}^t d_2\, \tilde{x}_t^b(2)^{\mathrm{j}} - \sum_{j=1}^{N} {h_{ij}}^t d_1\, \hat{x}_t(1)^{\mathrm{j}} \Big|^2 \quad (3.35)$$

Similarly, the branch metric for $S(L_b)$ is given by

$$\max_{\tilde{x}_t^a(2)\in\{x_t^a(2)\}} \sum_{i=1}^{M} \Big| r_t^i - \sum_{j=1,2} {h_{ij}}^t d_2\, \tilde{x}_t^a(2)^{\mathrm{j}} - \sum_{j=3,4} {h_{ij}}^t d_2\, x_t^b(2)^{\mathrm{j}} - \sum_{j=1}^{N} {h_{ij}}^t d_1\, \hat{x}_t(1)^{\mathrm{j}} \Big|^2 \quad (3.36)$$

3.4.5 Performance Evaluation of GMLSTTCs

The performance of the GMLSTTCs has been illustrated by using the signal constellation of 16-QAM partitioned in two levels with d_2/d_1=2. The simulation results are provided for GMLSTTCs with four transmit antennas and different number of receive

antennas. Each frame transmitted from the transmit antennas consists of 130 symbols and a quasi-static Rayleigh fading channel is considered for the transmission of symbols. The simulation results, as shown in figure 3.13, illustrates the performance of GMLSTTCs by varying the number of receive antennas. GMLSTTCs provide spectral efficiency of 6 bits/s/Hz in comparison to 4bits/s/Hz provided by MLSTTCs. The increase in spectral efficiency is achieved by grouping the transmit antennas and using separate component STTCs for each group of transmit antennas for transmitting more than one symbol per time slot.

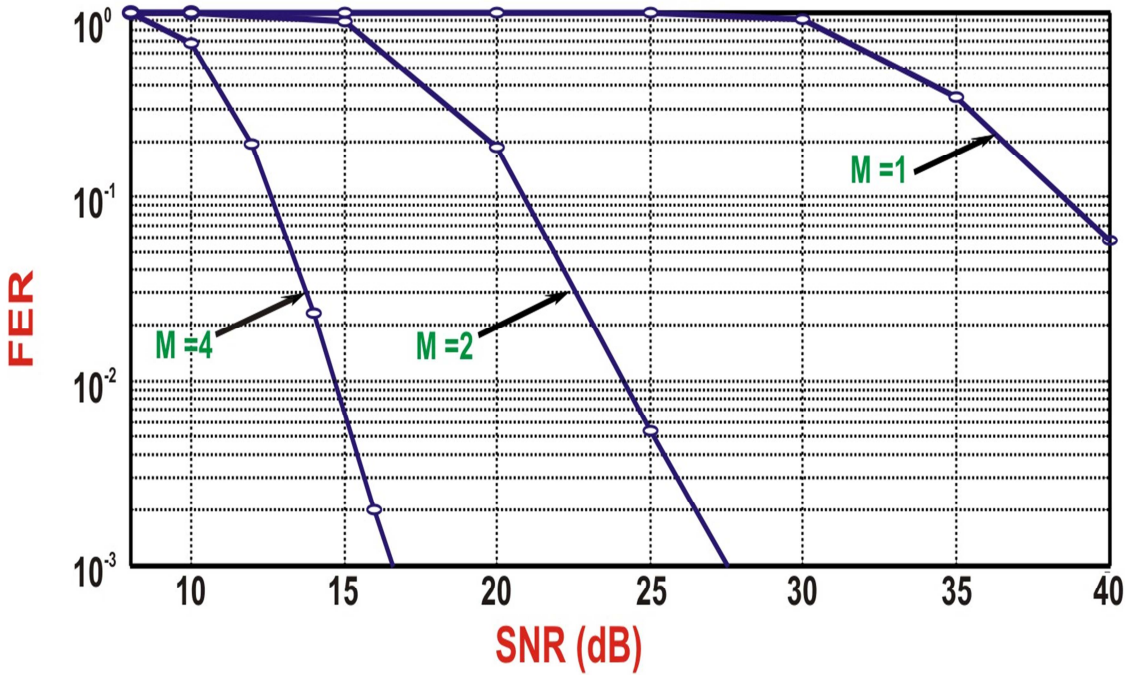

Figure 3.13: FER performance of GMLSTTCs by varying the number of receive antennas

3.5 DESIGN AND ANALYSIS OF GMLDSTTCs

GMLSTTCs use predefined STTCs as component codes in multilevel coding. The error performance of GMLSTTCs has been improved by combining GMLSTTCs with dynamic space-time coding using the CSI at the transmitter. The CSI at the transmitter is used to select a code set for generating dynamic STTCs. The dynamic STTCs are used as component codes in multilevel coding instead of predefined STTCs to generate novel

GMLDSTTCs. Analysis and simulation results show that GMLDSTTCs are superior in performance as compared to GMLSTTCs.

3.5.1 System Model and Encoding for GMLDSTTCs

A block diagram for GMLDSTTC system is shown in figure 3.14. Each STTC encoder receives a data stream and optimum generator sequences to perform dynamic space-time trellis coding. The encoders 1 to *L-1* generate the dynamic STTCs which span all *N* transmit antennas. The STTC encoder *l* output is given by

$$S(l) = x_t^{ci}(l)^1, x_t^{ci}(l)^2 \ldots x_t^{ci}(l)^N \qquad \textit{where } l=1, 2,\ldots L\text{-}1 \tag{3.37}$$

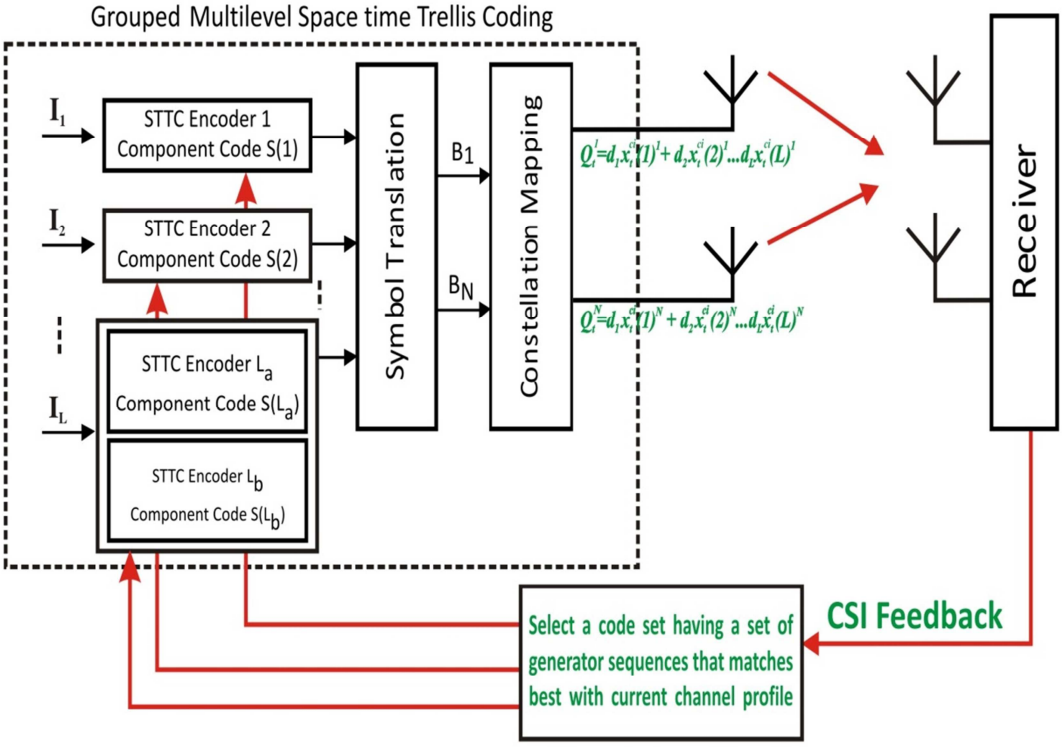

Figure 3.14: Block diagram of a GMLDSTTC system

Two parallel STTC encoders L_a and L_b are used at level *L* for generating dynamic STTCs, each spanning through a group of *N/2* transmit antennas. For example, STTC encoder L_a is used for generating dynamic STTCs which span through a group of transmit antennas 1 to *N/2* whereas STTC encoder L_b is used for generating dynamic STTCs which span through another group of transmit antennas *N/2+1* to *N*. The groups of

antennas are predefined while designing GMLSTTCs and cannot be changed dynamically. The STTC encoder L_a output is given by

$$S(L_a) = x_t^{ci}\ (L_a)^1, x_t^{ci}\ (L_a)^2, ..., x_t^{ci}\ (L_a)^{N/2} \quad (3.38)$$

In the same way, STTC encoder L_b output is represented as

$$S(L_b) = x_t^{ci}\ (L_b)^{N/2+1}, x_t^{ci}\ (L_b)^{N/2+2}, ..., x_t^{ci}\ (L_b)^N \quad (3.39)$$

The output at level L, which is combination of output of STTC encoders L_a and L_b, is given as

$$S(L) = x_t^{ci}\ (L_a)^1, x_t^{ci}\ (L_a)^2, ..., x_t^{ci}\ (L_a)^{N/2}, x_t^{ci}\ (L_b)^{N/2+1}, x_t^{ci}\ (L_b)^{N/2+2}, ..., x_t^{ci}\ (L_b)^N \quad (3.40)$$

The outputs from all L encoders, $S(1)...S(L)$, are applied to a symbol translator. The translated outputs are denoted by

$$B(1) = x_t^{ci}(1)^1, x_t^{ci}(2)^1 \dots x_t^{ci}(L_a)^1 \quad (3.41)$$

$$B(N) = x_t^{ci}(1)^N, x_t^{ci}(2)^N \dots x_t^{ci}(\mathrm{L_b})^N \quad (3.42)$$

Collectively, the outputs from the L levels, i.e. $S(1),...S(L)$, are fed in a symbol translator to generate N translated symbols. The translated symbols are mapped to M_{ary}-QAM signal constellations using a constellation mapper. The constellation mapper uses the $\mathcal{M}$-way partitioning strategy to map the translated symbols with the M_{ary}-QAM signal constellation as described in section 3.4.2. $x_t^{ci}(1)$ in each translated output is mapped to the actual constellation points, while $x_t^{ci}(2)\ \dots x_t^{ci}(L)$ respectively are mapped to the subset centre points. The mapped symbols are then transmitted through N antennas. The symbol $Q_t^{j,ci}$ transmitted at time t and channel condition ci by the j^{th} transmit antenna is denoted by

$$Q_t^{j,ci} = d_1 x_t^{ci}(1)^j + d_2 x_t^{ci}(2)^j \dots d_L x_t^{ci}(L_b)^j \quad (3.43)$$

where $j = 1... N$, and $d_1... d_L$ are the subset distances corresponding to $x_t^{ci}(1), ..., x_t^{ci}(L)$.

3.5.2 Decoding of GMLDSTTCs

The transmitted signals while travelling from transmitter to receiver are corrupted by Rayleigh fading. The faded and noisy signal received at the receive antenna *i* is given by:

$$r_t^i = \sum_{j=1}^{N} {h_{ij}}^t \, Q_t^{j,ci} + n_t^i \tag{3.44}$$

Substituting the equation (3.43) in equation (3.44)

$$r_t^i = \sum_{l=1}^{L} \sum_{j=1}^{N} {h_{ij}}^t \, d_l \, x_t^{ci}(l)^j + n_t^i \tag{3.45}$$

The received signal is decoded by the multistage decoder employing two parallel decoders at final stage which is shown in figure 3.12. The Viterbi algorithm used by the multistage decoder derives the branch metrics for each stage. At the 1st stage, the component code *S(1)* is estimated and the estimated value of *S(1)* is passed to the second decoding stage to estimate the value of *S(2)*. Similarly, the decoder at final stage which comprises of two parallel decoders uses the estimated values of previous stages to decode the values of $S(L_a)$ and $S(L_b)$.

3.5.3 Branch Metrics Calculation for GMLDSTTCs

To evaluate the performance of GMLDSTTCs, a system with four transmit antennas and a constellation of 16-QAM partitioned in two levels have been considered. The STTC encoder at level 1 generate component STTC *S(1)* which spans all four transmit antennas. At level 2, two STTC encoders generate identical component STTCs, each spanning a predefined group of two antennas. The transmit antennas in first group are 1 and 2 and antennas in second group are 3 and 4. The component code for group 1 has been referred to as $S(L_a)$ and for group 2 as $S(L_b)$. The received signal at the i^{th} receive antenna at time *t* for the system as considered above is given by

$$r_t^i = \sum_{j=1}^{4} {h_{ij}}^t \, d_1 \, x_t^{ci}(1)^j + \sum_{j=1}^{4} {h_{ij}}^t \, d_2 \, x_t^{ci}(2)^j + n_t^i \tag{3.46}$$

The conditional probability density function (pdf) of r_t^i conditioned on the channel matrix and encoder outputs for L levels may be written as $P\left(r_t^i \middle|\, x_t^{ci}(1), x_t^{ci}(2) \ldots x_t^{ci}(L), H_t\right)$.

In the 1st stage of decoding, the multistage decoder employing the Viterbi algorithm is used to hypothesize the value of $x_t^{ci}(1)$. The values of $x_t^{ci}(2)$ are unknown at this stage and therefore not considered while estimating the value of $x_t^{ci}(1)$. Based on this assumption, the conditional PDF can be written as

$$P\left(r_t^i \middle|\, x_t^{ci}(1), H_t\right) = \sum_{\substack{x_t(l),\\ l=1,2}} P\left(x_t^{ci}(2) \middle| x_t^{ci}(1), H_t\right) P\left(r_t^i \mid x_t^{ci}(2), H_t\right) \qquad (3.47)$$

Each STTC encoder operates independently, therefore $x_t^{ci}(1)$ and $x_t^{ci}(2)$ are considered as mutually independent. It is also assumed the channel is independent of the component STTCs and the probability of transmission of different component codes is same. Based on these assumptions, the probability $P\left(x_t^{ci}(2) \middle| x_t^{ci}(1), H_t\right)$ in the expression on the right hand side of equation 3.47 reduces to a constant and can be ignored when maximizing the likelihood function. Based on these assumptions, the equation 3.47 can be written as

$$P\left(r_t^i \middle| x_t^{ci}(1),\ x_t^{ci}(2),\ H_t\right) =$$

$$\frac{1}{\left(\sqrt{2\pi}{\sigma_n}^2\right)} exp\left[\frac{\left| \begin{array}{c} r_t^i - \sum_{j=1}^{2} {h_{ij}}^t\, d_2\, \tilde{x}_t^{a,ci}(2)^j - \sum_{j=3}^{4} {h_{ij}}^t\, d_2\, \tilde{x}_t^{b,ci}(2)^j \\ - \sum_{j=1}^{N} {h_{ij}}^t\, d_1\, x_t^{ci}(1)^j \end{array} \right|^2}{2{\sigma_n}^2}\right] \qquad (3.48)$$

Using the equation 3.48 and ignoring the constant term, the likelihood function for $x_t^{ci}(1)$ is given by

$$L\left(x_t^{ci}(1)\right) = P\left(r_t^i \middle| x_t^{ci}(1), H_t\right) \propto$$

$$exp\left[\frac{\left|\begin{array}{c} r_t^i - \sum_{j=1}^{2} {h_{ij}}^t\, d_2\, \tilde{x}_t^{a,ci}(2)^j - \sum_{j=3}^{4} {h_{ij}}^t\, d_2\, \tilde{x}_t^{b,ci}(2)^j \\ -\sum_{j=1}^{N} {h_{ij}}^t\, d_1 x_t^{ci}(1)^j \end{array}\right|^2}{2{\sigma_n}^2}\right] \tag{3.49}$$

Therefore, the branch metric for *S(1)* at level 1 is given by:

$$\max_{\substack{\tilde{x}_t^{a,ci}(2)\in\{x_t^{a,ci}(2)\} \\ \tilde{x}_t^{b,ci}(2)\in\{x_t^{b,ci}(2)\}}} \sum_{i=1}^{M} \left| r_t^i - \sum_{j=1}^{2} {h_{ij}}^t\, d_2\, \tilde{x}_t^{a,ci}(2)^j - \sum_{j=3}^{4} {h_{ij}}^t\, d_2\, \tilde{x}_t^{b,ci}(2)^j - \sum_{j=1}^{N} {h_{ij}}^t\, d_1\, x_t^{ci}(1)^j \right|^2 \tag{3.50}$$

In second stage, one decoder is used to decode $S(L_a)$ and another decoder is used to decode $S(L_b)$.

The branch metric for $S(L_a)$ is given by

$$\max_{\tilde{x}_t^{b,ci}(2)\in\{x_t^{b,ci}(2)\}} \sum_{i=1}^{M} \left| r_t^i - \sum_{j=1}^{2} {h_{ij}}^t\, d_2\, x_t^{a,ci}(2)^j - \sum_{j=3}^{4} {h_{ij}}^t\, d_2\, \tilde{x}_t^{b,ci}(2)^j - \sum_{j=1}^{N} {h_{ij}}^t\, d_1\, \widehat{x_t^{ci}}(1)^j \right|^2 \tag{3.51}$$

Similarly, the branch metric for $S(L_b)$ is given by

$$\max_{\tilde{x}_t^{a}(2)\in\{x_t^{a}(2)\}} \sum_{i=1}^{M} \left| r_t^i - \sum_{j=1}^{2} {h_{ij}}^t\, d_2\, \tilde{x}_t^{a,ci}(2)^j - \sum_{j=3}^{4} {h_{ij}}^t\, d_2\, x_t^{b,ci}(2)^j - \sum_{j=1}^{N} {h_{ij}}^t\, d_1\, x_t^{ci}(1)^j \right|^2 \tag{3.52}$$

3.5.4 Simulation Results for GMLDSTTCs

The simulation results are provided for GMLDSTTCs with four transmit antennas, 16-QAM signal constellation partitioned in two levels, and different number of receive antennas. The transmitter is assumed to have knowledge of four different possible predefined channel profiles. The generator sequences for each encoder in the selected code set CS^{ci} at the predefined channel profiles *ci* are given in table 3.1. Figure 3.15

depicts the performance comparison of GMLSTTCs and proposed GMLDSTTCs. The simulation results show that FER performance of GMLDSTTCs is superior by 1.6 dB to the GMLSTTCs at FER of 10^{-2} and M=2.

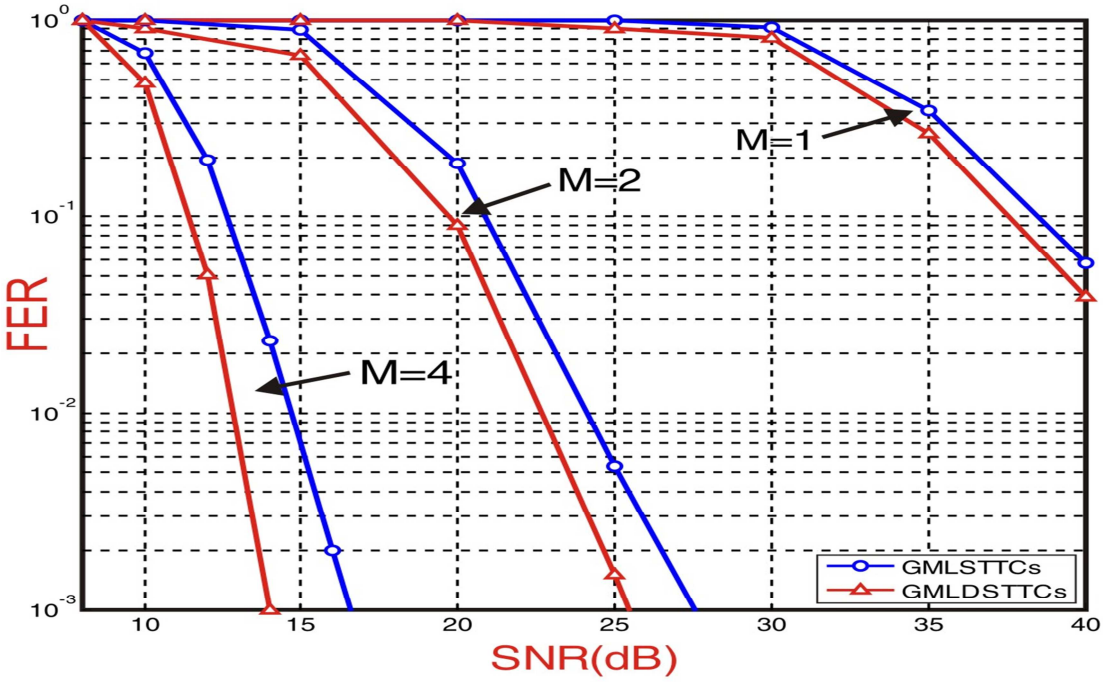

Figure 3.15: Performance comparison of GMLSTTCs and proposed GMLDSTTCs with 4 transmit and 1, 2, and 4 receive antennas.

3.6 COMPLEXITY CONSIDERATIONS

It has been shown in [181] that the system combining STTCs and multilevel coding offers significantly low complexity in comparison to the STTC system. The main reason for the low complexity is mapping of simpler component codes to different partitions of the enlarged signal constellation and using a multistage decoder at the receiver. The complexity of the STTC system increases exponentially in comparison with the complexity of the system using the combination of multilevel coding and STTCs where the complexity increases linearly with the size of the underlying constellation.

The minimum complexities of MLSTTCs, GMLSTTCs, MLDSTTCs, and GMLDSTTCs have been compared by assuming that these codes are designed using 16-

QAM constellation, multilevel coding with two levels (i.e. L=2), and component STTCs with N_s states and N_b branches per state. $N_s \times N_b$ has been used to measure the minimum complexity of these codes for comparison purposes. Table 3.2 presents comparison of different aspects of the GMLDSTTCs, MLSTTCs, MLDSTTCs, and GMLSTTCs.

Table 3.2: Comparison of MLSTTCs, MLDSTTCs, GMLSTTCs, and GMLDSTTCs (For L=2 levels, 16 QAM Constellation).

Parameter/Criteria	MLSTTCs	MLDSTTCs	GMLSTTCs	GMLDSTTCs
Constellation Partitioning	MRM partitioning	MRM partitioning	$\mathcal{M}$- way partitioning	$\mathcal{M}$-way partitioning
Spectral Efficiency	4 bits/s/Hz (2 STTC encoders required, each providing a spectral efficiency of 2 bits/s/Hz. The level 2 is not partitioned into sublevels)	4 bits/s/Hz (2 STTC encoders required, each providing a spectral efficiency of 2 bits/s/Hz. The level 2 is not partitioned into sublevels)	6 bits/s/Hz (3 STTC encoders required, each providing a spectral efficiency of 2 bits/s/Hz. The level 2 is being partitioned into two sublevels.)	6 bits/s/Hz (3 STTC encoders required, each providing a spectral efficiency of 2 bits/s/Hz. The level 2 is being partitioned into two sublevels.)
Error Performance, SNR required (at FER of 10^{-1}, using 2 receive antennas)	16.2 dB	15.8 dB	21 dB	19.4 dB
Channel State Information	Perfect CSI at receiver only	Perfect CSI at receiver only. Transmitter receives index of selected code set	Perfect CSI at receiver only	Perfect CSI at receiver and transmitter
Minimum Complexity	32	52	48	72
Transmit Antenna Grouping	No	No	Yes	Yes
Component Code Selection	No, Predefined component STTCs used.	Yes, Component STTCs are dynamically selected based on the index bits	No, Predefined component STTCs used.	Yes, Component STTCs are dynamically selected based on perfect CSI at transmitter.

In STTCs, for transmitting b bits/sec/Hz, the number of branches leaving each state of the trellis is 2^b which is same as the size of signal constellation. For 16-QAM, minimum 16 states with 16 branches leaving each state are required for the data transmission rate of 4 bits/sec/Hz in STTCs. Therefore, the minimum complexity of STTC system for

providing the data transmission rate of 4 bits/sec/Hz is 16×16 whereas for 6 bits/sec/Hz, the minimum value of the complexity is 64 × 64. Thus, it can be seen that the minimum complexity for STTCs increase exponentially with increase in the data rate.

In contrast to STTCs, MLSTTCs use the multilevel coding and constellation partitioning to resolve the problem of increase in complexity with the size of constellation. Since 16-QAM is partitioned into two 4-QAM subsets, the number of states are equal to 4×2 (4×L) and number of branches leaving each state are 4. Therefore, the minimum complexity in MLSTTCs for providing the data transmission rate of 4 bits/sec/Hz is 4×2×4 whereas for 6 bits/sec/Hz, the minimum value of the complexity is 4×3×4. Thus, the minimum complexity for MLSTTCs increases linearly with the increase in data rate.

In GMLSTTCs, the second level is split into two sub-levels. For minimum complexity, the level 1 and each sub-level at level 2 use 4-QAM STTCs as component codes with 4 branches leaving each state. Therefore, three 4-QAM STTCs are required as the component codes. The minimum complexity for GMLSTTCs is given by 4×3×4 = 48.

MLDSTTCs and GMLDSTTCs are designed by selecting optimum generator sequences for each component STTCs based on the feedback information from the receiver. The minimum complexity for MLSTTCs for providing the data transmission rate of 4 bits/sec/Hz is 4×2×4 =32. The selection of the code set including optimum generator sequences for each component STTCs results in an increase in the minimum complexity. For the system having two transmit antennas and two receive antennas, the calculation of power gain as given in equation 3.12 results in minimum increase in the complexity by 2×2=4.

For four predefined channel profiles, the comparison of total power gain *G* at the current channel profile with total power gains corresponding to the predefined channel

profiles results in an increase in the minimum complexity by 4×4=16. This increase in the minimum complexity entirely depends on the number of predefined channel profiles. The minimum complexity of MLDSTTCs for 4 predefined channel profiles is given by 32+ 4+ 16=52. Similarly, the minimum complexity for GMLDSTTCs for the system having four transmit antennas and two receive antennas 48+ 8+ 16=72.

3.7 SUMMARY OF THE CHAPTER

In this chapter, the design and performance analysis of MLSTTCs and GMLSTTCs has been presented by combining the MLC and STTCs. MLSTTCs and GMLSTTCs have been designed by assuming that the perfect CSI is available at the receiver only and there is no availability of the perfect CSI at the transmitter. The simulation results have been shown the performance of MLSTTCs and GMLSTTCs by varying the number of receive antennas.

The effect of CSI at the transmitter has been analysed to improve the performance of MLSTTCs and GMLSTTCs. In this chapter, the CSI at the transmitter has been utilized to generate the dynamic component STTCs used for multilevel coding. Dynamic STTCs have been generated by using the CSI to dynamically select the optimum generator sequences for each STTC encoder. Dynamic STTCs are used as component codes in MLSTTCs and GMLSTTCs instead of predefined STTCs to generate MLDSTTCs and GMLDSTTCs. The simulation results have shown that MLDSTTCs and GMLDSTTCs outperform MLSTTCs and GMLSTTCs by 1.1.dB and 1.6 dB respectively. In the next chapter, the CSI is used to improve the performance of GMLSTTCs by adaptive grouping of the transmit antennas.

CHAPTER 4

IMPROVEMENT IN PERFORMANCE OF GMLSTTCs BASED ON ADAPTIVE GROUPING OF TRANSMIT ANTENNAS

4.1 INTRODUCTION

MIMO wireless communication systems use multiple antennas at the transmitter and the receiver to increase the reliability of communication, data rate, and the spectral efficiency of the wireless systems operating in the fading channels. However, increasing the number of antennas at the transmitter and the receiver beyond a particular limit do not improve the performance significantly. Moreover, there will be an increase in cost and complexity of the systems on increasing the number of antennas. Even further, search for optimal antennas become computationally intensive when the number of antennas is large which results in more power consumption and delay in data transmission. This motivates the need for efficient antenna selection algorithms with reasonable power requirements and minimum latency.

Antenna selection [119]-[121] is a powerful signal processing technique in the wireless systems with multiple antennas at the transmitter and receiver. The main advantage of the antenna selection is that it decreases the system cost, reduces the computational complexity, and preserves the diversity of the system. In an antenna selection technique, a subset of antennas is optimally selected from a large number of antennas. An exhaustive search is performed on all possible combinations of antennas such that the selected combination provides minimum error.

GMLSTTCs [182] use the predefined grouping of transmit antenna. The groups of antennas defined in GMLSTTCs do not change with the change in the CSI at the transmitter. In this chapter, adaptively grouped multilevel space-time trellis codes

(AGMLSTTCs) have been designed by adaptive grouping of transmit antennas using the perfect CSI at the transmitter. An adaptive antenna grouping algorithm is presented to group the transmit antennas. The simulation results have shown that AGMLSTTCs provide better error performance than GMLSTTCs in quasi static Rayleigh fading channel conditions.

4.2 DESIGN AND ANALYSIS OF AGMLSTTCs

The predefined grouping of transmit antennas limits the performance of GMLSTTCs. The performance of GMLSTTCs has been improved by adaptive grouping of transmit antennas using the CSI at the transmitter. Instantaneous channel power gain is calculated between each transmit antenna and all the receive antennas. A subset of transmit antennas having maximum channel power gain is selected to form a group. In adaptive antenna grouping, the transmit antennas in the groups change with the change in the CSI at the transmitter.

4.2.1 System Model: AGMLSTTCs

A MIMO system having *N* transmit antennas and *M* receive antenna is presented in figure 4.1. The channel is assumed to exhibit quasi-static Rayleigh fading. The system comprises a transmitter having STTC encoders for encoding the input data stream and a receiver having a multistage decoder for decoding the received signal. At least one or more levels use two or more STTCs. It is assumed that the transmitter and receiver have perfect knowledge of the CSI.

4.2.2 Encoding for AGMLSTTCs

At the transmitter, each STTC encoder receives a data stream, and performs space-time trellis coding on the data stream. The encoders 1 to *L-1* generate the STTCs which span all *N* transmit antennas. The STTC encoder *l* output is given by:

$$S(l) = x_t(l)^1, x_t(l)^2, ..., x_t(l)^N \quad where\ l=1, 2,\ldots L-1 \tag{4.1}$$

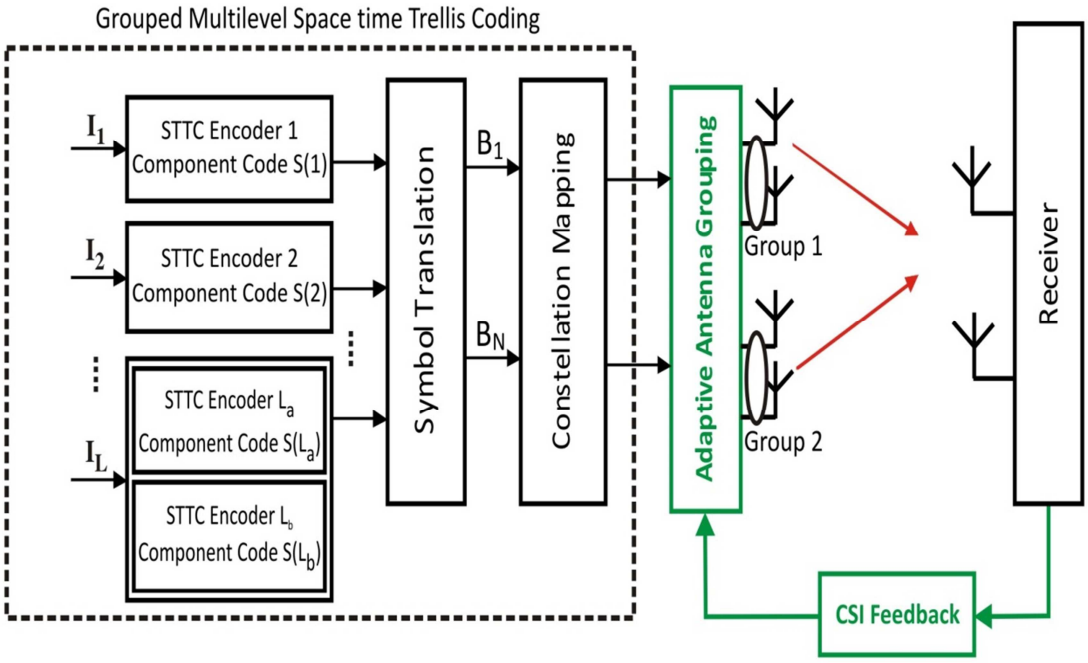

Figure 4.1 Block diagram of AGMLSTTC system

Two parallel STTC encoders L_a and L_b are used at level L for generating STTCs which span through a group of $N/2$ transmit antennas. For example, STTC encoder L_a is used for generating STTCs which span through a first group of transmit antennas whereas STTC encoder L_b is used for generating STTCs which span through another group of $N/2$ transmit antennas. The antennas in each group are selected using an adaptive antenna grouping algorithm. The antennas in each group change dynamically with the change in CSI. The main purpose of adaptive grouping of transmit antennas at level L is to improve the performance of codes in comparison with predefined antenna grouping.

The output from STTC encoder L_a is given by

$$S(L_a) = x_t(L_a)^1, x_t(L_a)^2, ..., x_t(L_a)^{N/2} \quad (4.2)$$

Similarly, STTC encoder L_b output is given by

$$S(L_b) = x_t(L_b)^{N/2+1}, x_t(L_b)^{N/2+2}, ..., x_t(L_b)^N \quad (4.3)$$

The output at level L is given as

$$S(L) = x_t(L_a)^1, x_t(L_a)^2, ..., x_t(L_a)^{N/2}, x_t(L_b)^{N/2+1}, x_t(L_b)^{N/2+2}, ..., x_t(L_b)^N \quad (4.4)$$

Each component STTC has been designed using trace criteria for a 4-QAM signal constellation. The symbols, $x_t(1)$ to $x_t(L)$, in complex form are represented as

$$x_t(l) = a + jb \quad a, b \in \{1, -1\} \tag{4.5}$$

Collectively, the outputs from the L levels, $S(1),...S(L)$, are fed into a symbol translator to generate the translated symbols. These translated symbols are denoted by

$$B(1) = x_t(1)^1, x_t(2)^1 ... x_t(L_a)^1 \tag{4.6}$$

$$B(N) = x_t(1)^N, x_t(2)^N ... x_t(L_b)^N \tag{4.7}$$

The translated N symbols are mapped to M_{ary}-QAM (i.e 16-QAM) signal constellation using an $\mathcal{M}$-way partitioning scheme in which the M_{ary}-QAM signal constellation is partitioned in two levels such that the Euclidean distance increases with each level of partition. The 16-QAM constellation is partitioned in subsets, each comprising four constellation points. Each subset of four points is further partitioned in four subsets, each subset comprising a single constellation point. The $\mathcal{M}$-way partitioning is shown in figure 3.11. The Euclidean distance of subsets (d_2) is greater than the Euclidean distance of sets (d_1). One or more number of component codes can be used for each partition depending upon the number of encoders used at the corresponding level. The component code $S(1)$ at level 1 selects one of the subsets and the two component codes $S(L_a)$ and $S(L_b)$ at level 2 select the constellation points from the selected subset.

It is possible to use higher modulation techniques (e.g. 64-QAM) in multilevel coding. The use of 64-QAM would result in partitioning the constellation in 3 levels. The 3 levels would require at least 4 space-time encoders at the transmitter and would therefore increase data rate and complexity of the system but the complexity is manageable for large order modulations. Thus, higher order modulation techniques are generally able to offer much faster data rates and higher levels of spectral efficiency but will also increase complexity of the system. Another limitation of using the higher order

modulation techniques is that they are significantly less resistant to effects of noise present in the channel. This is because the constellation points are close and the transmission becomes more susceptible to noise. This results in a higher error rate in higher order modulation. In this way, a balance is required between the data rate and an acceptable error rate for the system.

The mapped signals are then transmitted through N antennas. The symbol Q_t^j transmitted at time t by the j^{th} transmit antenna is given by

$$Q_t^j = d_1 x_t(1)^j + d_2 x_t(2)^j \dots d_L x_t\left(L_{(b)}\right)^j \quad (4.8)$$

where $j = 1, \dots, N$, and $d_1, \dots, d_L$ a represent the subset distances for levels 1 to L.

4.2.3 Adaptive Antenna Grouping Algorithm

The symbols at level L are transmitted through two groups of transmit antennas. The groups are formed using the perfect CSI at the transmitter with the help of an adaptive antenna grouping algorithm. The steps of the adaptive antenna grouping algorithm are:

- Calculate the instantaneous channel power gain between the transmit antenna i and all the receive antennas.

  $$G_i = \sum_{j=1}^{M} \left| h_{ij}{}^t \right|^2 \quad 1 \leq i \leq N \quad (4.9)$$

- Arrange the calculated values of G_i in an increasing order.
- Select two antennas, denoted by u and v to form a first group of antennas. The antennas u and v are selected such that the total instantaneous channel power gain of antennas u and v is maximum i.e.

  $$\{u, v\} = argmax\ (\{G_u + G_v\})\ 1 \leq u, v \leq N, u \neq v \quad (4.10)$$

- After, the formation of first group, second group is formed in the same way. The second group of the antennas is formed by selecting next two antennas from the

remaining transmit antennas. This procedure continues till all the transmit antennas are grouped.

4.2.4 MULTISTAGE DECODING OF AGMLSTTCs

The transmitted signals while travelling from transmitter to receiver are corrupted by Rayleigh fading. The faded and noisy signal received at the receive antenna *i* is given by:

$$r_t^i = \sum_{j=1}^{N} {h_{ij}}^t \, Q_t^j + n_t^i \tag{4.11}$$

In matrix form the received signal can be represented as

$$\begin{bmatrix} r_t^1 \\ r_t^2 \\ \vdots \\ r_t^M \end{bmatrix} = \begin{bmatrix} {h_{11}}^{\mathrm{t}} & \cdots & {h_{1N}}^{\mathrm{t}} \\ {h_{21}}^{\mathrm{t}} & \ldots & {h_{2N}}^{\mathrm{t}} \\ \vdots & \ddots & \vdots \\ {h_{M1}}^{\mathrm{t}} & \cdots & {h_{MN}}^{\mathrm{t}} \end{bmatrix} \begin{bmatrix} Q_t^1 \\ Q_t^2 \\ \vdots \\ Q_t^N \end{bmatrix} + \begin{bmatrix} n_t^1 \\ n_t^2 \\ \vdots \\ n_t^M \end{bmatrix} \tag{4.12}$$

In compact form, the received signal is given as

$$r_t = H_t Q_t + n_t \tag{4.13}$$

where H_t is known as channel matrix. Substituting the equation 4.8 in equation 4.11

$$r_t^i = \sum_{l=1}^{L} \sum_{j=1}^{N} {h_{ij}}^t \, d_l \, x_t(l)^j + n_t^i \tag{4.14}$$

The received signal is decoded by a multistage decoder employing two parallel decoders at final stage which is shown in figure 3.12. Viterbi algorithm is used by the multistage decoder to derive the branch metrics for each stage. At the 1st stage, the component code *S(1)* is estimated and the estimated value of *S(1)* is passed to the second decoding stage to estimate the value of *S(2).* The decoder at the second stage comprises two parallel decoders which use the estimated values of previous stages to estimate the values of $S(L_a)$ and $S(L_b)$.

4.2.5 BRANCH METRICS CALCULATION FOR AGMLSTTCs

A MIMO system having four transmit antennas and a 16-QAM signal constellation partitioned in two levels have been used to evaluate the performance of AGMLSTTCs. The STTC encoder at level 1 generates component STTC, *S(1)* which spans all four

transmit antennas. At level 2, two STTC encoders generate identical component STTCs, each spanning a group of two transmit antennas. The transmit antennas in each group are adaptively selected based on the CSI at the transmitter. The selected antennas in each group are determined by

$$\text{Group 1=antennas}\{u, v\} = argmax\ (\{G_u + G_v\})\ 1 \leq u, v \leq 4, u \neq v \quad (4.15)$$

$$\text{Group 2=antennas}\{y, z\} = arg(\{G_y + G_z\}) \quad (4.16)$$

where $1 \leq y, z \leq 4, y \neq z, argmax\ (\{G_u + G_v\}) > arg(\{G_y + G_z\})$

For the system as considered above, r_t^i is given by

$$r_t^i = \sum_{j=1}^{N} {h_{ij}}^t\, d_1\, x_t(1)^j + \sum_{j=1}^{N} {h_{ij}}^t\, d_2\, x_t(2)^j + n_t^i \quad (4.17)$$

A conditional probability density function (PDF) for the received signal is given by

$$P(r_t|x_t(1), x_t(2), H_t) \quad (4.18)$$

In the 1st stage of decoding, the multistage decoder employing the Viterbi algorithm is used to hypothesize the value of $x_t(1)$. The values of $x_t(2)$ are unknown at this stage and therefore not considered while estimating the value $x_t(1)$. Based on this assumption, the PDF can be written as

$$P(r_t|\, x_t(1), H_t) = \sum_{\substack{x_t(l),\\ l=1,2}} P\ (x_t(2)|\, x_t(1), H_t)\ P(r_t|\, x_t(2), H_t) \quad (4.19)$$

Each STTC encoder operates independently, therefore, $x_t(1)$ and $x_t(2)$ are considered as mutually independent. It is also assumed the channel is independent of the component STTCs and the probability of transmission of different component codes is same. Based on these assumptions, the equation 4.19 can be written as

$$P(r_t|x_t(1), H_t) =$$

$$\frac{1}{(\sqrt{2\pi}{\sigma_n}^2)} \exp\left[\frac{\left| r_t^i - \sum_{j=u,v} {h_{ij}}^t d_2\, \tilde{x}_t^a(2)^{\mathrm{j}} - \sum_{j=y,z} {h_{ij}}^t d_2\, \tilde{x}_t^b(2)^{\mathrm{j}} - \sum_{j=1}^{N} {h_{ij}}^t d_1\, x_t(1)^{\mathrm{j}} \right|^2}{2{\sigma_n}^2}\right] \quad (4.20)$$

Based on equation 4.20, the likelihood function for $x_t(1)$ is given by

$$L\big(x_t(1)\big) = P(r_t|x_t(1), H_t)$$

$$\propto \exp\left[\frac{\left| r_t^i - \sum_{j=u,v} h_{ij}{}^t d_2\, \tilde{x}_t^a(2)^{\mathrm{j}} - \sum_{j=y,z} h_{ij}{}^t d_2\, \tilde{x}_t^b(2)^{\mathrm{j}} - \sum_{j=1}^{N} h_{ij}{}^t d_1\, x_t(1)^{\mathrm{j}} \right|^2}{2\sigma_n{}^2}\right] \quad (4.21)$$

Therefore, the branch metric for component code *S(1)* is given by

$$\max_{\substack{\tilde{x}_t^a(2)\in\{x_t^a(2)\} \\ \tilde{x}_t^b(2)\in\{x_t^b(2)\}}} \sum_{i=1}^{M} \Big| r_t^i - \sum_{j=u,v} h_{ij}{}^t\, d_2\, \tilde{x}_t^a(2)^{\mathrm{j}} - \sum_{j=y,z} h_{ij}{}^t\, d_2\, \tilde{x}_t^b(2)^{\mathrm{j}} - \sum_{j=1}^{N} h_{ij}{}^t\, d_1\, x_t(1)^{\mathrm{j}} \Big|^2 \quad (4.22)$$

In the second stage, one decoder is used to decode $S(L_a)$ and another decoder is used to decode $S(L_b)$. The branch metric for the component code $S(L_a)$ is computed as

$$\max_{\tilde{x}_t^b(2)\in\{x_t^b(2)\}} \sum_{i=1}^{M} \Big| r_t^i - \sum_{j=u,v} h_{ij}{}^t\, d_2\, x_t^a(2)^{\mathrm{j}} - \sum_{j=y,z} h_{ij}{}^t\, d_2\, \tilde{x}_t^b(2)^{\mathrm{j}} - \sum_{j=1}^{N} h_{ij}{}^t\, d_1\, \hat{x}_t(1)^{\mathrm{j}} \Big|^2 \quad (4.23)$$

Similarly, the branch metric for component code $S(L_b)$ is computed as

$$\max_{\tilde{x}_t^a(2)\in\{x_t^a(2)\}} \sum_{i=1}^{M} \Big| r_t^i - \sum_{j=u,v} h_{ij}{}^t\, d_2\, \tilde{x}_t^a(2)^{\mathrm{j}} - \sum_{j=y,z} h_{ij}{}^t\, d_2\, x_t^b(2)^{\mathrm{j}} - \sum_{j=1}^{N} h_{ij}{}^t\, d_1\, \hat{x}_t(1)^{\mathrm{j}} \Big|^2 \quad (4.24)$$

4.2.6 SIMULATION RESULTS FOR AGMLSTTCs

The performance of AGMLSTTCs has been illustrated by using the signal constellation of 16-QAM partitioned in two levels with d_2/d_1=2. The simulation results have been calculated using four transmit antennas and different number of receive antennas. Each frame transmitted from the transmit antennas consists of 130 symbols and a quasi-static Rayleigh fading channel is considered for the transmission of symbols. The perfect CSI is assumed to be available at the transmitter and receiver. The CSI information at the transmitter has been used for adaptive grouping of the transmit antennas.

The FER performance of AGMLSTTCs, as shown in figure 4.2, is plotted against SNR for four transmit antennas and different number of receive antennas. Figure 4.2 exhibits that the FER performance of AGMLSTTCs is superior over GMLSTTCs due to the adaptive grouping of the transmitting antennas using the CSI at the transmitter. The comparison results show that AGMLSTTCs are superior to GMLSTTCs by about 1.5 dB at the FER of 10^{-2} and M=2, whereas the spectral efficiency of 6 bits/sec/Hz is achieved in both the codes.

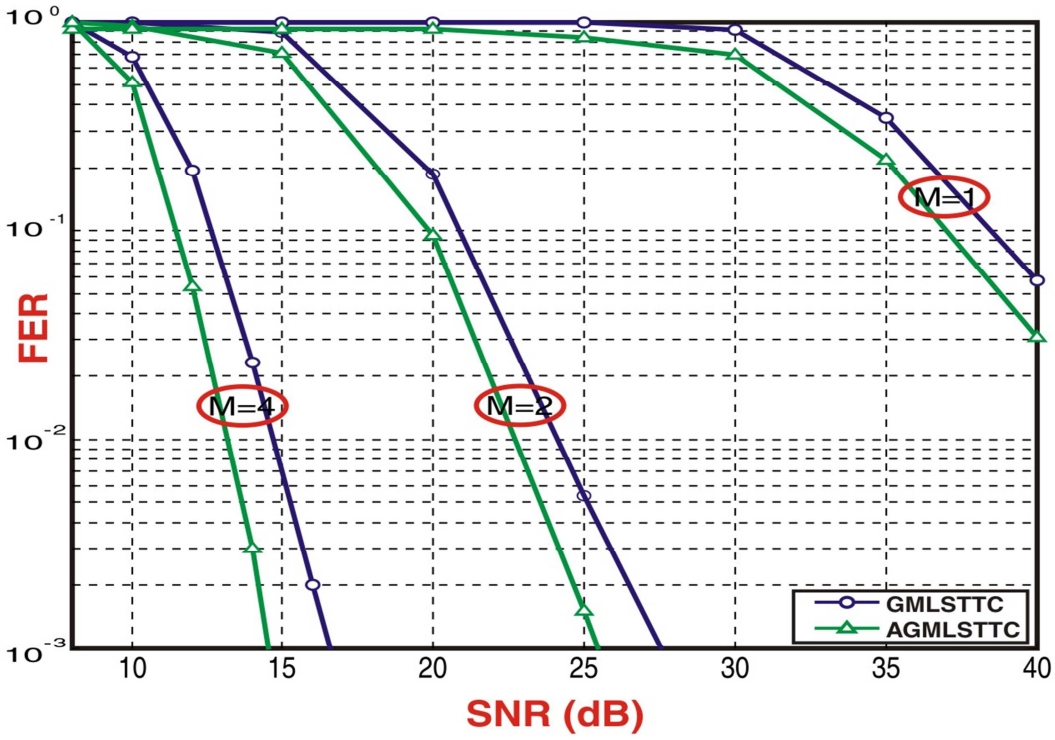

Figure 4.2: Performance comparison of AGMLSTTCs and GMLSTTCs

4.3 SUMMARY OF THE CHAPTER

In this chapter, the use of the CSI at the transmitter has presented for adaptive grouping of transmit antennas to improve the performance of GMLSTTCs. A new adaptive antenna grouping algorithm is presented which uses the CSI at the transmitter to optimally group the transmit antennas. Novel AGMLSTTCs have been designed by replacing the predefined antenna grouping in GMLSTTCs with adaptive antenna

grouping. The simulation results have shown that AGMLSTTCs using the adaptive grouping of transmit antennas perform considerably better than GMLSTTCs.

In the next chapter, the CSI at transmitter is used to provide a beamforming scheme to improve the performance of AGMLSTTCs. The CSI is also used optimally simultaneously for dynamic component code selection, adaptive grouping of transmit antennas, and beamforming.

CHAPTER 5

IMPROVEMENT IN PERFORMANCE OF AGMLSTTCs BASED ON BEAMFORMING AND DYNAMIC COMPONENT CODE SELECTION

5.1 INTRODUCTION

In recent years, to alleviate the problem of scarce radio spectrum and to fulfill the tremendously increasing demand for reliable transmission of high speed data, beamforming is another prominent technique used in MIMO systems. It has been shown that the beamforming [154]-[159] improves the spectral efficiency, decreases the outage probability, and improves the error performance for space-time coded systems. WMLSTTCs [183], designed by combining MLSTTCs and beamforming using the CSI at the transmitter, has shown better performance than MLSTTCs.

In AGMLSTTCs, the transmit power is equally distributed across all transmit antennas. The CSI at the transmitter in AGMLSTTCs has been used for adaptive grouping of transmit antennas only. In this chapter, the CSI at the transmitter has been utilized for adaptive antenna grouping as well as for beamforming to further improve the performance of AGMLSTTCs. The CSI is used to provide a beamforming scheme for dynamically allocating the transmit power to transmit antennas. The dynamic allocation of transmit power is performed by weighting transmitting signals based on the CSI. Novel WAGMLSTTCs are proposed and the simulation results show that performance of WAGMLSTTCs is better than AGMLSTTCs in the quasi-static Rayleigh channel conditions.

This chapter further introduces an optimum utilization of the CSI at the transmitter. In

the earlier chapters, the CSI has been used separately for adaptive antenna grouping and dynamic code selection to improve the error performance of GMLSTTCs. The combined effect of these schemes along with beamforming on GMLSTTCs has not been explored yet. The CSI at the transmitter has been used simultaneously for beamforming, adaptive antenna grouping, and dynamic code selection to design WAGMLDSTTCs. It is shown that WAGMLDSTTCs provide better error performance than WAGMLSTTCs.

5.2 BEAMFORMING

Beamforming is a signal processing technique for directional transmission or reception of the signal. This is achieved by multiplying the signals with beamforming/weighting coefficients to adjust the magnitude and phase of the signals in such a way that signals in a particular direction experience constructive interference while others experience destructive interference.

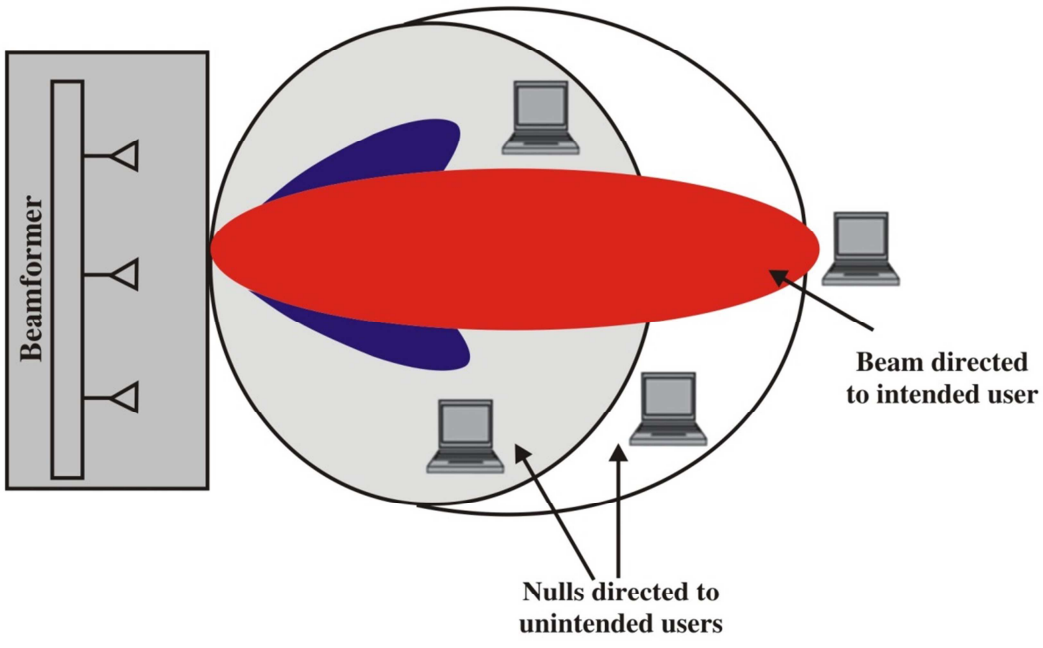

Figure 5.1: Beamforming for intended user

Figure 5.1 shows that beamforming emphasizes the signals in a particular direction while attenuates signals in other directions. The beams directed to desired users are

amplified, while beams for unintended users have been attenuated to increase received SNR for the desired user. Therefore, the beamforming results in a stronger link for the desired user and improves error performance.

5.2.1 Weighting Coefficients and the Weighted Response

Figure 5.2 illustrates that the signal $x_i(t)$ from antenna i is multiplied with a weighting coefficient w_i^*, where the * represents the complex conjugate. The weighted signals are added together at the receiver to generate the received signal.

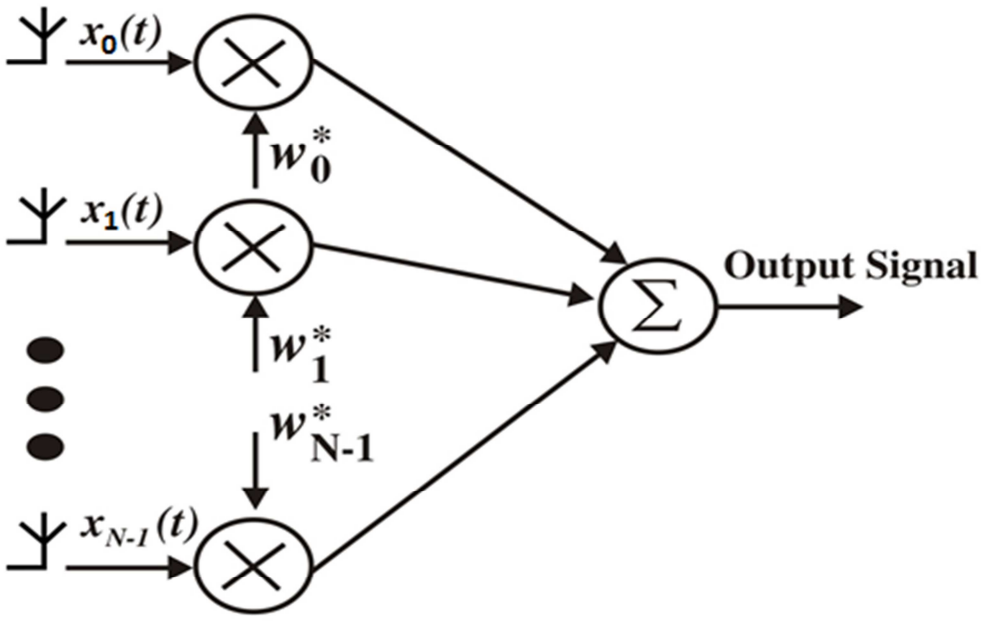

Figure 5.2: A general beamforming system

The output signal *r* corresponds to weighted response and is given by

$$r = \sum_{i=0}^{N-1} x_i w_i^* = w^H x \quad (5.1)$$

where *w* represents a vector of weights with length *N*, *x* represents a vector of received signals with length *N* and the superscript *H* represents the Hermitian of a vector (the conjugate transpose). w^H is given as

$$w^H = [w_0^*, w_1^*, w_2^*, \ldots . w_{N-1}^*] = [w^T]^* \quad (5.2)$$

5.2.2 Fixed Beamforming and Adaptive Beamforming

Based on whether the values of weighting coefficients are fixed or varying, the beamforming techniques are classified in two categories:

(a) Fixed Beamforming: Fixed beamforming is a beamforming technique in which weighting coefficients are fixed during the operation. A fixed set of weighting coefficients are used for multiplying the corresponding signals. For example, as shown in figure 5.3, beamforming based on switched-beam antennas is one of fixed beamforming techniques in which a finite number of beams are used and each beam is provided one radio frequency signal.

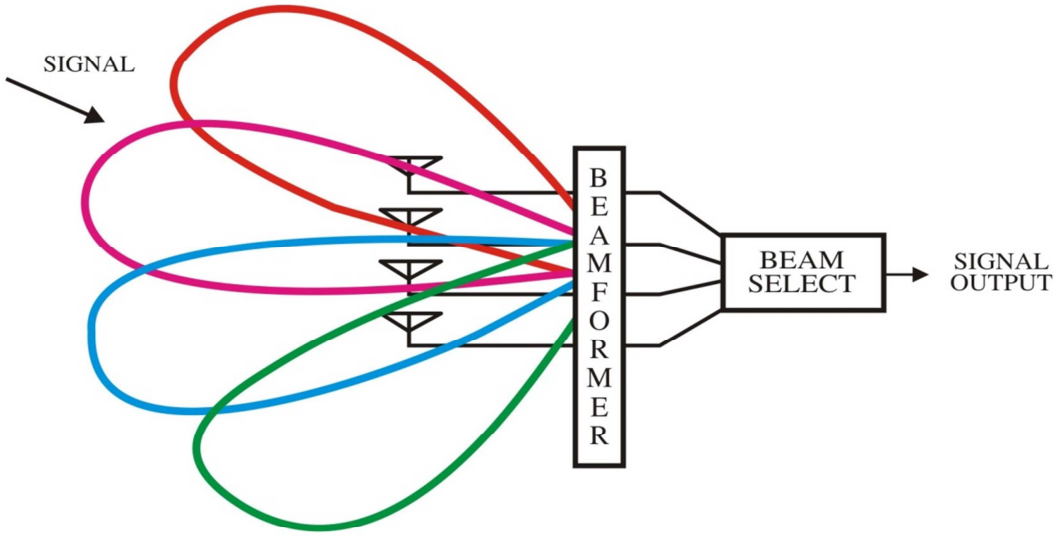

Figure 5.3: Fixed Beamforming

In fixed beamforming, a beam providing the optimum performance is selected using a beam select signal. The transmitter or receiver searches for the optimum beam periodically which can provide best performance and switches the transmission or reception of the signals to that beam. The fixed beamforming using the beam switching technique can provide an array gain of Y with Y weighting coefficients.

(b) Adaptive Beamforming: Adaptive Beamforming is a beamforming technique in which the weighting coefficients change dynamically to enhance the desired signal while suppressing interference signals to maximize SNR at the receiver. This adaptive beamforming approach leads to optimal performance, but is more expensive and needs considerable implementation efforts. Figure 5.4 shows a generic adaptive beamforming system which requires a reference signal to adjust the weighting coefficients.

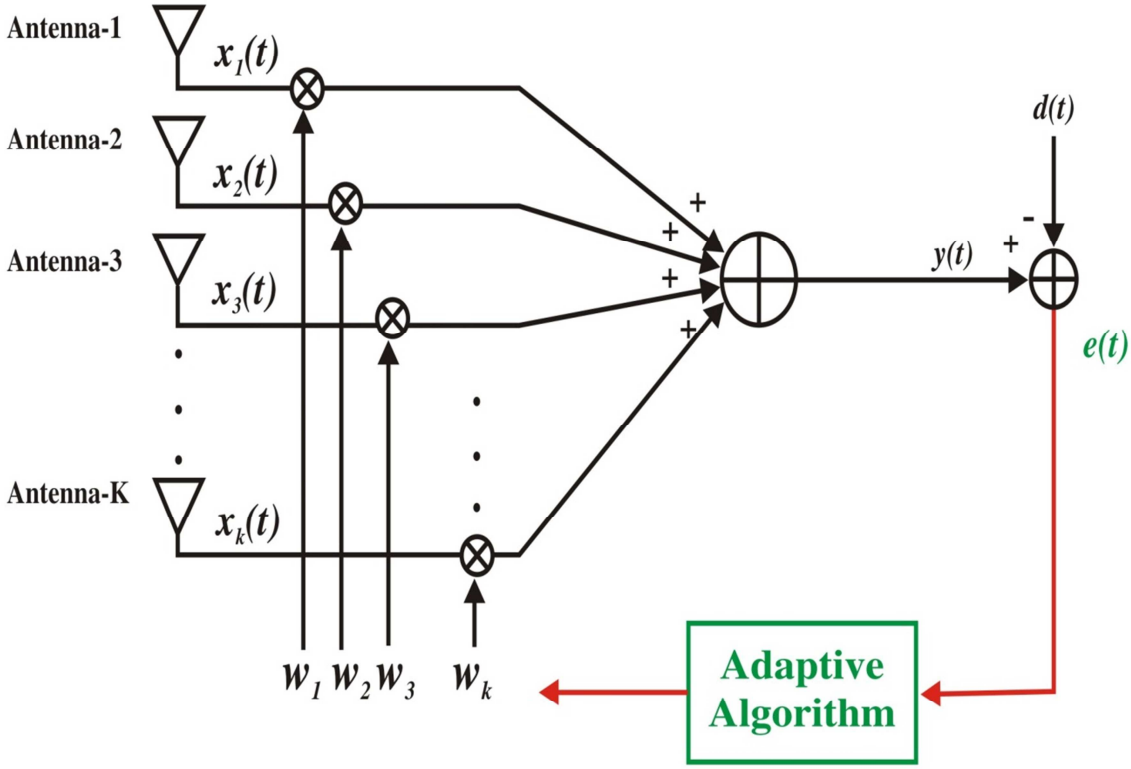

Figure 5.4: An adaptive beamforming system

The signal $x(t)$ received by each antenna is multiplied with a coefficient in a weight vector w (series of amplitude and phase coefficients) which adjusts the phase and amplitude of the signal accordingly. This weighted signal is summed up, resulting in the array output $y(t)$. An adaptive algorithm is then employed to minimize the error $e(t)$ between a desired signal $d(t)$ and the array output $y(t)$.

A reference signal is generated based on the adaptive algorithm to dynamically adjust the weighting coefficients. The adaptive algorithm is generally derived by first setting a performance criterion and then generating a set of iterative equations to adjust the weights so that the performance criterion is met. As the weights are iteratively adjusted, the performance of beamformer approaches the desired criterion. The algorithm is said to be converged when the performance of the desired criterion is met.

The systems using MIMO and beamforming techniques hold advantages of both MIMO and beamforming. These systems can not only obtain spatial diversity gain due to MIMO, but also array gain using the beamforming. Thereby, beamforming is being widely utilized to increase the coverage, improve the throughput effectively, and reducing network construction and maintenance costs greatly. It brings space multiplexing gain and also reduces the co-channel interference, thereby, improving the spectrum efficiency to meet the demand for high-speed data transmission.

5.3 DESIGN AND ANALYSIS OF WAGMLSTTCs

The novel design of WAGMLSTTCs is proposed by using the CSI at the transmitter for adaptive grouping of transmit antennas and providing beamforming for the transmitting signals. The beamforming is provided by dynamically distributing the power across the transmit antennas using the beamforming coefficients. It is shown using the simulation results that WAGMLSTTCs provide better performance than AGMLSTTCs over quasi-static Rayleigh channel conditions.

5.3.1 System Model: WAGMLSTTCs

A MIMO system having N transmit antennas and M receive antennas is presented in figure 5.5. The channel is assumed to exhibit quasi-static Rayleigh fading. The system comprises a transmitter having STTC encoders for encoding the input data stream and a receiver having a multistage decoder for decoding the received signal. The perfect CSI is

assumed to be available at the receiver and the transmitter. A beamformer and an antenna grouper are applied at the transmitter which use the CSI at the transmitter for providing the beamforming and adaptive grouping of the transmit antennas.

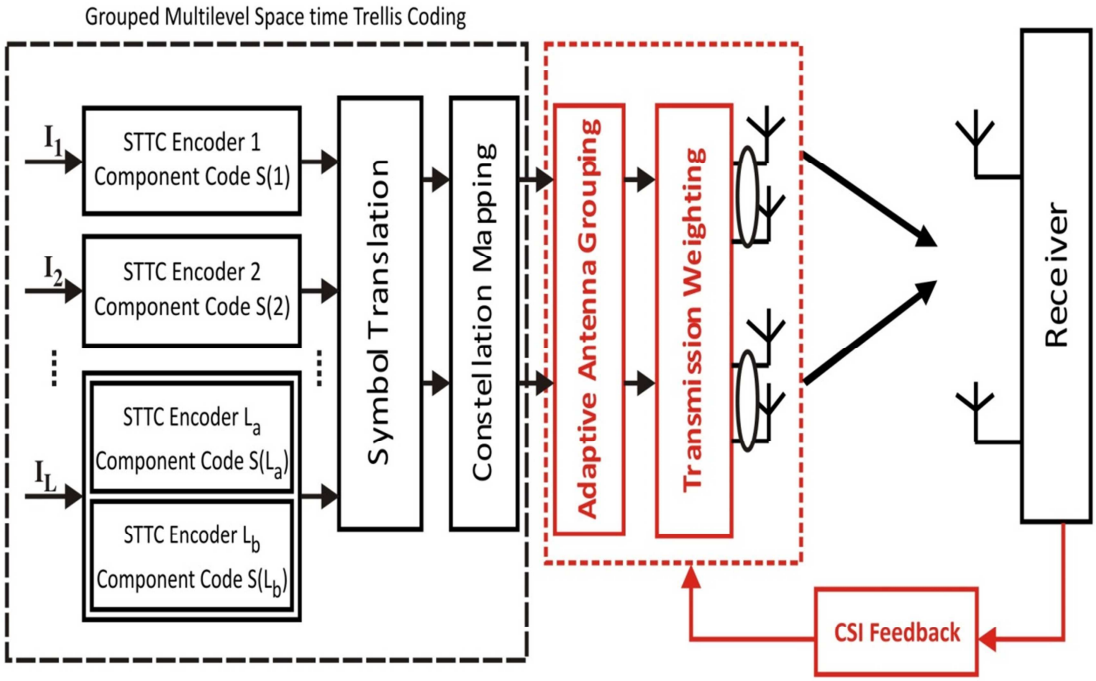

Figure 5.5: Block diagram of a WAGMLSTTC system

5.3.2 Encoding for WAGMLSTTCs

At the transmitter, each STTC encoder receives a data stream, and performs space-time trellis coding on the data stream. The encoders 1 to *L-1* generate the STTCs which span all *N* transmit antennas. The STTC encoder *l* output is given by:

$$S(l) = x_t(l)^1, x_t(l)^2, ..., x_t(l)^N \text{ where } l=1, 2,\ldots L\text{-}1 \quad (5.3)$$

Two parallel STTC encoders L_a and L_b are used at level L for generating STTCs which span through a group of *N/2* transmit antennas. For example, STTC encoder L_a is used for generating STTCs which span through a first group of *N/2* transmit antennas whereas STTC encoder L_b is used for generating STTCs which span through another

group of *N/2* transmit antennas. The groups of antennas are defined using an adaptive antenna grouping algorithm as described below:

- Calculate the instantaneous channel power gain between transmit antenna *i* and all the receive antennas.

  $G_i=\sum_{j=1}^{M}\left|h_{ij}{}^{t}\right|^2 \quad 1\leq i\leq N$ (5.4)

- Arrange the calculated values of G_i in an increasing order.
- Select two antennas, denoted by *u* and *v* to form a first group of antennas. The antennas *u* and *v* are selected such that the total the instantaneous channel power gain of antennas *u* and *v* is maximum i.e.

  $\{u, v\} = argmax\ (\{G_u + G_v\})\ 1 \leq u, v \leq N, u \neq v$ (5.5)

- After, the formation of first group, second group is formed in the same way. The second group of antennas is formed by selecting next two antennas from the remaining transmit antennas. This procedure continues till all the transmit antennas are grouped.

The antennas in each group changes dynamically with the change in CSI. The main purpose of adaptive grouping of transmit antennas at level *L* is to improve the performance of codes in comparison with codes designed based on predefined antenna grouping. The STTC encoder L_a output is given by

$S(L_a) = x_t(L_a)^1, x_t(L_a)^2, ..., x_t(L_a)^{N/2}$ (5.6)

In the same way, STTC encoder L_b output is represented as

$S(L_b) = x_t(L_b)^{N/2+1}, x_t(L_b)^{N/2+2}, ..., x_t(L_b)^N$ (5.7)

The output at level *L*, which is the combination of output of STTC encoders L_a and L_b, is given as:

$S(L)= x_t(L_a)^1, x_t(L_a)^2, ..., x_t(L_a)^{N/2}, x_t(L_b)^{N/2+1}, x_t(L_b)^{N/2+2}, ..., x_t(L_b)^N$ (5.8)

Collectively, the outputs from L levels, $S(1),...S(L)$, are input to a symbol translator. The translated symbols are denoted by

$$B(1) = x_t(1)^1, x_t(2)^1 ... x_t(L_a)^1 \quad (5.9)$$

$$B(N) = x_t(1)^N, x_t(2)^N ... x_t(L_b)^N \quad (5.10)$$

The N translated symbols are mapped to M_{ary}-QAM signal constellations using a constellation mapper. The constellation mapper uses the $\mathcal{M}$-way partitioning strategy to map the translated symbols with the signal constellation as described in section 3.4.2. $x_t(1)$ in each translated output is mapped to the actual constellation points, while $x_t(2)$ $... x_t(L)$ respectively are mapped to the subset centre points. The mapped symbols are weighted to provide the beamforming before transmission.

The weighting coefficient for j^{th} transmit antenna are given as

$$w_j = {h_{ij}}^t (\sum_{j=1}^{N} \left|{h_{ij}}^t\right|^2)^{-1/2} \quad (5.11)$$

The weights satisfy the power normalization constraint

$$\sum_{j=1}^{N} \left|w_j\right|^2 = 1 \quad (5.12)$$

The weighted symbols are then transmitted through N antennas. The symbol Q_t^j transmitted at time t by the j[th] transmit antenna is given by.

$$Q_t^j = w_j\{d_1 x_t(1)^j + d_2 x_t(2)^j ... d_L x_t\left(L_{(b)}\right)^j\} \quad (5.13)$$

where $j = 1, ...,N$, and $d_1, ..., d_L$ are the subset distances corresponding to $x_t(1), ...,$ $x_t(L)$.

5.3.3. Multistage Decoding of WAGMLSTTCs

The transmitted signals while travelling from transmitter to receiver are corrupted by Rayleigh fading. The faded and noisy signal received at the receive antenna i is given by

$$r_t^i = \sum_{l=1}^{L} \sum_{j=1}^{N} w_j {h_{ij}}^t \; d_l \, x_t(l)^j + \; n_t^i \quad (5.14)$$

The received signal is decoded by a multistage decoder employing two parallel decoders at final stage which is shown in figure 3.12. Viterbi algorithm is used by the multistage decoder to derive the branch metrics for each stage. At the 1st stage, the component code *S(1)* is estimated and the estimated value of *S(1)* is passed to the second decoding stage to estimate the value of *S(2.)* Similarly, the decoder at final stage which comprises of two parallel decoders uses the estimated values of previous stages to estimate the values of $S(L_a)$ and $S(L_b)$.

5.3.4 Branch Metrics Calculation for WAGMLSTTCs

A system with four transmit antennas and a 16-QAM signal constellation partitioned in two levels have been used to evaluate the performance of WAGMLSTTCs. The STTC encoder at level 1 generate component STTC *S(1)* which spans all four transmit antennas. At level 2, two STTC encoders generate identical component STTCs, each spanning a group of two transmit antennas. The transmit antennas in each group are adaptively selected based on the CSI at the transmitter. The selected antennas in each group are determined by

For Group 1: *antennas* $\{u, v\} = argmax\ (\{G_u + G_v\}$ (5.15)

where $1 \leq u, v \leq 4, u \neq v$

For Group 2 *antennas* $\{y, z\} = arg(\{G_y + G_z\})$ (5.16)

where $1 \leq y, z \leq 4, y \neq z$, argmax $(\{G_u + G_v\}) > \arg(\{G_y + G_z\})$

The received signal at the i^{th} receive antenna at time t is

$$r_t^i = \sum_{j=1}^{N} w_j {h_{ij}}^t\, d_1\, x_t(1)^j + \sum_{j=1}^{N} w_j {h_{ij}}^t\, d_2\, x_t(2)^j + n_t^i \quad (5.17)$$

The conditional PDF of r_t^i conditioned on the channel matrix and encoder outputs is written as $P(r_t | x_t(1), x_t(2), \ldots x_t(L),\ H_t)$. In the 1st stage of decoding, the multistage decoder employing Viterbi algorithm is used to hypothesize the value of $x_t(1)$. The value

of $x_t(2)$ is unknown at this stage and therefore it is not considered while estimating the value $x_t(1)$. Based on this assumption, the conditional PDF can be written as

$$P(r_t|\, x_t(1), H_t) = \sum_{\substack{x_t(l),\\ l=1,2}} P\,(x_t(2) \mid x_t(1),\ H_t)\, P(r_t|\, x_t(2), H_t) \tag{5.18}$$

Each STTC encoder operates independently, therefore, $x_t(1)$ and $x_t(2)$ are considered as mutually independent. It is also assumed that the channel is independent of the component STTCs and the probability of transmission of different component codes is same. Based on these assumptions, the equation 5.18 can be written as

$$P(r_t|x_t(1), H_t) = \frac{1}{\left(\sqrt{2\pi}{\sigma_n}^2\right)} exp\left[\frac{\left|\begin{array}{c} r_t^i - \sum_{j=u,v} w_j {h_{ij}}^t\, d_2\, \tilde{x}_t^a(2)^j - \\ \sum_{j=y,z} w_j {h_{ij}}^t\, d_2\, \tilde{x}_t^b(2)^j - \\ \sum_{j=1}^{N} w_j {h_{ij}}^t\, d_1\, x_t(1)^j \end{array}\right|^2}{2{\sigma_n}^2}\right] \tag{5.19}$$

Based on equation 5.19, the likelihood function for $x_t(1)$ is given by

$$L\big(x_t(1)\big) = P(r_t|x_t(1), H_t) \propto\ exp\left[\frac{\left|\begin{array}{c} r_t^i - \sum_{j=u,v} w_j {h_{ij}}^t\, d_2\, \tilde{x}_t^a(2)^j - \\ \sum_{j=y,z} w_j {h_{ij}}^t\, d_2\, \tilde{x}_t^b(2)^j - \\ \sum_{j=1}^{N} w_j {h_{ij}}^t\, d_1\, x_t(1)^j \end{array}\right|^2}{2{\sigma_n}^2}\right] \tag{5.20}$$

Therefore, the branch metric for *S(1)* is given by

$$\max_{\substack{\tilde{x}_t^a(2)\in\{x_t^a(2)\}\\ \tilde{x}_t^b(2)\in\{x_t^b(2)\}}} \sum_{i=1}^{M} \left| r_t^i - \sum_{j=u,v} w_j {h_{ij}}^t\, d_2\, \tilde{x}_t^a(2)^j - \sum_{j=y,z} w_j {h_{ij}}^t\, d_2\, \tilde{x}_t^b(2)^j - \sum_{j=1}^{N} {h_{ij}}^t\, d_1\, x_t(1)^j \right|^2 \tag{5.21}$$

In the second stage, one decoder is used to decode $S(L_a)$ and another decoder is used to decode $S(L_b)$ corresponding to group 1 and group 2 of the transmit antennas. The branch metric for component code $S(L_a)$ is computed as

$$\max_{\tilde{x}_t^b(2)\in\{x_t^b(2)\}} \sum_{i=1}^{M} \left| r_t^i - \sum_{j=u,v} w_j {h_{ij}}^t \, d_2 \, x_t^a(2)^j - \sum_{j=y,z} w_j {h_{ij}}^t \, d_2 \, \tilde{x}_t^b(2)^j - \sum_{j=1}^{N} w_j {h_{ij}}^t \, d_1 \, \widehat{x_t}(1)^j \right|^2 \tag{5.22}$$

Similarly, the branch metric for component code $S(L_b)$ is computed as

$$\max_{\tilde{x}_t^a(2)\in\{x_t^a(2)\}} \sum_{i=1}^{M} \left| r_t^i - \sum_{j=u,v} w_j {h_{ij}}^t \, d_2 \, \tilde{x}_t^a(2)^j - \sum_{j=y,z} w_j {h_{ij}}^t \, d_2 \, x_t^b(2)^j - \sum_{j=1}^{N} w_j {h_{ij}}^t \, d_1 \, \widehat{x_t}(1)^j \right|^2 \tag{5.23}$$

5.3.5 Simulation Results for Performance Analysis of WAGMLSTTCs

The performance of WAGMLSTTCs has been illustrated by using the signal constellation of 16-QAM partitioned in two levels with d_2/d_1=2. The FER performance of AGMLSTTCs obtained after the grouping the transmit antennas is shown in figure 4.2. It can be seen that AGMLSTTCs are superior to GMLSTTCs by about 1.5 dB at the FER of 10^{-2}. AGMLSTTCs are further weighted using the beamforming coefficients before the transmission to obtain WAGMLSTTCs.

Figure 5.6 exhibits the FER performance comparison of WAGMLSTTCs and GMLSTTCs. It can be noted that the performance of WAGMLSTTCs is further improved by the adaptive weighting of the transmitting signals. The simulation results depict that the performance of WAGMLSTTCs is superior to GMLSTTCs by about 2.6 dB at the FER of 10^{-2} and M=2.

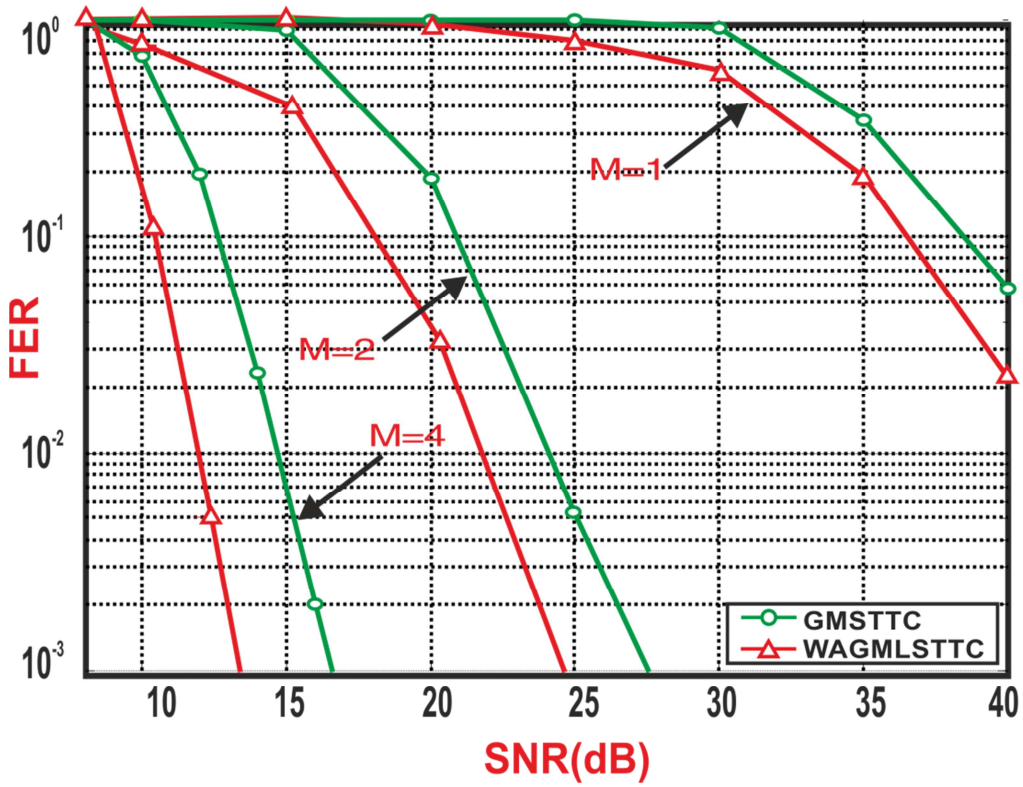

Figure 5.6: Performance comparison of WAGMLSTTCs and GMLSTTCs

5.4 DESIGN AND ANALYSIS OF WAGMLDSTTCs

With the objective to improve the error performance of WAGMLSTTCs, the CSI at the transmitter is also used for dynamic component code selection in WAGMLSTTCs. Therefore, the CSI is used for simultaneously providing the adaptive grouping of transmit antennas, beamforming, and dynamic component code selection in GMLSTTCs. The codes generated based on this optimum utilization of the CSI are referred to as WAGMLDSTTCs. The simulation results have shown that these codes provide significant improvement in error performance over WAGMLSTTCs, AGMLSTTCs, and GMLSTTCs in the quasi static Rayleigh fading channel conditions.

5.4.1 System Model: WAGMLDSTTCs

The system model for WAGMLDSTTCs, as shown in figure 5.7, comprises a system for WAGMLSSTCs and a component code selector for selecting the optimum generator sequences for generating the dynamic STTCs which are used as component codes.

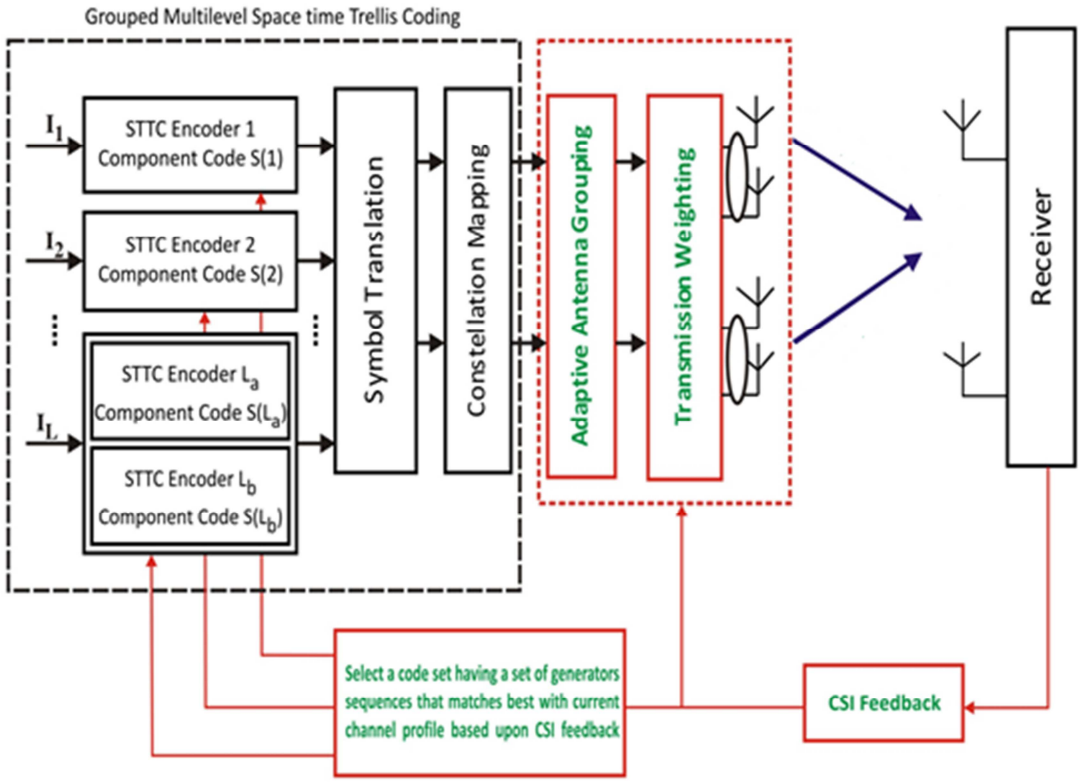

Figure 5.7 System Model for WAGMLDSTTCs

5.4.2 Encoding of WAGMLDSTTCs

The input symbols are de-multiplexed into several independent data streams, with each stream encoded using a space-time trellis encoder. Each space-time trellis encoder uses optimum generator sequences selected using a code set selection algorithm. The outputs of the encoders are referred to as dynamic STTCs. The dynamic STTCs are mapped to new symbols from the enlarged constellation. These mapped symbols are distributed to different antenna groups where they are weighted, and then transmitted simultaneously.

A (*N, M, C*) codeset selection scheme is used for selecting a codeset that matches best with the current CSI at the transmitter. *N* represents number of transmit antennas, *M* represents number of receive antennas, and *C* represents number of predefined CSI at the transmitter. A predefined CSI represents one of the most frequent channel conditions

observed between the transmitter and receiver at different times. The predefined CSI is defined based on the channel power gain between all transmit antennas and all the receive antennas. The predefined CSI is selected based on the frequency of occurrence of the predefined CSI when channel is analysed randomly at different times.

The steps of codeset selection algorithm are:

- Calculate the sum of channel power gain between all the transmit antennas *N* and all the receive antennas *M* at current CSI.

  $G=\sum_{j=1}^{N}\sum_{i=1}^{M}\left|h_{ij}{}^{t}\right|^{2}\ 1\le i\le M,\ 1\le j\le N$ (5.24)

- Compare power gain at the current CSI with power gains corresponding to a predefined CSI.
- Select one of the predefined CSI which has power gain closest to the power gain of the current CSI.
- Retrieve a code set with generator sequences corresponding to the selected predefined CSI.

For example, a code set CS^{ci} selected at the current CSI *ci* is given as

$$CS^{ci} = [(G_1^{1,ci}, G_1^{2,ci}, \dots G_1^{m,ci}), (G_2^{1,ci}, G_2^{2,ci}, \dots G_2^{m,ci}),$$
$$\dots (G_l^{1,ci}, G_l^{2,ci}, \dots G_l^{m,ci}), \dots\ G_L^{1,ci}, G_L^{2,ci}, \dots G_L^{m,ci}] \quad (5.25)$$

where $(G_l^{1,ci}, G_l^{2,ci}, \dots G_l^{m,ci})$ is set of generator sequences for the STTC encoder *l* represented as:

$$G_l^{1,ci} = [(g_{0,1}^{1,ci} \dots g_{0,N}^{1,ci}), (g_{1,1}^{1,ci} \dots g_{1,N}^{1,ci}) \dots (g_{v1,1}^{1,ci} \dots g_{v1,N}^{1,ci}] \quad (5.26)$$

$$G_l^{2,ci} = [(g_{0,1}^{2,ci} \dots g_{0,N}^{2,ci}), (g_{1,1}^{2,ci} \dots g_{1,N}^{2,ci}) \dots (g_{v2,1}^{2,ci} \dots g_{v2,N}^{2,ci})\ ] \quad (5.27)$$

$$G_l^{m,ci} = [(g_{0,1}^{m,ci} \dots g_{0,N}^{m,ci}), (g_{1,1}^{m,ci} \dots g_{1,N}^{m,ci}) \dots (g_{vm,1}^{m,ci} \dots g_{vm,N}^{m,ci})] \quad (5.28)$$

where $g_{j,i}^{k,ci}$, k = 1, 2, . . . ,*m*, *j* = 1, 2, . . . , *vk*, i = 1, 2, . . . , *N*, is an element of the 4-

QAM constellation set and v_k is the memory order of the k^{th} shift register.

When these generator sequences are used by STTCs encoder, they generate dynamic STTCs. The encoders 1 to *L-1* generate dynamic STTCs which span all *N* transmit antennas. The STTC encoder outputs for levels 1 to *L-1* is given by

$$S(l) = x_t^{ci}(l)^1, x_t^{ci}(l)^2 \ldots x_t^{ci}(l)^N \qquad \textit{where } l=1, 2,\ldots L\text{-}1 \tag{5.29}$$

Two parallel STTC encoders L_a and L_b are used at level *L* for generating dynamic STTCs which span through a group of *N/2* transmit antennas. The STTC encoder L_a output is given by

$$S(L_a) = x_t^{ci}\,(L_a)^1, x_t^{ci}\,(L_a)^2, \ldots, x_t^{ci}\,(L_a)^{N/2} \tag{5.30}$$

Similarly, STTC encoder L_b ouput is given by

$$S(L_b) = x_t^{ci}\,(L_b)^{N/2+1}, x_t^{ci}\,(L_b)^{N/2+2}, \ldots, x_t^{ci}\,(L_b)^N \tag{5.31}$$

The output at level *L*, which is combination of output of STTC encoders L_a and L_b, is given as:

$$S(L) = x_t^{ci}\,(L_a)^1, x_t^{ci}\,(L_a)^2, \ldots, x_t^{ci}\,(L_a)^{N/2}, x_t^{ci}\,(L_b)^{N/2+1}, x_t^{ci}\,(L_b)^{N/2+2}, \ldots, x_t^{ci}\,(L_b)^N \tag{5.32}$$

The outputs from all *L* encoders, *S (1)...S (L),* are applied to a symbol translator. The translated outputs are denoted by

$$B(1) = x_t^{ci}(1)^1, x_t^{ci}(2)^1 \ldots x_t^{ci}(L_a)^1 \tag{5.33}$$

$$B(N) = x_t^{ci}(1)^N, x_t^{ci}(2)^N \ldots x_t^{ci}(\mathrm{L_b})^N \tag{5.34}$$

Collectively, the outputs from *L* levels, i.e. *S(1),...S(L),* are input in a symbol translator to generate *N* translated symbols which are mapped to M_{ary}-QAM signal constellations using a constellation mapper. The constellation mapper uses the *M*-way partitioning strategy to map the translated symbols with the signal constellation.

An example of $\mathcal{M}$ way partitioning of 16-QAM signal constellation partitioned in two levels is illustrated in figure 5.8. The 16-QAM constellation is partitioned in subsets, each comprising four constellation points as shown by circle in blue color.

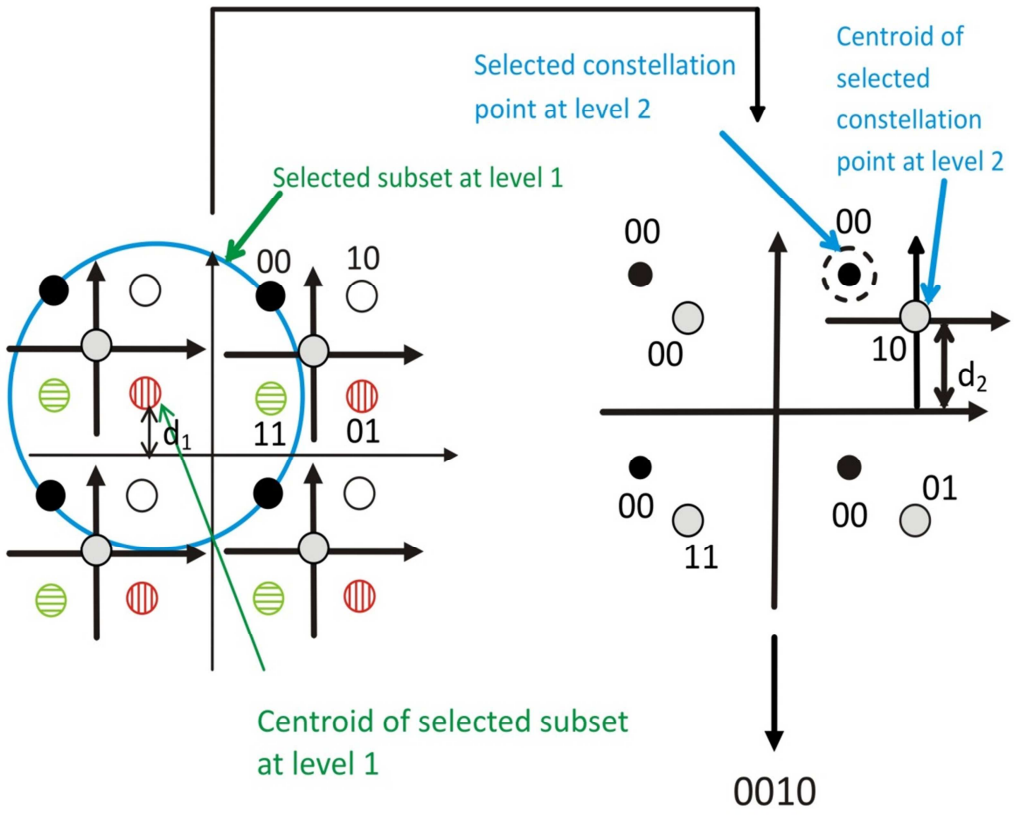

Figure 5.8: Constellation partitioning used in WAGMLDSTTCS

Each subset of four points is further partitioned into four subsets, each subset comprising a single constellation point as shown by a dotted circle in figure 5.8. The Euclidean distance of level 2 (d_2) is greater than the Euclidean distance of level 1 (d_1). One or more number of component codes can be used for each partition depending on the number of encoders used at the corresponding level. The component code *S(1)* at level 1 selects one of the subsets and the two component codes $S(L_a)$ and $S(L_b)$ select constellation points from the selected subset.

The mapped symbols are then weighted and transmitted through adaptively grouped antennas. The symbol Q_t^j transmitted at time *t* and the CSI *ci* by the j^{th} transmit antenna is given by

$$Q_t^j = w_j\{d_1 x_t^{ci}(1)^j + d_2 x_t^{ci}(2)^j \ldots d_L x_t^{ci}(L_b)^j\} \quad (5.35)$$

where j = 1... N, and d_1... d_L are the subset distances corresponding to $x_t^{ci}(1)$, ..., $x_t^{ci}(L)$.

5.4.3. Decoding of WAGMLDSTTCs

The transmitted signals while traveling from transmitter to receiver are corrupted by Rayleigh fading. The faded and noisy signal received at receive antenna *i* is given by

$$r_t^i = \sum_{j=1}^{N} {h_{ij}}^t \, Q_t^j + \, n_t^i \quad (5.36)$$

In matrix form the received signal can be represented as:

$$\begin{bmatrix} r_t^1 \\ r_t^2 \\ \vdots \\ r_t^M \end{bmatrix} = \begin{bmatrix} {h_{11}}^t & \cdots & {h_{1N}}^t \\ {h_{21}}^t & \ldots & {h_{2N}}^t \\ \vdots & \ddots & \vdots \\ {h_{M1}}^t & \cdots & {h_{MN}}^t \end{bmatrix} \begin{bmatrix} Q_t^1 \\ Q_t^2 \\ \vdots \\ Q_t^N \end{bmatrix} + \begin{bmatrix} n_t^1 \\ n_t^2 \\ \vdots \\ n_t^M \end{bmatrix} \quad (5.37)$$

In compact form, the received signal is given as

$$r_t = H_t Q_t + \, n_t \quad (5.38)$$

Substituting equation 5.35 in equation 5.36

$$r_t^i = \sum_{l=1}^{L} \sum_{j=1}^{N} w_j {h_{ij}}^t \, d_l \, x_t^{ci}(l)^j + \, n_t^i \quad (5.39)$$

The received signal is decoded by a multistage decoder employing two parallel decoders at final stage as shown in figure 5.9. The Viterbi algorithm is used by the multistage decoder to derive the branch metrics for each stage. At 1st stage, the component code *S(1)* is estimated and the estimated value of *S(1)* is passed to the second decoding stage to estimate the value of $S(2)$. Similarly, the decoder at final stage which comprises of two parallel decoders uses the estimated values of previous stages to estimate the values of $S(L_a)$ and $S(L_b)$.

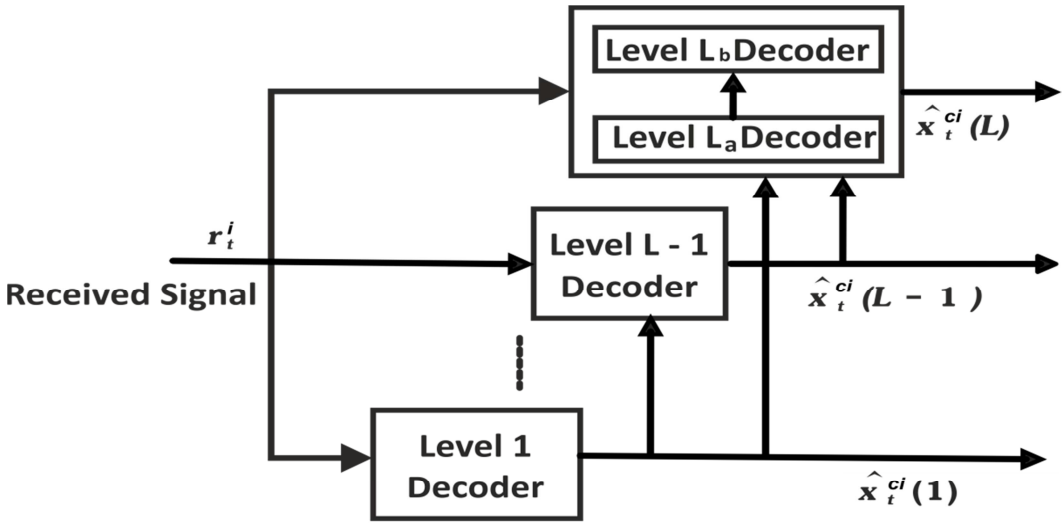

Figure 5.9: Multistage decoder for WAGMLDSTTCs

5.4.4 Branch Metrics Calculation for WAGMLDSTTCs

The branch metrics for each component codes are obtained similarly as described in section 5.3.4. The branch metrics for WAGMLDSTTCs have been calculated by replacing the predefined component codes with dynamic component codes. Therefore, the branch metric for the component code *S(1)* is given by

$$\max_{\substack{\tilde{x}_t^{a,ci}(2)\in\{x_t^{a,ci}(2)\}\\ \tilde{x}_t^{b,ci}(2)\in\{x_t^{b,ci}(2)\}}} \sum_{i=1}^{M} \left| r_t^i - \sum_{j=u,v} {w_j h_{ij}}^t \, d_2 \, \tilde{x}_t^{a,ci}(2)^j - \sum_{j=y,z} w_j {h_{ij}}^t \, d_2 \, \tilde{x}_t^{b,ci}(2)^j \right.$$

$$\left. - \sum_{j=1}^{N} w_j {h_{ij}}^t \, d_1 \, x_t^{ci}(1)^j \right|^2 \qquad (5.40)$$

In the second stage, one decoder is used to decode $S(L_a)$ and another decoder is used to decode $S(L_b)$. The branch metric for $S(L_a)$ is given by

$$\max_{\tilde{x}_t^{b,ci}(2)\in\{x_t^{b,ci}(2)\}} \sum_{i=1}^{M} \left| r_t^i - \sum_{j=u,v} {h_{ij}}^t \, d_2 \, x_t^{a,ci}(2)^j - \sum_{j=y,z} {h_{ij}}^t \, d_2 \, \tilde{x}_t^{b,ci}(2)^j \right.$$

$$\left. - \sum_{j=1}^{N} {h_{ij}}^t \, d_1 \, \widehat{x_t^{ci}}(1)^j \right|^2 \qquad (5.41)$$

The branch metric for $S(L_b)$ is given by

$$\max_{\tilde{x}_t^a(2)\in\{x_t^a(2)\}} \sum_{i=1}^{M} \left| r_t^i - \sum_{j=u,v} {w_j h_{ij}}^t \, d_2 \, \tilde{x}_t^{a,ci}(2)^j - \sum_{j=y,z} {w_j h_{ij}}^t \, d_2 \, x_t^{b,ci}(2)^j \right.$$

$$\left. - \sum_{j=1}^{N} {w_j h_{ij}}^t \, d_1 \, \widehat{x_t^{ci}}(1)^j \right|^2 \qquad (5.42)$$

5.4.5. Simulation Results for Performance Analysis of WAGMLDSTTCs

The simulation results have been shown for WAGMLDSTTCs using four transmit antennas, 16-QAM signal constellation partitioned in two levels, and different number of receive antennas. Four different possible predefined channel profiles have been considered at the transmitter. The generator sequences for each encoder in the selected code set CS^{ci} at predefined channel profiles are given in table 3.1.

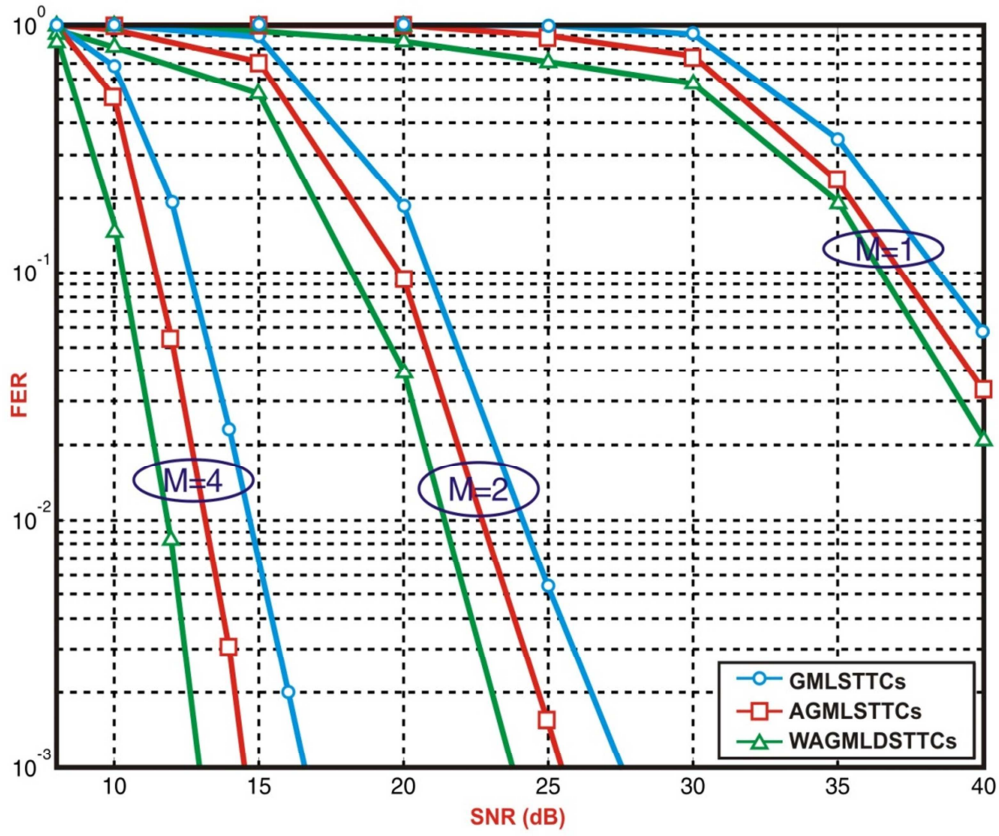

Figure 5.10: Performance comparison of GMLSTTCs, AGMLSTTCs, and WAGMLDSTTCs

Figure 5.10 exhibits the FER performance comparison of WAGMLDSTTCs, AGMLSTTCs, and GMLSTTCs. It can be noted that the performance of WAGMLSTTCs is improved by the using dynamic STTCs as component codes. The comparison results show that WAGMLDSTTCs are superior to GMLSTTCs and AGMLSTTCs by about 3.2 dB and 1.6 dB respectively at the FER of 10^{-2} and M=2.

5.5 COMPLEXITY CONSIDERATIONS

The minimum complexities for MLSTTCs, GMLSTTCs, MLDSTTCs, and GMLDSTTCs have been calculated in section 3.6 and the table 3.2 presented their comparison based on different parameters. Similarly, in this section, the minimum complexities of AGMLSTTCs, WAGMLSTTCs, and WAGMLDSTTCs are calculated.

AGMLSTTCs are designed by adaptive grouping of transmit antennas based on the CSI at the transmitter. As calculated in section 3.6, the minimum complexity for GMLSTTCs is 48. The adaptive grouping of the transmit antennas increases the complexity of AGMLSTTCs. For the system having four transmit antennas and two receive antennas, the calculation of power gain as given in equation 4.9 results in a minimum increase in the complexity by 4×2=8. The sorting the power gains using a merge sort algorithm increases the complexity by (n x log n) i.e. by 8. The formation of two groups of antennas increases the complexity by 2. Therefore, the minimum complexity for AGMLSTTCs is 48+ 8 +8+2=66.

The complexity of WAGMLSTTCs is more due to weighting of the transmitting signals to provide the beamforming. For four transmit antennas, four beamforming coefficients needs to be calculated based on the CSI at the transmitter. Considering minimum complexity, there will be an increase in the complexity by 4 due to beamforming. Therefore, the minimum complexity of WAGMLSTTCs is 66+4=70.

Similarly, the complexity of WAGMLDSTTCs is more than WAGMLSTTCs due to the dynamic component code selection. As presented in the section 3.6, for the system having four transmit antennas and two receive antennas, the calculation of power gain results in an increase in the complexity by 8. For four predefined channel profiles, the comparison of total power gain *G* at the current channel profile with total power gains corresponding to the predefined channel profiles results in an increase in the minimum complexity by 16. Therefore, the minimum complexity for WAGMLDSTTCs for the system having four transmit antennas and two receive antennas is 70+ 8+16=94.

Thus, the complexity of WAGMLDSTTCs is highest among all the presented codes but at the same time WAGMLDSTTCs provide the maximum coding gain. The table 5.1 given below presents a comparison of different aspects of the GMLSTTCs AGMLSTTCs, WAGMLSTTCs, and WAGMLDSTTCs.

Table 5.1: Comparison of GMLSTTCs, AGMLSTTCs, WAGMLSTTCs, and WAGMLDSTTCs (For L=2 levels, 16-QAM Constellation).

Parameter/Criteria	**GMLSTTCs**	**AGMLSTTCs**	**WAGMLSTTCs**	**WAGMLDSTTCs**
Constellation Partitioning	$\mathcal{M}$-way partitioning	$\mathcal{M}$-way partitioning	$\mathcal{M}$-way partitioning	$\mathcal{M}$-way partitioning
Spectral Efficiency	6 bits/s/Hz	6 bits/s/Hz	6 bits/s/Hz	6 bits/s/Hz
Channel State Information	Perfect CSI at receiver only	Perfect CSI at receiver and transmitter	Perfect CSI at receiver and transmitter	Perfect CSI at receiver and transmitter
Minimum Computational Complexity	48	66	70	94
Transmit Antenna Grouping	Predefined antenna grouping	Adaptive antenna grouping	Adaptive antenna Grouping	Adaptive antenna Grouping
Component Code Selection	No, Predefined component STTCs used.	No, Predefined component STTCs used.	No, Predefined component STTCs used.	Yes, Component STTCs are dynamically selected based on perfect CSI at transmitter.
Beamforming	No	No	Yes	Yes

5.6 SUMMARY OF THE CHAPTER

In this chapter, improvement in the performance of AGMLSTTCs has been presented by employing a beamforming technique at the transmitter. The CSI at the transmitter has been utilized for adaptive grouping of the transmit antennas and providing beamforming for the transmitting signals to design WAGMLSTTCs. In the beamforming technique, the transmitting signals are multiplied with beamforming coefficients calculated with the help of the CSI at the transmitter. The simulation results have shown that WAGMLSTTCs outperform GMLSTTCs by 2.6 dB.

The performance of WAGMLSTTCs has been further improved by using the CSI at the transmitter to dynamically select the component codes for multilevel coding. WAGMLDSTTCs have been presented which optimally utilize the CSI at the transmitter for grouping of transmit antennas, beamforming, and dynamic component code selection. The simulation results have manifested that WAGMLDSTTCs are superior to the GMLSTTCs and AGMLSTTCs by about 3.2 dB and 1.6 dB. Thus, WAGMLDSTTCs provide best performance over all other codes presented in the thesis.

CHAPTER 6

CONCLUDING REMARKS AND FUTURE SCOPE

6.1 CONCLUDING REMARKS

The main aim of the research work presented in this thesis was to improve the performance of MLSTTCs and GMLSTTCs using CSI at the transmitter. This thesis has discussed and showed the use of CSI at the transmitter for dynamic component code selection, adaptive antenna grouping, and beamforming. In this research work, design and analysis of different dynamically grouped multilevel space-time trellis codes have been presented based on combination of MLSTTCs or GMLSTTCs with the CSI at the transmitter. The presented system models, mathematical expressions for branch metric calculation, and simulation results confirm that the use of the CSI at the transmitter can significantly improve the performance of MLSTTCs and GMLSTTCs.

In the first approach, the CSI at the transmitter has been used for dynamic selection of the component STTCs. MLSTTCs and GMLSTTCs use predefined STTCs as the component codes in the multilevel coding. A code set selection algorithm has been proposed for dynamic selection of the optimum generator sequences with the help of the CSI at the transmitter. The selected generator sequences are used for designing the dynamic STTCs. The simulation results have shown that the coding gain of dynamic STTCs is superior to existing STTCs by 0.7 dB at FER of 10^{-2}. Dynamic STTCs have been used as the component codes in multilevel coding for designing novel MLDSTTCs and GMLDSTTCs. It may be inferred from the simulation results that MLDSTTCs are superior to MLSTTCs by 1.1 dB at FER of 10^{-1} and GMLDSTTCs are superior to GMLSTTCs by 1.6 dB at FER of 10^{-2}.

In the second approach, the CSI at the transmitter has been used for adaptive grouping of the transmit antennas. GMLSTTCs use static and predefined grouping of transmit antennas. In the presented research work, the performance of GMLSTTCs has been improved by performing adaptive grouping of the transmit antennas based on the CSI. An adaptive antenna algorithm is proposed for adaptive grouping of the transmit antennas. In the adaptive antenna grouping, instantaneous channel power gain is calculated between each transmit antenna and all the receive antennas. A subset of transmit antennas having maximum instantaneous channel power gain is selected to form a group of transmit antennas. Novel AGMLSTTCs have been designed by replacing the predefined antenna grouping in GMLSTTCs with adaptive grouping of the transmit antennas with the help of the CSI at the transmitter. From the presented results, it is evident that AGMLSTTCs are superior to GMLSTTCs by 1.5 dB at the FER of 10^{-2}.

In a third approach, the CSI at the transmitter has been used for providing beamforming for the transmitting signals by dynamically distributing the transmit power across the transmit antennas. In GMLSTTCs, the transmit power is equally distributed across all transmit antennas. The performance of GMLSTTCs has been improved by dynamically allocating the power to the transmit antennas. Novel WAGMLSTTCs have been presented by using the CSI for both the antenna grouping and weighting the transmitting signals. Finally, the CSI has been optimally used for simultaneously providing the adaptive grouping of the transmit antennas, beamforming, and dynamic component code selection. WAGMLDSTTCs have been designed by combining adaptive grouping of the transmit antennas, beamforming, and dynamic component code selection. It has been shown that the performance of WAGMLSTTCs is superior to GMLSTTCs by 2.6 dB and the performance of WAGMLDSTTCs is superior to GMLSTTCs by 3.2 dB. Hence, it can be concluded that the proposed codes designed using the CSI at the transmitter

provide improved error performance in comparison to the existing multilevel codes. The proposed codes can be used to improve the performance of the wireless communication systems such as GSM, CDMA, TDMA, and FDMA.

6.2 FUTURE SCOPE

The advantages of using the CSI at the transmitter in MLSTTCs and GMLSTTCs have been demonstrated in the thesis, nevertheless, there is always scope for improvements. An objective for future work of the presented mathematical framework can be expanded by considering different channel models other than quasi-static Rayleigh fading channel model. For example, the performance of the proposed codes can be analyzed for Rician channel, Nagakami channel, and frequency selective channel. In the presented work, the multistage decoder has been used to minimize the probability of error. The minimum mean square error (MMSE) and iterative decoding can be investigated to minimize the probability of symbol error. Moreover, other research directions could be followed by considering higher size signal constellation e.g. a 32-QAM or 64-QAM signal constellation can be used to further improve the data transmission rate to 8b/s/Hz. Another possibility is to develop other types of multilevel codes by using the component codes other than STTCs in multilevel coding. For example, other types of multilevel codes can be designed by using OSTBCs and SOSTBCs as component codes.

LIST OF PUBLICATIONS

[1] D. Jain and S. Sharma, "Adaptively grouped multilevel space-time trellis codes," *Wireless Pers. Commun.*, ***Springer***, vol. 74, no. 2, pp. 415-426, Jan. 2014, **(SCI Indexed; Impact Factor: 0.979)**.

[2] D. Jain and S. Sharma, "A novel grouped multilevel dynamic space-time trellis code scheme," *Int. J. Commun. Systems*, ***John Wiley & Sons***, DOI: 10.1002/dac.2754, Feb. 2014, **(SCI Indexed; Impact Factor: 1.106)**.

[3] D. Jain, and S. Sharma, "Adaptive generator sequence selection in multilevel space–time trellis codes," *Wireless Pers. Commun.*, ***Springer***, vol. 75, no. 4, pp. 1851-1862, Apr. 2014. **(SCI Indexed; Impact Factor: 0.979)**.

[4] D. Jain and S. Sharma, "Weighted adaptively grouped multilevel space-time trellis codes," *Int. J. Electron.*, ***Taylor and Francis***, DOI:10.1080/00207217.2014.942889, Aug. 2014. **(SCI Indexed; Impact Factor: 0.751)**.

[5] D. Jain and S. Sharma, "Adaptively grouped multilevel space–time trellis codes combined with beamforming and component code selection," *Wireless Pers. Commun.*, ***Springer***, vol. 77, no. 4, pp. 2549-2563, Aug. 2014, **(SCI Indexed; Impact Factor: 0.979)**.

REFRENCES

[1] A. Pierce, B. B. Barrow, B. Goldberg, and J. Tucker, “Effective application of forward-acting error-control coding to multichannel HF data modems,” *IEEE Trans. Commun.*, vol. 18, no. 4, pp 281-294, Aug. 1970.

[2] J. L. Massey, “Coding and modulation in digital communications,” *in Int. Zurich Seminar Digital Commun.*, Switzerland, Mar. 1974, pp 1-4.

[3] G. Ungerboeck and I. Csajka, “On improving data-link performance by increasing channel alphabet and introducing sequence coding,” in *Proc. IEEE Int. Symp. Inform. Theory (ISIT)*, Sweden, June 1976.

[4] H. Imai and S. Hirakawa, “A new multilevel coding method using error correcting codes,” *IEEE Trans. Inform. Theory*, vol. 23, pp. 371-377, May 1977.

[5] G. Ungerboeck, “Channel coding with multilevel/phase signals,” *IEEE Trans. Inform. Theory*, vol. 28, pp. 55-67, Jan. 1982.

[6] G. Ungerboeck, “Trellis-coded modulation with redundant signal sets, Part I: Introduction,” *IEEE Commun. Mag.*, vol. 25, pp. 5-11, Feb. 1987.

[7] G. Ungerboeck, “Trellis-coded modulation with redundant signal sets, Part II: State of the art,” *IEEE Commun. Mag.*, vol. 25, pp. 12-21, Feb. 1987.

[8] G. D. Forney, R. G. Gallager, G. Lang, F. Longstaff, and S. Qureshi, “Efficient modulation for band-limited channels,” *IEEE J. Select. Areas Commun. (JSAC)*, vol. 2, pp. 632-647, Sept. 1984.

[9] A. R. Calderbank and J. E. Mazo, “A new description of trellis codes,” *IEEE Trans. Inform. Theory*, vol. 30, pp. 781-791, Nov. 1984.

[10] A. R. Calderbank and N. Sloane, “New trellis codes based on lattices and cosets,” IEEE Trans. Inform. Theory, vol. 33, pp. 177-195, Mar. 1988.

[11] E. Biglieri, D. Divsalar, P. J. McLane, and M. K. Simon, *Introduction to trellis coded modulation*. N.Y.: MacMillan, 1991.

[12] T. K. Moon, *Trellis Coded Modulation, in Error Correction Coding: Mathematical Methods and Algorithms*. N.J.: John Wiley & Sons, 2005.

[13] V. V. Ginzburg, "Multidimensional signals for a continuous channel," *Problemy Peredachi Informatsii*, vol. 20, no. 1, pp. 28-46, Jan. 1984.

[14] E. Biglieri and M. Elia, "Multidimensional modulation and coding for band limited digital channels," *IEEE Trans. Inform. Theory*, vol. 34, no. 4, pp. 803-809, July 1988.

[15] S. I. Sayegh, "A class of optimum block codes in signal space," *IEEE Trans. Commun.*, vol. 34, pp. 1043-1045, Oct. 1986.

[16] R. M. Tanner, "Algebraic construction of large Euclidean distance combined coding/modulation systems," in *IEEE Int. Symp. Inform. Theory*, Ann Harbor. Oct. 6-9, 1986.

[17] L. Duan, B. Rimoldi, and R. Urbanke, "Approaching the AWGN channel capacity without active shaping," in *Proc. IEEE Int. Symp. Inform. Theory*, ULM, Germany, Jun. 1997, pp. 374.

[18] X. Ma and L. Ping, "Coded modulation using superimposed binary codes," *IEEE Trans. Inform. Theory*, vol. 50, no. 12, pp. 3331–3343, Dec. 2004.

[19] G. J. Pottie and D. P. Taylor, "Multilevel codes based on partitioning," *IEEE Trans. Inform. Theory*, vol. 35, pp. 387-98, Jan. 1989.

[20] U.Waschmann, R. F. Fischer, and J. B. Huber, "Multilevel codes: Theoretical concepts and practical design rules," *IEEE Trans. Inform. Theory*, vol. 45, pp. 1361-1391, July 1999.

[21] A. Calderbank, “Multilevel codes and multistage decoding,” *IEEE Trans. Commun*., vol. 37, pp. 222-229, Mar. 1989.

[22] M. Isaka and H. Imai, “On the iterative decoding of multilevel codes,” *IEEE J. Select. Areas Commun*, vol. 19, no. 5, pp. 935-943, May 2001.

[23] E. Zehavi, “8-PSK trellis codes for a Rayleigh channel,” *IEEE Trans. Commun.*, vol. 40, pp. 873-884, May 1992.

[24] G. Caire, G. Taricco, and E. Biglieri, “Bit-interleaved coded modulation,” *IEEE Trans. Inform. Theory*, vol. 44, no. 3, pp. 927–946, May 1998.

[25] S. H. Muller-Weinfurtner, “Coding approaches for multiple antenna transmission in fast fading and OFDM,” *IEEE Trans. Signal Process.*, vol. 50, no. 10, pp. 2442-2450, Oct. 2002.

[26] M. McKay and I. Collings, “Capacity and performance of MIMO-BICM with zero-forcing receivers,” *IEEE Trans. Commun*., vol. 53, no. 1, pp. 74-83, Jan. 2005.

[27] J. Hamkins and B. Moision, “Multipulse pulse-position modulation on discrete memoryless channels,” *JPL Interplanetary Netw. Progress Report*, vol. 42, pp. 1-13, May 2005.

[28] J. Proakis, *Digital Communications.* 4th edition, New York: McGraw-Hill, 2001.

[29] J. Huber and U. Wachsmann, “Capacities of equivalent channels in multilevel coding schemes,” *Electron. Lett.*, vol. 30, pp. 557-558, Mar. 1994.

[30] R. Fischer, J. Huber, and U. Wachsmann, “Multilevel coding: aspects from information theory,” in *Proc IEEE Global Telecommun. Conf. (GLOBEGOM’96)*, London, U.K., Nov. 1996, pp. 26-30.

[31] A. R. Calderbank and N. Seshadri, “Multilevel codes for unequal error protection,” *IEEE Trans. Inform. Theory*, vol. 39, no. 4, pp. 1234-1248, July 1993.

[32] L. F. Wei, “Trellis coded modulation with multidimensional constellations,” *IEEE Trans. Inform. Theory,* vol. 33, no.4, pp. 483-501, July 1987.

[33] S. Mallik, *Multilevel coding schemes for underspread fading channels.* Master Thesis, University of Illinois at Urbana-Champaign, U.S.A., 2004.

[34] R. Morelos-Zaragoza, M. Fossorier, S. Lin, and H. Imai, “Multilevel coded modulation for unequal error protection-Part I: symmetrical constellations,” *IEEE Trans. Commun.*, vol. 48, pp 204-213, Feb. 2000.

[35] T. Cover, “Broadcast channels,” *IEEE Trans. Inform. Theory*, vol. 18, pp. 2-14, Jan. 1972.

[36] K. Fazel and M. Ruf, “Combined multilevel coding and multiresolution modulation,” *in Proc. IEEE Int. Conf. Commun. (ICC), Geneva, Switzerland*, May 1993, vol. 2, pp. 1081-1085.

[37] G.D. Forney and Jr. Coset, “Codes part I: Introduction and geometrical classification,” *IEEE Trans. Inform. Theory,* vol. 34, pp. 1123-1151, Sept. 1988.

[38] G.D. Forney and Jr. Coset, “Codes part II: Binary lattices and related codes,” *IEEE Trans. Inform. Theory*, vol. 34, pp. 1152-1187, Sept. 1988.

[39] A. Wittneben, “A new bandwidth efficient transmit antenna modulationdiversity scheme for linear digital modulation,” in *Proc. IEEE Int. Conf. Commun. (ICC), Geneva, Switzerland*, May 1993, pp. 1630–1634.

[40] N. Seshadri and J. H. Winters, “Two signalling schemes for improving the error performance of frequency-division-duplex (FDD) transmission systems using transmitter antenna diversity,” in *Proc. IEEE Veh. Technol. Conf. (VTC), Secaucus, New Jersey, USA*, May 1993, pp.508–511.

[41] S. Ogose, K. Murota, and K. Hirade, “A transmitter diversity for MSK with two-bit differential detection,” *IEEE Trans. Veh. Technol.*, vol. VT-33, no. 1, pp. 37–43, Feb. 1984.

[42] V. M. DaSilva and E. S. Sousa, “Fading-resistant modulation using several transmitter antennas,” *IEEE Trans. Commun.*, vol. 45, no. 10, pp. 1236–1244, Oct. 1997.

[43] J. Winters, “On the capacity of radio communication systems with diversity in a Rayleigh fading environment,” *IEEE J. Select. Areas Commun*., vol. 5, pp. 871–878, June 1987.

[44] G. J. Foschini, “Layered space-time architecture for wireless communication in fading environments when using multi-element antennas,” *Bell Labs Tech. J.*, pp. 41–59, Autumn 1996.

[45] E. Telatar, “Capacity of multi-antenna Gaussian channels,” *Eur. Trans. Telecomm. ETT*, vol. 10, pp. 585–596, Nov. 1999.

[46] R. K. Hawkins, P. J F. Manning, J. R. Gibson, and K. P. Singh, “Calibration of the CCRS airborne scatterometers,” *IEEE Trans. Antennas Propagation*, vol. 38, no. 6, pp. 903-918, June 1990.

[47] V. Tarokh, N. Seshadri, and A. R.Calderbank, “Space-time codes for high data rate wireless communication: Performance criterion and code construction,” *IEEE Trans. Inform. Theory*, vol. 44, pp. 744-765, Mar. 1998.

[48] W. Firmanto, B. Vucetic, and J. Yuan, “Space-time TCM with improved performance on fast fading channels,” *IEEE Commun. Lett.*, vol. 5, pp. 154–156, Apr. 2001.

[49] J. Yuan, Z. Chen, B. Vucetic, and W. Firmanto, “Performance and design of space-time coding in fading channels,” *IEEE Trans. Commun.*, vol. 51, pp. 1991–1996, Dec. 2003.

[50] M. Tao and R. S. Cheng, “Improved design criteria and new trellis codes for space-time coded modulation in slow flat fading channels,” *IEEE Commun. Lett.*, vol. 5, pp. 313–315, July 2001.

[51] J. Zhang, Y. Qiang, J. Wang, and D. Li, “On the design of space-time code for fast fading channels,” in *Proc. IEEE Personal, Indoor and Mobile Radio Commun. PIMRC 2003*, Sept. 2003, vol. 2, pp. 1045–1048.

[52] Q. Yan and R. S. Blum, “Improved space-time convolutional codes for quasi-static slow fading channels,” *IEEE Trans. Wireless Commun.*, vol. 1, pp. 563–571, Oct. 2002.

[53] V. Tarokh, H. Jafarkhani, and A. R. Calderbank, “Space-time block codes from orthogonal designs,” *IEEE Trans. Inform. Theory*, vol. 45, pp. 1456–1466, July 1999.

[54] V. Tarokh, H. Jafarkhani, and A. R. Calderbank, “Space-time block coding for wireless communciations: performance results,” *IEEE J. Select. Areas Commun.*, vol. 17, pp. 451–459, Mar. 1999.

[55] S. M. Alamouti, “A simple transmit diversity technique for wireless communications,” *IEEE J. Select. Areas Commun.*, vol. 16, no. 8, pp. 1451–1458, Oct. 1998.

[56] J. Zhu, W.C. Wong, and C D. S. Liyanage, “Study of performance of OFDM-CDMA in Mobile Fading Channels,” *IEICE Trans. Commun.*, vol. E-84 B, no. 3, pp. 674 -681, Mar. 2001.

[57] S. S. Anderson, G. A. Punchihewa, and C. D. S. Liyanage, “Alamouti space-time block code receiver implementation in a fixed - point DSP”, in *Proc 11th Electron. New Zealand Conf. (ENZCON 2004), Palmerston North New Zealand*, Nov. 2004, pp. 212-217.

[58] W. Su, X. G. Xia, and K. J. R. Liu, “A systematic design of high-rate complex orthogonal space-time block codes,” *IEEE Commun. Lett.*, vol. 8, no. 6, pp. 380-382, June 2004.

[59] X. B. Liang, “Orthogonal designs with maximal rates,” *IEEE Trans. Inform. Theory*, vol. 49, no. 10, pp. 2468-2503, Oct. 2003.

[60] K. Lu, S. Fu, and X. G. Xia, “Closed-form designs of complex orthogonal space-time block codes of rates (k+ 1)/(2k) for 2k-1or 2k transmit antennas,” *IEEE Trans. Inform. Theory*, vol. 51, no. 12, pp. 4340-4347, Dec. 2005.

[61] S. Sandhu and A. Paulraj, “Space-time block codes: A capacity perspective,” *IEEE Commun. Lett.*, vol. 4, no. 12, pp. 384-386, Dec. 2000.

[62] T. Niyomsataya, A. Miri, and M. Nevins, “Pairwise error probability of space–time codes for a keyhole channel,” *IET commun.*, vol. 1, no. 1, pp. 101-105, Feb. 2007.

[63] H. Jafarkhani, “A quasi-orthogonal space-time block code,” *IEEE Trans. Commun.*, vol. 49, no. 1, pp. 1–4, July 2001.

[64] N. Sharma and C. B. Papadias, “Improved quasi-orthogonal codes through constellation rotation,” *IEEE Trans. Commun.*, vol. 51, pp. 332–335, Mar. 2003.

[65] W. Su and X.-G. Xia, “Signal constellations for quasi-orthogonal space-time block codes with full diversity,” *IEEE Trans. Inform Theory*, vol. 50, pp. 2331–2347, Oct. 2004.

[66] C. Yuen, Y. L. Guan, and T. T. Tjhung, “Quasi-orthogonal STBC with minimum decoding complexity,” *IEEE Trans. Wireless Commun.*, vol. 4, no. 5, pp. 2089–2094, Sep. 2005.

[67] T. H. Liew and L. Hanzo, “Space-time codes and concatenated channel codes for wireless communications,” in *Proc. IEEE*, vol. 90, no. 2, pp. 187-219, Feb. 2002.

[68] H. Jafarkhani and N. Seshadri, “Super-orthogonal space-time trellis codes,” *IEEE Trans. Inform. Theory*, vol. 49, no. 4, pp. 937–950, Apr. 2003.

[69] D. Ionescu, K. Mukkavilli, Y. Zhiyuan, and J. Lilleberg, “Improved 8-and 16-state space-time codes for 4PSK with two transmit antennas,” *IEEE Commun. Lett.*, vol. 5, no. 7, pp. 301–303, July 2001.

[70] S. Siwamogsatham and M. Fitz, “Improved high-rate space-time codes via concatenation of expanded orthogonal block code and M-TCM,” in *Proc. IEEE Int. Conf. Commun. ICC* 2002, May 2002, vol. 1, pp. 636–640.

[71] M. Bale, B. Laska, D. Dunwell, F. Chan, and H. Jafarkhani, “Computer design of super-orthogonal space-time trellis codes,” *IEEE Trans. Wireless Commun.*, vol. 6, no. 2, pp. 463–467, Feb. 2007.

[72] H. Jafarkhani and N. Hassanpour, “Super-quasi-orthogonal space-time trellis codes for four transmit antennas,” *IEEE Trans. Wireless Commun.*, vol. 4, no. 1, pp. 215–227, Jan. 2005.

[73] O. Tirkkonen and A. Hottinen, “Square-matrix embeddable space-time block codes for complex signal constellations,” *IEEE Trans. Inform. Theory*, vol. 48, no. 2, pp. 384-395, Feb. 2002.

[74] M. O. Damen, K. Abed-Meraim, and J. C. Belfiore, “Diagonal algebraic space-time: block codes,” *IEEE Trans. Inform. Theory*, vol. 48, no. 3, pp. 628-636, Mar. 2002.

[75] M. O. Damen, A. Tewfik, and J. C. Belfiore, “A construction of a space-time code based on number theory,” *IEEE Trans. Inform. Theory*, vol. 48, no. 3, pp. 753-760, Mar. 2002.

[76] Y. Xia, Z. Wang, and G. B. Giannakis, “Space-time diversity systems based on linear constellation precoding,” *IEEE Trans. Wireless Commun.*, vol. 2, no. 2, pp. 294-309, Mar. 2003.

[77] S. Banerjee and M. Agrawal, “A simple analytical design approach to space-time trellis codes,” *Wireless Pers. Commun.*, vol. 75, no. 2, pp 1141-1154, Mar. 2014.

[78] Z. Chen, B. Vucetic, and J. Yuan, “Improved space-time trellis coded modulation scheme on slow Rayleigh fading channels,” *Electron. Lett.*, vol. 37, pp. 440-441, Mar. 2001.

[79] M. Tao and R. S. Cheng, “Improved design criteria and new trellis codes for space-time coded modulation in slow at fading channels,” *IEEE Commun. Lett*., vol. 5, pp. 313-315, July 2001.

[80] S. Baro, G. Bauch, and A. Hansmanna, “Improved codes for space-time trellis-coded modulation,” *IEEE Commun. Lett.*, vol. 4, pp. 20-22, Jan. 2000.

[81] Q. Yan and R. S. Blum, “Improved space-time convolutional codes for quasi-static slow fading channels,” *IEEE Trans. Wireless Commun.*, vol. 1, pp. 563-571, Oct. 2002.

[82] G. Tarricco and E. Biglieri, “Exact pairwise error probability of space-time codes,” *IEEE Trans. Inform. Theory*, vol. 48, pp. 510-513, Feb. 2002.

[83] P. Dharmawansa and N. Rajatheva, “Pairwise error probability of space-time codes in frequency selective Rician channels,” *IEEE Commun. Lett*., vol. 9, no. 10, pp. 894-896, Oct. 2005.

[84] M. Uysal and C. N. Georghiades, “Error performance analysis of space-time codes over Rayleigh fading channels,” *J. Commun. Netw.*, vol. 2, pp. 351-355, Dec. 2000.

[85] M. Uysal, “Diversity analysis of space-time coding in cascaded Rayleigh fading channels”, *IEEE Commun. Lett.*, vol. 10, no. 3, pp. 165-167, Mar. 2006.

[86] F. Behnamfar, F. Alajaji, and T. Linder, “MAP decoding for multi-antenna systems with non-uniform sources: exact pairwise error probability and applications,” *IEEE Trans. Commun.*, vol. 57, no. 1, pp. 242-254, Jan. 2009.

[87] Z. Zhang, S. W. Cheung, and T. I. Yuk, “An exact close-form PEP and a new PEP for space-time codes in Rayleigh fading channels,” in *Proc. Singapore Inter. Conf. Commun. Syst. (ICCS 2008)*, Nov. 2008, pp.82-86.

[88] J. Zhang, Y. Qiang, J. Wang, and D. Li, “On the design of space-time code for fast fading channels,” in *14th Proc. Personal, Indoor and Mobile Radio Commun., PIMRC 2003*, Sept. 2003, vol. 2, pp. 1045-1048.

[89] M. K. Byun, D. Park, and B. G. Lee, “Performance and distance spectrum of space-time codes in fast Rayleigh fading channels,” in *Proc. IEEE Conf. WCNC 2003*, Mar. 2003, vol. 1, pp. 257-261.

[90] L. Yan and P. Y. Kam, “Space-time trellis codes over rapid Rayleigh fading channels with channel estimation—part II: performance analysis and code design for non-identical channels,” *IEEE Trans. Commun.*, vol. 57, no. 2, pp 343-347, Feb. 2009.

[91] A. Graell, “Design of space-time trellis codes for transmit-correlated fading channels,” *IEEE Trans. Commun.*, vol. 55, no. 1, Jan. 2007.

[92] C. Liao and V. K. Prabhu, “Design of space-time trellis codes in fast and flat fading channel,” in *Proc. IEEE Int. Symp. Microwave, Antenna*, Aug. 2005, vol. 2, pp 1111–1114.

[93] T. M. N. Ngatched, A. S. Alfa, and J. Cai, “Cooperative sensing with transmit diversity based on randomised STBC in CR networks,” *Int. J. Autonomous and Adaptive Commun. Syst*., vol.6, no. 4, pp. 403-416, Oct. 2013.

[94] Z. Zhong, S. Zhu, and A. Nallanathan, “Distributed space-time trellis code for asynchronous cooperative communications under frequency-selective channels,” *IEEE Trans. Wireless Commun.*, vol. 8, no. 2, pp. 796-805, Feb. 2009.

[95] L. Chu, J. Yuan, and Y. Li, “Performance analysis and code design of distributed space-time trellis codes for a detection-and-forward system,” 66th *IEEE Veh. Tech. Conf., VTC-2007 Fall*, Oct. 2007, pp.1172-1176.

[96] K. G. Seddik, A. K. Sadek, A. S. Ibrahim, and K. J. Liu, “Design criteria and performance analysis for distributed space-time coding,” *IEEE Trans. Veh. Tech.*, vol. 57, no. 4, July 2008.

[97] T. Wang, Y. Yao, and G. B. Gainnakis, “Non-coherent distributed space-time processing for multiuser cooperative transmissions,” *IEEE Trans. Wireless Commun*., vol. 5, no. 12, pp. 3339-3343, Dec. 2006.

[98] R. U. Nabar, H. Bolcskei, and F. W. Kneubuhler, “Fading relay channels: performance limits and space-time signal design,” *IEEE J. Select. Areas Commun.*, vol. 22, no. 6, pp. 1099-1109, Aug. 2004.

[99] M. Uysal, O. Canpolat, and M. M. Fareed, “Asymptotic performance analysis of distributed space-time codes,” *IEEE Commun. Lett.*, vol. 10, no. 11, pp. 775-777, Nov. 2006.

[100] A. Stefanov and E. Erkip, “Cooperative space-time coding for wireless networks,” *IEEE Trans. Commun.*, vol. 53, no. 11, pp. 1804-1809, Nov. 2005.

[101] O. Canpolat, M. Uysal, and M. M. Fareed, “Analysis and design of distributed space-time trellis codes with amplify-and-forward relaying,” *IEEE Trans. Veh. Tech.*, vol. 56, no. 4, pp. 1649-1660, July 2007.

[102] Y. Li, X.Guo, J.Hui, and X. Wang, “A new high rate serially concatenated space-time code,” in *Proc. IEEE Int. Symp. Inform. Theory*, Sept. 2005, pp.1043-1047.

[103] F. Shengli, X. Xia, and H. Wang, “Recursive space–time trellis codes using differential encoding,” *IEEE Trans. Inform. Theory*, vol. 55, no. 2, Feb. 2009.

[104] G. D. Golden, G. J. Foschini, R. A. Valenzuela, and P. W. Wolniansky, “Detection algorithm and initial laboratory results using the V-BLAST space-time communication architecture,” *Electron. Lett.*, vol. 35, pp. 14-15, Jan. 1999.

[105] H. E. Gamal and R. Hammons, “A new approach to layered space-time coding and signal processing,” *IEEE Trans. Inform. Theory*, vol. 47, pp. 2321-2334, Sept. 2001.

[106] G. Caire and G. Colavolpe, “On low-complexity space-time coding for quasi-static channels,” *IEEE Trans. Inform. Theory*, vol. 49, pp. 1400-1416, June 2003.

[107] C. B. Papadias and G. J. Foschini, “Capacity-approaching space-time codes for systems employing four transmitter antennas,” *IEEE Trans. Inform. Theory*, vol. 49, pp. 726-733, Mar. 2003.

[108] B. L. Hughes, “Differential space-time modulation,” *IEEE Trans. Inform. Theory*, vol. 46, pp. 1496-1501, Nov. 2000.

[109] B. M. Hochwald and W. Sweldens, “Differential unitary space-time modulation,” *IEEE Trans. Commun.*, vol. 48, pp. 1496-1501, Dec. 2000.

[110] J. K. Cavers, “An analysis of pilot symbol assisted modulation for Rayleigh fading channels,” *IEEE Trans. Veh. Technol.*, vol. 40, pp. 686-693, Nov. 1991.

[111] N. S. Ferdinand and N. Rajatheva, “Performance Analysis of Imperfect Channel Estimation in MIMO Two Hop Fixed Gain Relay Network with Beamforming,” *IEEE Commun. Lett.*, vol.15, no.2, pp. 208-210, Feb. 2011.

[112] A. Kumar, N. Lakshay, and S. P. Singh. “Cognitive Radios: A Survey of Methods for Channel State Prediction,” *arXiv preprint arXiv:1311.2869,* Nov. 2013.

[113] V. Tarokh, N. Seshadri, and A. R. Calderbank, “Space-time codes for high data rate wireless communication: performance criteria in the presence of channel estimation errors, mobility, and multiple paths,” *IEEE Trans. Commun*., vol. 47, pp. 199-207, Feb. 1999.

[114] P. Garg, R. K. Mallik, and H. M. Gupta, “Performance analysis of space-time coding with imperfect channel estimation,” *IEEE Trans. Wireless Commun.*, vol. 4, pp. 257-265, Jan. 2005.

[115] A. U. Alahakone and S. M. N. A. Senanayake, “A combination of inertial sensors and vibrotactile feedback for balance improvements in therapeutic applications,” in *Proc. Innovative Technologies in IEEE Intelligent Systems and Industrial Applications*, CITISIA 2009, July 2009, pp. 5-10.

[116] A. J. Goldsmith and P. P. Varaiya, “Capacity of fading channels with channel side information,” *IEEE Trans. Inform. Theory*, vol. 43, pp. 1986-1992, Nov. 1997.

[117] A. Narula, M. J. Lopez, M. D. Trott, and G. W. Wornell, “Efficient use of side information in multiple-antenna data transmission over fading channels,” *IEEE J. Select. Areas Commun.*, vol. 16, pp. 1423-1436, Oct. 1998.

[118] V. K. N. Lau, Y. Liu, and T. Chen, “The role of transmit diversity on wireless communications-reverse link analysis with partial feedback,” *IEEE Trans. Commun.*, vol. 50, pp. 2082-2090, Dec. 2002.

[119] A. F. Molisch and M. Z. Win, “MIMO systems with antenna selection,” *IEEE Microwave Mag.*, vol. 5, no. 1, pp. 46–56, Mar. 2004.

[120] D. A. Gore and A. J. Paulraj, “MIMO antenna subset selection with space-time coding,” *IEEE Trans. Signal Process.*, vol. 50, no. 10, pp. 2580–2588, Oct. 2002.

[121] A. Ghrayeb and T. M. Duman, “Performance analysis of MIMO systems with antenna selection over quasi-static fading channels,” *IEEE Trans. Veh. Tech.*, vol. 52, no. 2, pp. 281–288, Mar. 2003.

[122] D. Gore, R. Nabar, and A. Paulraj, “Selecting an optimal set of transmit antennas for a low rank matrix channel,” in *Proc. Int. Conf. Acoustics, Speech, and Signal Process. ICASSP*, June 2000, vol.5, pp.2785-2788.

[123] A. F. Molisch, M. Z. Win, and J. H.Winter, “Capacity of MIMO systems with antenna selection,” in *Proc. IEEE Int. Conf. Commun.*, Jun. 2001, vol. 2, pp. 570-574.

[124] R. S. Blum and J. H. Winters, “On optimum MIMO with antenna selection,” *IEEE Commun. Lett.*, vol. 6, no. 8, pp. 322-324, Aug. 2002.

[125] R. W. Heath, Jr., S. Sandhu, and A. Paulraj, “Antenna selection for spatial multiplexing systems with linear receivers,” *IEEE Commun. Lett.*, vol. 5, no. 4, pp. 142-144, Apr. 2001.

[126] A. Gorokhov, D. Gore, and A. Paulraj, “Receive antenna selection for MIMO flat-fading channels: theory and algorithms,” *IEEE Trans. Inform. Theory*, vol. 49, no. 10, pp. 2687–2696, Oct. 2003.

[127] I. Bahceci, T. M. Duman, and Y. Altunbasak, “Antenna selection for multiple-antenna transmission systems: performance analysis and code construction,” *IEEE Trans. Inform. Theory*, vol. 49, no. 10, pp. 2669 – 2681, Oct. 2003.

[128] X. N. Zeng and A. Ghrayeb, “Performance bounds for space-time block codes with receive antenna selection,” *IEEE Trans. Inform. Theory*, vol. 50, no. 9, pp. 2130–2137, Sep. 2004.

[129] A. Sanei, A. Ghrayeb, Y. Shayan, and T. M. Duman, “On the diversity order of space-time trellis codes with receive antenna selection over fast fading channels,” *IEEE Trans. Wireless Commun.*, vol. 5, no. 7, pp. 1579–1585, July 2006.

[130] Q. Ma and C. Tepedelenlioglu, “Antenna selection for space-time coded systems with imperfect channel estimation,” *IEEE Trans. Wireless Commun*., vol. 6, no. 2, pp. 710–719, Feb. 2007.

[131] S. Thoen, L. Perre, B. Gyselwckx, and M. Engels, “Performance analysis of combined transmit-SC/receive-MRC,” *IEEE Trans. Commun*., vol. 49, pp. 5-8, Jan 2001.

[132] Z. Chen, B. Vucetic, J. Yuan, and K. Lo, “Analysis of transmit antenna selection/maximal-ratio combining in Rayleigh fading channels,” *IEEE Trans. Veh. Tech*., vol. 54, no. 4, pp. 1312-1321, July 2005.

[133] W. H. Wong and E. G. Larsson, “Orthogonal space-time block coding with antenna selection and power allocation,” *Electron. Lett.*, vol. 39, no. 4, pp. 379–381, Feb. 2003.

[134] M. Tao, Q. Li, and H. K. Garg, “Extended space-time block coding with transmit antenna selection over correlated fading channels,” *IEEE Trans. Wireless Commun.*, vol. 6, no. 9, pp. 3137–3141, Sept. 2007.

[135] Z. Chen, B. Vucetic, and J. Yuan, “Space-time trellis codes with transmit antenna selection,” *Electron. Lett.*, vol. 39, no. 11, pp. 854–855, May 2003.

[136] R. Narasimhan, “Spatial multiplexing with transmit antenna and constellation selection for correlated MIMO fading channels,” *IEEE Trans. Signal Process.*, vol. 51, no. 11, pp. 2829-2838, Nov. 2003.

[137] J. Yuan, “Adaptive transmit antenna selection with pragmatic space- time trellis codes,” *IEEE Trans. Wireless Commun.*, vol. 5, no. 7, pp. 1706–1715, July 2006.

[138] V. Tarokh, A. Naguib, N.Seshadri, and A. R. Calderbank, “Combined array processing and space-time coding,” *IEEE Trans. Inform. Theory*, vol. 45, no. 4, pp. 1121-1128, May 1999.

[139] Y. Huang, D. Xu, and L. Yang, “Adaptive antenna grouping for space-time block coding and spatial multiplexing hybrid system,” in *Proc. Int. Conf. First Mobile Computing and Wireless Commun., MCWC 2006*, Sept. 2006, pp. 88-92.

[140] H. K. Mohammed, R. Tripathi, and K. Kant, “Performance of adaptive modulation in multipath fading channel,” *8th Int. Conf Advanced Commun. Tech. ICACT 2006*, Feb. 2006, vol. 2, pp. 1277-1282.

[141] I. Alam, V. Srivastva, A. Prakash, R. Tripathi, and A. K. Shankhwar, “Performance evaluation of adaptive modulation based MC-CDMA system,” *Wireless Eng. and Tech.*, vol. 4, pp. 54-58, Jan. 2013.

[142] F. Rashid-Farrokhi, K. J. R. Liu, and L. Tassiulas, “Transmit beamforming and power control for cellular wireless systems,” *IEEE J. Select. Areas Commun*., vol. 16, pp. 1437–1450, Oct. 1998.

[143] A. Kumar and R. Tripathi, “Impact of antenna beam joining on resource utilization in wireless mesh networks using smart antenna,” in *Int. Conf. on Computer and Commun. Tech. (ICCCT)*, Sept. 2010, pp.377-382.

[144] S. A. Jafar and A. Goldsmith, “On optimality of beamforming for multiple antenna systems with imperfect feedback,” in *Proc. IEEE Int. Symp. Inform. Theory*, June 2001, pp. 321-325.

[145] M. Agrawal and S. Prasad, “Robust adaptive beamforming for wideband, moving and coherent jammer via uniform linear arrays,” *IEEE Trans. Antennas and Prop*., vol. 47, pp. 1267-1275, Aug. 1999.

[146] M. Agrawal and S. Prasad, “Optimum broadband beamforming for coherent broadband signals and interferences,” *Signal Process., Elsevier*, vol. 77, no. 1, pp. 21-36, Aug. 1999.

[147] M. Agrawal, R. Abrahamsson, and P. Åhgren, “Optimum beamforming for a near field source in signal-correlated interferences,” *Signal Process., Elsevier*, vol. 86, no. 5, pp. 915-923, May 2006.

[148] G. Jongren, M. Skoglund, and B. Ottersten, “Combining beamforming and orthogonal space-time block coding,” *IEEE Trans. Inform. Theory*, vol. 48, no. 3, pp. 611-627, Mar. 2002.

[149] S. Zhou and G. B. Giannakis, “Optimal transmitter eigen-beamforming and space-time block coding based on channel correlations,” *IEEE Trans. Inform. Theory*, vol. 49, pp. 1673 –1690, July 2003.

[150] M. Katz, E. Tiirola, and J. Ylitalo, “Combining space-time block coding with diversity antenna selection for improved downlink performance,” in *Proc. IEEE Int. Veh. Tech. Conf.*, Jan. 2001, vol. 1, pp. 178–182.

[151] X. Yu, X. Liu, Q. Zhu, and D. Xu, “Adaptive modulation with constrained variable power for space–time coded MIMO systems,” *Int. J. Commun. Syst.* doi: 10.1002/dac.2425, Sep. 2012.

[152] S. Cho, I. Hwang, V. Tarokh, and C. You, “A practical transmit beamforming strategy for closed-loop MIMO communication,” *Int. J. Commun. Syst.*, vol. 25, pp. 1091–1099, Aug. 2012.

[153] L. Tang, X. Zhang, Y. Bai, and P. Zhu, “Performance analysis of MIMO beamforming with imperfect feedback,” *Int. J. Commun. Syst.* doi: 10.1002/dac.2461, Oct. 2012.

[154] J. N. Pillai and S. H. Mneney, “Adaptively Weighted space-time trellis codes,” in *Proc. Southern African Telecommun. Netw. Application Conf.*, pp. 39-44, Sept. 2004.

[155] A. Santoso, Y. Li, and B. Vucetic, “Weighted space-time trellis codes,” *Electron. Lett.*, vol. 40, pp. 254-256, Feb. 2004.

[156] A. Santoso, L. Yonghui, J. Allan, and B. Vucetic, “Dynamic transmit power allocation in space-time trellis coded systems,” *IEEE Trans. Wireless Commun.*, vol. 7, no. 8, pp. 3079-3089, Aug. 2008.

[157] Y. Li, B. Vucetic, A. Santoso, and Z. Chen, “Space-time trellis codes with adaptive weighting,” *Electron. Lett.*, vol. 39, no. 25, pp. 1833-1834, Dec. 2003.

[158] Y. Li and B. Vucetic, “Combined space-time trellis codes and beamforming on fast fading channels,” *Veh. Tech. Conf.*, June 2005, vol. 2, pp. 1181-1185.

[159] Y. Li and B. Vucetic, “Code design for combined space-time trellis codes and beamforming on slow fading channels,” *IEEE Inform. Theory Workshop*, pp. 473-477, Oct. 2006.

[160] D. Mavares and R. P. Torres, “Space-time code selection for transmit antenna diversity systems,” in *Proc. First Int. Conf. Mobile Computing and Wireless Commun.*, Sept 2006; pp. 83-87.

[161] L. Liu and H. Jafarkhani, “Space–time trellis codes based on channel-phase feedback,” *IEEE Trans. Commun.*, vol. 54, pp. 2186-2198, Dec. 2006.

[162] M. E. Celebi, S. Sahin, and U. Aygolu, “Full rate full diversity space-time block code selection for more than two transmit antennas,” *IEEE Trans. Wireless Commun.*, vol. 6, pp. 16-19, Jan. 2007.

[163] A. Eksim and M. E. Celebi, “Received SNR based code and antenna selection for limited feedback communication,” in *Proc. 18th conf. IEEE Signal Process. Commun.*, Apr. 2010, pp. 21-24.

[164] T. Ginige, N. Rajatheva, and K. M. Ahmed, “Dynamic spreading code selection method for PAPR reduction in OFDM-CDMA systems with 4-QAM modulation,” *IEEE Commun. Lett.*, vol. 5, no. 10, pp. 408-410, Oct. 2001.

[165] J. Blanz and H. D. Schotten, “Dynamic space-time coding for a communication system,” U.S. Patent 8,320,499, Nov. 27, 2012.

[166] D. M. Teran, R. P. T. Jimenez, and R. A. U. Vargas, “Constant-rate adaptive space-time code selection technique for Wireless Communications,” in *Proc. 6th Int. Conf. Digital Telecommun., ICDT 2011*, Apr. 2011, pp. 7-11.

[167] L. Lampe, R. Schober, and R. F. Fischer, “Multilevel coding for multiple-antenna transmission,” *IEEE Trans. Wireless Commun.*, vol. 3, no. 1, pp. 203-208, Jan. 2004.

[168] D. F. Yuan, F. Zhang, A. F. Sui, and Z. W. Li, “Concatenation of space-time block codes and multilevel codes over Rayleigh fading channels,” in *Proc. IEEE Veh. Tech. Conf. VTC Fall*, Oct. 2001, vol. 1, pp. 192-196.

[169] D. F. Yuan, P. Zhang, and Q. Wang, “Multilevel codes (MLC) with multiple antennas over Rayleigh fading channels,” *IEEE 54th Veh. Tech. Conf. VTC Fall*, Oct. 2001, vol. 3, pp. 1289–1293.

[170] T. Woerz and J. Hagenauer, “Multistage coding and decoding for a M-PSK system,” In *Proc. IEEE Global Telecommun. Conf. Exhibition Commun. Connecting the Future, GLOBECOM ’90*, Dec.1990, pp. 698–703.

[171] T. Woerz and J. Hagenauer, “Multistage coding and decoding for a M-PSK system,” in *Proc. IEEE Global Telecommun. Conf., GLOBECOM’92’*, Dec. 1992, pp. 1779 –1784.

[172] P. A. Martin, D.M. Rankin, and D. P. Taylor, “Multi-dimensional space-time multilevel codes,” *IEEE Trans. Wireless Commun.*, vol. 5, no. 9, pp. 2569-2577, Sept. 2006.

[173] P. A. Martin, D. M. Rankin, and D. P. Taylor, “Space-time multilevel codes,” *IEEE 61st Veh. Tech. Conf. VTC Spring*, June 2005, vol.2, pp.1201-120.

[174] L. F. Wei, “Trellis coded modulation with multidimensional constellations,” *IEEE Trans. Inform. Theory*, vol. 33, no. 4, pp. 483-501, July 1987.

[175] O. Oruc, I. Altunbas, and U. Aygolu, “Multilevel super-orthogonal space-time coding,” in *Proc. IEEE 12th Signal Process. Commun. Applications Conf.*, Apr. 2004, pp.724-727.

[176] M. A. Shang-Chih, “Multilevel concatenated space-time block codes,” *IEICE Trans. Fundamentals Electron., Commun. Computer Sciences*, vol. 93, no. 10, pp. 1845-1847, Jan. 2010.

[177] R. Y. Tee, O. R. Alamri, S. X. Ng, and L. Hanzo, “Equivalent Capacity-Based Joint Multilevel Coding and Space–Time Transmit Diversity Design,” *IEEE Trans. Veh. Tech.*, vol. 57, no. 5, pp. 3006-3014, Sept. 2008.

[178] J. Chui and A. R. Calderbank, “Multilevel diversity-embedded space-time codes for video broadcasting over WiMAX,” in *Proc. IEEE Int. Symp. Inform. Theory, ISIT-2008*, July 2008, pp. 1068-1072.

[179] S. N. Diggavi, A. R. Calderbank, S. Dusad, and N. Al-Dhahir, “Diversity embedded space-time codes,” *IEEE Trans. Inform. Theory*, vol. 54, pp. 33–50, Jan. 2008.

[180] S. C. Ma, “Extended space-time multilevel coded spatial modulation,” *J. Chinese Institute Engineers*, vol. 36, no. 6, pp. 715-720, June 2013.

[181] A. M. Baghaie, *Multilevel space-time trellis codes for Rayleigh fading channels*. ME Thesis, University of Canterbury, New Zealand. http://ir.canterbury.ac.nz/bitstream/10092/2101/1/Thesis_fulltext.pdf.

[182] A. M. Baghaie, P. A. Martin, and D. P. Taylor, “Grouped multilevel space-time trellis codes,” *IEEE Commun. Lett*., vol. 14, no. 3, pp. 232-234, Mar. 2010.

[183] S. Sharma, “A novel weighted multilevel space–time trellis coding scheme,” *Computers & Mathematics Applications*, vol. 63, no. 1, pp. 280–287, Jan. 2012.